UNIVERSITE PARIS XIII –SORBONNE PARIS NORD

École doctorale Sciences, Technologies, Santé Galilée

Élaboration de matériaux hybrides Titane/Polymère pour améliorer la réponse biologique des cellules osseuses

Elaboration of Titanium/Polymer hybrid materials to improve the biological response of bone cells

---

THÈSE DE DOCTORAT
présentée par

Caroline Rosada Joaquina PEREIRA

Laboratoire des Biomatériaux Pour la Santé

Unité de recherche CSPBAT UMR 7244

Institut Galilée, Université Paris XIII, Sorbonne Paris Nord

pour l'obtention du grade de
DOCTEUR EN CHIMIE DES MATÉRIAUX

Soutenue le 16 mai 2023 devant le jury d'examen constitué de :

M HOURDET Dominique, Professeur des Universités, Sorbonne Université, Rapporteur.
Mme DEGOUTIN Stéphanie, Maître de Conférences-HDR, Université de Lille, Rapportrice.
Mme CARRADÒ Adele, Professeur des Universités, Institut de physique et chimie des matériaux de Strasbourg, Examinatrice.
M CHAUBET Frédéric, Professeur des Universités, Université Sorbonne Paris Nord, Examinateur.
Mme FALENTIN-DAUDRÉ Céline, Maître de Conférences-HDR, Université Sorbonne Paris Nord, Directrice de thèse.

ACKNOWLEDGMENTS

This research project was conducted at the Laboratoire des Biomatériaux Pour la Santé (LBPS-CSPBAT UMR 7244, CNRS), Institut Galilée, from Université Sorbonne Paris Nord.

First of all, I would like to express my sincere gratitude to my thesis supervisor Doctor Céline Falentin-Daudré, director in functions of the LBPS/CSPBAT laboratory, for accepting me as her PhD student. Her support, avaibility, patience and guidance were very encouraging during the three years of this thesis. Many thanks for her help in finalising the thesis manuscript. It was a pleasure to be guided by her.

I want to express grateful thanks to the members of my thesis jury. I am very honoured by the presence on this jury of Professor Dominique Hourdet (Sorbonne Université) and Doctor Stéphanie Degoutin (Université de Lille). I extent my gratitude for their acceptance to become a jury of this thesis and for the attention and time given to evaluate this work.

I am very grateful to Professor Frédéric Chaubet (Université Sorbonne Paris Nord) and Professor Adele Carradò (Institut de Physique et Chimie des Matériaux de Strasbourg) for giving me the honour of evaluating my work and for their participation as members of the jury.

I would like to acknowledge Pr. Heinz Palkowski, Dr. Patrick Masson, Dr. Flavien Mouillard, Gargi Shankar Nayak and Dr. Jean-Sébastien Baumann for all their valuable insights, discussion and friendship during the ANR BIOSMS meetings. I would like to extend this thank you note to all the former and current students and researchers at the LBPS team. Special thanks to André and Véronique for their help throught the first year of my thesis.

I also thank Dr. Sophie Le Cann, Pr. Guillaume Haïat and all the team at Paris Est Créteil for their collaboration and material production on the BioMint project. To Dr. Vincent Humblot, I express my gratitude for his help and enriching suggestions on the XPS characterization.

A big thank you to the whole team of teachers and researchers at Bobigny: Carole, Marilyne, Maelle, Dominique and Philippe. Thank you to all the students I was able to guide

during my thesis. Special thanks to Alexia Barjavel and Claire Semedo Da Moura for their great work during their internship.

I would like to thank all my PhD Student friends (Aurélie, Fatma, Nouha, Memona, Célia) for their support and the good times we had together.

Many thanks to the support given by all my friends (Marie, Transley, Emma, Joseph, Linda, Diana, Boris, Riri, Emna, Phil, Hiru, Bryan, Raphaël, Julien, team Jussieu, team GG).

I am grateful to Maverick, Rozenn and Philippe for their constant motivation and for their kind advices.

Finally, I thank my parents and my brother, Elder, for being always unconditionnaly present in my life. Their support and motivation especially in the most difficult times were precious.

This thesis is dedicated in the memory of my cousin, Jovin Pereira who passed away on the 3rd February 2022 at the age of 20 years of a motocycle accident.

TABLE OF CONTENTS

LIST OF FIGURES

LIST OF TABLES

NOMENCLATURE

ALP: Alkaline Phosphatase

AIBN: 2,2'-azobis (2-methylpropionitrile)

ATR/FTIR: Attenuated total reflection Fourier transform infrared spectroscopy

BSA: Bovine serum albumin

D-MEM: Dulbecco's Mod Eagle Medium

DMSO: dimethylsufoxide

ECM: Extracellular matrix

EDS: Energy Dispersive x-ray Spectroscopy

FBS: Fetal Bovine Serum

Fn: Fibronectin

HA: Hydroxyapatite

ISO: International Organization for Standardization

MC 3 T3-E1: osteoblast cells ATCC n°CRL-2593

MMA: Methyl Methacrylate

NaSS: Sodium styrene sulfonate

PBS: Phosphate Buffer Saline solution

Poly(MMA) or PMMA: Poly (methyl methacrylate)

Poly (NaSS) or PNaSS: Poly (sodium styrene sulfonate)

Poly(VBP) or PVBP: Poly (Vinyl Benzyl Phosphonic acid)

RANKL: receptor activating NF-kB ligand

RAFT: Reversible Addition-Fragmentation chain Transfer

NMR: Nuclear magnetic resonance

SBF: Sérum Bovin Foetal

SEM: Scanning Electron Microscopy

TB: Toluidine Blue

Ti: Titanium

TA6Al4V: Titanium alloy with 6% aluminium and 4% vanadium

UV: UltraViolet

Vn: Vitronectin

XPS: X-Ray Photoelectron Spectroscopy

INTRODUCTION

Scope of the thesis

The craniofacial bone structures, which include the skull, maxillae, and mandible, support several essential body functions, such as the protection of the brain and the allocution. Significant loss of craniofacial bone substances is usually caused by lesions or pathologies, such as tumoral or congenital malformations [1].

Skull fracture is among the most severe bone injuries as they may directly damage the brain. The leading cause of skull fractures remains head trauma. In France, each year, around 150 000 people suffer from head trauma injuries [2]. The seriousness of skull bone lesions depends on the nature and location of the fracture. Despite the remarkable capacity of the bone tissue to regenerate minor defects, the repair of larger lesions often requires surgery.

Although autograft is frequently used to restore bone, this method presents considerable disadvantages, such as substantial morbidity at the donor site and limited availability of bone tissue. Other techniques, such as allogenic grafts, are also unsatisfactory due to immune rejection and the high risk of disease transmission [3]. These limitations have prompted the pursuit of alternative bone reconstruction techniques that reduce the danger of infection and rejection.

Presently, the elaboration of functional cranial prosthetic devices constitutes a very active field of research, both in fundamental research and engineering, in terms of improving the mechanical properties, biocompatibility of implants, and tailoring the most suitable shapes. The main challenge is selecting suitable biomaterials closer to the surrounding tissues with mechanical and biological properties. In this view, bone substitutes like implants provide an interesting research direction for replacing and remodelling the damaged bone flap.

The most widely used materials for cranioplasty reconstruction are poly (methyl methacrylate) (PMMA) [4], hydroxyapatite [5–7], and titanium [6,8,9]. In particular, titanium (Ti) and its alloys have proven to have successful biological and mechanical qualities in elaborating functional biomedical devices [10]. However, despite their acceptable biocompatibility, pure titanium implants are not optimally osseointegrated. In the long term, an inflammatory process leading to the development of a fibrous capsule detaches pure Ti implants from the bone tissue and causes the failure of the implant [11,12].

To solve the problems correlated with Ti implants' osseointegration, researchers have developed numerous functionalization approaches (heat and plasma treatment [13–14], silane treatments and protein coating [15], anodic oxidation [16,17]). Among these approaches, using a coating made up of a bioactive polymer covalently grafted onto the prosthetic titanium surface is a solution that avoids loosening the implant and increases its lifespan.

The speciality of the "Laboratoire des Biomatériaux Pour la Santé" (CSPBAT, UMR CNRS 7244) research team, is to covalently functionalized Ti and its alloys with various chemical groups, such as hydroxyl groups [18], carboxyl [19], sulfonic [20], and phosphate [21]. LBPS team worked for several years (since 2000) on grafting anionic polymers onto Ti and its alloys surfaces. The technologies developed by the LBPS team make it possible to graft bioactive polymers to the Ti surfaces by free radical polymerization route.

Previous work carried out at LBPS on the development of bioactive prosthesis has shown excellent *in vitro* and *in vivo* results of radical grafting of sodium styrene sulfonate monomer (NaSS) onto Ti implants [22-24]. The grafting procedure of NaSS recently developed by our team, is particularly appealing as it is a direct ultraviolet (UV) irradiation process [25]. The grafting process is done in two steps: activation of the surface by oxidation to create Ti hydroperoxides which decompose by UV irradiation to create free radicals on the surface. These radicals then allow the initiation and the radical polymerization of the monomer. The UV irradiation process is a straightforward, fast, and inexpensive approach that allows the introduction of the desired functional groups on materials surfaces without modifying their general characteristics.

Nowadays, there is a great interest in developing composite materials [26]. In this context, a part of the work presented in this manuscript focuses on the elaboration of Titanium/Polymer (Ti/P) hybrid materials for designing functional bone prostheses. Sandwich structure (Ti/P/Ti) are appealing for the design of innovative cranial prostheses because they combine the properties of both, (metallic and polymeric) materials. Depending on the polymer used to conceive the implant, it is possible to incorporate new functionalities to Ti surfaces (flexibility, lightness, control of the hydrophilic/hydrophobic balance, etc..). In addition, to improve the osseointegration of prostheses, the other part of our work focused on the grafting of a bioactive polymer based on phosphonic acid. In this PhD project, the grafting process of

this polymer was optimized to graft pure titanium surfaces as well as textured TA6V titanium alloy implants.

Research objectives

In the framework of the elaboration of three-layered biocompatible hybrid structures composed of titanium and polymer sheets Ti/P/Ti, we have worked on the ANR "BIOSMS" project in collaboration with the Institute de Physique et Chimie des Matériaux of Strasbourg (IPCMS, CNRS UMR 7504) and the Institute of Metallurgy at Clausthal University of Technology (IMET TUC).

Due to its strong resistance to corrosion, its good transparency properties and its high refractive index, PMMA is used in many fields: in optics, for the manufacture of sensors or for the separation of molecules [27]. In addition, its biocompatibility makes it the most widely used polymer in implant-type medical devices (orthopedic, vascular, cardiac, artificial organ, catheter, etc.), in the preparation of bone cements [28], and as a release system. It is also used in the composition of suture threads, adhesives, contact lenses [29] in dental implants [30,31] or even for cranioplasty reconstruction. Poly (NaSS) is the model polymer for the bio-functionalization of the implant and its biological impact once integrated into the living system. This polymer possesses bioactive and anti-inflammatory properties [32].

The work presented in this thesis has several objectives:

In collaboration with the IPCMS, the first objective of this work was to develop sandwich structures by grafting PMMA onto Ti surfaces using the indirect grafting technique developed within the LBPS.

The second objective of this work was to develop the grafting of bioactive polymers carrying sulfonate groups onto Ti sandwich structures in order to improve the osseointegration properties.

The third objective of this work was to develop a method to improve bone-implant integration by covalently grafting Ti with phosphonic acid-based monomers: vinyl benzyl phosphonic acid (VBP). This monomer has a similar a structure similar to that of NaSS. Studies have shown that titanium and polymers functionalized with phosphate groups (-PO_3H_2) exhibit

increased bioactivity due to their ability to generate bone-like apatite [33–35]. In recent years, vinyl phosphonic acid has been used as a coating to make bone graft substitutes [36] and functionalize bone scaffolds [37] for bone regeneration. These results suggest the beneficial influence of phosphonate groups on the osseointegration of implants. Various factors making it possible to optimize the grafting of poly (VBP) on titanium substrates have been studied. This study used UV-induced two-step graft polymerization of VBP to functionalize Ti surfaces with phosphonate groups. The oxidation of Ti produces peroxides on the surface, which generate radicals when exposed to UV irradiation, initiating the polymerization of the VBP monomer. The effect of VBP grafting has been characterized chemically. Moreover, *in vitro* studies with MC3T3-E1 osteoblastic cells were conducted to assess the influence of VBP grafting on bone cell adhesion, spreading, and differentiation.

Thesis outline

This work reports the development of Ti functionalization by different bioactive polymers carrying sulfonate and phosphonate groups, in order to improve the biological response of sandwich structures. The results are presented in the form of a thesis in articles. This thesis is the subject of 4 publications.

Each chapter has been described as follows:

Chapter I describes the context of the subject of cranioplasty and the thesis project on developing titanium/polymer hybrid materials to improve the biological response of bone cells.

Chapter II describes the development of dual functionalization with two polymers having different functionalities on titanium surfaces. The objective of this part was therefore to graft 1) PMMA on one side of the titanium surface in order to improve the adhesion properties of the sandwich structures and 2) a bioactive polymer on the other part of the surface in order to improve the osseointegration of sandwich structures for cranioplasty reconstruction.

Chapter III describes another way to develop sandwich structures functionalized by two different polymers without using the technique of double functionalization. Thus, a direct grafting technique of PMMA and of bioactive polymers on Ti-PMMA surfaces was developed in order to improve the osseointegration properties of sandwich structures. To demonstrate the

efficiency and the necessity of this grafting, the *in vitro* study of the cellular response with bone cells (MC3T3-E1 osteoblasts) is reported.

In the literature, it has been shown that polymers bearing phosphonate groups improve osseointegration properties. In chapter IV, the development of direct grafting of polymers bearing phosphonate groups on titanium surfaces is presented, as well as the study of the cellular response *in vitro* with bone cells (MC3T3-E1 osteoblasts).

The results of the work are therefore articulated around four articles presented below, followed by a conclusion and work perspectives.

This thesis was carried out thanks to the support of an ANR "BIOSMS" and a doctoral grant from the Ministry of Research and Higher Education. Part of this work was carried out in collaboration with the teams of the Institute of Physics and Chemistry of Materials of Strasbourg (IPCMS, CNRS UMR 7504) (Pr Adele Carrado, Dr Patrick Masson, Dr Geneviève Pourroy, Dr Flavien Mouillard) and the Institute of Metallurgy at Clausthal University of Technology (IMET TUC) (Gargi Shankar Nayak and Pr Heinz Palkowski).

References

[1] P. Solaro, E. Pierangeli, C. Pizzoni, P. Boffi and G. Scalese, "From computerized tomography data processing to rapid manufacturing of custom-made prostheses for cranioplasty." Case report. J Neurosurg Sci., 52(4):113–6; discussion 116, 2008.

[2] Chiffres donnés par l'Institut du Cerveau https://institutducerveau-icm.org/fr/traumatismes-craniens/

[3] P. V. Giannoudis, H. Dinopoulos and E. Tsiridis: Bone substitutes: An update. Injury 36S, S20-S27 (2005)

[4] T. Origitano, R. Izquierdo, and L. B. Scannicchio, Reconstructing complex cranial defects with a preformed cranial prosthesis, Skull Base Surgery, vol. 5, no. 02, pp. 109–116, 1995.

[5] B. L. Eppley, L. Hollier, and S. Stal, Hydroxyapatite cranioplasty: 2. clinical experience with a new quick-setting material, Journal of Craniofacial Surgery, vol. 14, no. 2, pp. 209–214, 2003.

[6] Y. Ducic, Titanium mesh and hydroxyapatite cement cranioplasty: a report of 20 cases, Journal of Oral and Maxillofacial Surgery, vol. 60, no. 3, pp. 272–276, 2002.

[7] P. D. Costantino, C. D. Friedman, K. Jones, L. C. Chow, and G. A. Sisson, Experimental hydroxyapatite cement cranioplasty, Plastic and Reconstructive Surgery, vol. 90, no. 2, pp. 174–hyhen, 1992.

[8] A. Thien, N. K. King, B. T. Ang, E. Wang, and I. Ng, Comparison of polyetheretherketone and titanium cranioplasty after decompressive craniectomy, World neurosurgery, vol. 83, no. 2, pp. 176–180, 2015.

[9] M. Cabraja, M. Klein, and T.-N. Lehmann, Long-term results following titanium cranioplasty of large skull defects, Neurosurgical Focus, vol. 26, no. 6, p. E10, 2009.

[10] P.-I. Brånemark, U. Breine, R. Adell, B.O. Hansson, J. Lindström, Å. Ohlsson, Intra-Osseous Anchorage of Dental Prostheses: I. Experimental Studies 3 (1969) 81–100. https://doi.org/10.3109/02844316909036699.

[11] M. Esposito, J.-M. Hirsch, U. Lekholm, P. Thomsen, Biological factors contributing to failures of osseointegrated oral implants, European Journal of Oral Sciences. 106 (1998) 527–551. https://doi.org/10.1046/j.0909-8836..t01-2-.x.

[12] A.M. Roos-Jansaker, S. Renvert, J. Egelberg, Treatment of peri-implant infections: a literature review, J. Clin. Periodontol. 30 (2003) 467–485. https://doi.org/10.1034/j.1600-051X.2003.00296.x.

[13] Y.-J. Park, H.-J. Song, I. Kim, H.-S. Yang, Surface characteristics and bioactivity of oxide film on titanium metal formed by thermal oxidation, J Mater Sci: Mater Med. 18 (2007) 565–575. https://doi.org/10.1007/s10856-007-2303-7.

[14] L. Saldaña, V. Barranco, J.L. González-Carrasco, M. Rodríguez, L. Munuera, N. Vilaboa, Thermal oxidation enhances early interactions between human osteoblasts and alumina blasted Ti6Al4V alloy, J. Biomed. Mater. Res. 81A (2007) 334–346. https://doi.org/10.1002/jbm.a.30994.

[15] A. Carradó, Structural, Microstructural, and Residual Stress Investigations of Plasma-Sprayed Hydroxyapatite on Ti-6Al-4 V, ACS Appl. Mater. Interfaces. 2 (2010) 561–565. https://doi.org/10.1021/am900763j.

[16] Y. Liu, P. Layrolle, J. de Bruijn, C. van Blitterswijk, K. de Groot, Biomimetic coprecipitation of calcium phosphate and bovine serum albumin on titanium alloy, J. Biomed. Mater. Res. 57 (2001) 327–335. https://doi.org/10.1002/1097-4636(20011205)57:3 <327::AID-JBM1175>3.0.CO;2- J.

[17] Y.-T. Sul, C.B. Johansson, S. Petronis, A. Krozer, A. Wennerberg, T. Albrektsson, Characteristics of the surface oxides on turned and electrochemically oxidized pure titanium implants up to dielectric breakdown: the oxide thickness, micropore configurations, surface roughness, crystal structure and chemical composition, Biomaterials 23 (2002) 491–501. https://doi.org/10.1016/S0142-9612 (01)00131-4.

[18] L. Le Guéhennec, A. Soueidan, P. Layrolle, Y. Amouriq, Surface treatments of titanium dental implants for rapid osseointegration, Dental Materials. 23 (2007) 844–854. https://doi.org/10.1016/j.dental.2006.06.025.

[19] Y.-J. Park, H.-J. Song, I. Kim, H.-S. Yang, Surface characteristics and bioactivity of oxide film on titanium metal formed by thermal oxidation, J Mater Sci: Mater Med. 18 (2007) 565–575. https://doi.org/10.1007/s10856-007-2303-7.

[20] A. Michiardi, G. Hélary, P.-C.T. Nguyen, L.J. Gamble, F. Anagnostou, D.G. Castner, V. Migonney, Bioactive polymer grafting onto titanium alloy surfaces, Acta Biomaterialia. 6 (2010) 667–675. https://doi.org/10.1016/j.actbio.2009.08.043.

[21] N. Adden, L.J. Gamble, D.G. Castner, A. Hoffmann, G. Gross, H. Menzel, Phosphonic Acid Monolayers for Binding of Bioactive Molecules to Titanium Surfaces, Langmuir. 22 (2006) 8197–8204. https://doi.org/10.1021/la060754c.

[22] H. Chouirfa, M.D.M. Evans, D.G. Castner, Grafting of architecture controlled poly(styrene sodium sulfonate) onto titanium surfaces using bio-adhesive molecules: Surface characterization and biological properties, Biointerphases 12, 02C418 (2017). http://dx.doi.org/10.1116/1.4985608.

[23] F. El Khadali, G. Hélary, G. Pavon-Djavid, V. Migonney, Modulating Fibroblast Cell Proliferation with Functionalized Poly(methyl methacrylate) Based Copolymers: Chemical Composition and Monomer Distribution Effect, Biomacromolecules. 3 (2002) 51–56. https://doi.org/10.1021/bm015563x.

[24] F. Anagnostou, A. Debet, G. Pavon-Djavid, Z. Goudaby, G. Hélary, V. Migonney, Osteoblast functions on functionalized PMMA-based polymers exhibiting Staphylococcus aureus adhesion inhibition, Biomaterials. 27 (2006) 3912–3919. https://doi.org/10.1016/j.biomaterials.2006.03.004.

[25] H. Chouirfa, V. Migonney, C. Falentin-Daudré, Grafting bioactive polymers onto titanium implants by UV irradiation, RSC Adv. 6 (2016) 13766–13771. https://doi.org/10.1039/C5RA24497H.

[26] B. Harris, A perspective view of composite materials development, Materials & Design, vol. 12, no. 5, pp. 259–272, 1991.

[27] U. Ali, KJBtA Karim, NA.Buang, A Review of the Properties and Applications of Poly(Methyl Methacrylate) (PMMA). Polymer Reviews 55 (2015) 678–705. https://doi.org/10.1080/15583724.2015.1031377.

[28] S.M. Kenny, M. Buggy Bone cements and fillers: a review. Journal of Materials Science: Materials in Medicine 14 (2003) 923–38. https://doi.org/10.1023/A:1026394530192.

[29] T. Goda, K. Ishihara, Soft contact lens biomaterials from bioinspired phospholipid polymers. Expert Review of Medical Devices 3 (2006) 167–74. https://doi.org/10.1586/17434440.3.2.167.

[30] R.Q. Frazer, R.T. Byron, P.B. Osborne, K.P. West, PMMA: an essential material in medicine and dentistry. J Long Term Eff Med Implants 15 (2005) 629–39. https://doi.org/10.1615/jlongtermeffmedimplants.v15.i6.60.

[31] H. Kaur, A.Thakur, Applications of poly(methyl methacrylate) polymer in dentistry: A review. Materials Today: Proceedings 50 (2022) 1619–25. https://doi.org/10.1016/j.matpr.2021.09.125.

[32] H.P. Felgueiras, M.D.M. Evans, V. Migonney, Contribution of fibronectin and vitronectin to the adhesion and morphology of MC3T3-E1 osteoblastic cells to poly(NaSS) grafted Ti6Al4V, Acta Biomaterialia. 28 (2015) 225–233. https://doi.org/10.1016/j.actbio.2015.09.030.

[33] P. Datta, J. Chatterjee, S. Dhara, Electrospun nanofibers of a phosphorylated polymer—A bioinspired approach for bone graft applications, Colloids and Surfaces B: Biointerfaces. 94 (2012) 177–183. https://doi.org/10.1016/j.colsurfb.2012.01.033.

[34] C. Viornery, Y. Chevolot, D. Léonard, B.-O. Aronsson, P. Péchy, H.J. Mathieu, P. Descouts, M. Grätzel, Surface Modification of Titanium with Phosphonic Acid To Improve Bone Bonding: Characterization by XPS and ToF-SIMS, Langmuir. 18 (2002) 2582–2589. https://doi.org/10.1021/la010908i.

[35] C. Viornery, H.L. Guenther, B.-O. Aronsson, P. Péchy, P. Descouts, M. Grätzel, Osteoblast culture on polished titanium disks modified with phosphonic acids: Osteoblast Culture on Polished Titanium, J. Biomed. Mater. Res. 62 (2002) 149–155. https://doi.org/10.1002/jbm.10205.

[36] R.E. Dey, I. Wimpenny, J.E. Gough, D.C. Watts, P.M. Budd, Poly (vinylphosphonic acid- co -acrylic acid) hydrogels: The effect of copolymer composition on osteoblast adhesion and proliferation: PVPA- co -AA HYDROGELS, J. Biomed. Mater. Res. 106 (2018) 255–264. https://doi.org/10.1002/jbm.a.36234.

[37] R.E. Dey, X. Zhong, P.J. Youle, Q.G. Wang, I. Wimpenny, S. Downes, J.A. Hoyland, D.C. Watts, J.E. Gough, P.M. Budd, Synthesis and Characterization of Poly (vinylphosphonic acid- co -acrylic acid) Copolymers for Application in Bone Tissue Scaffolds, Macromolecules. 49 (2016) 2656–2662. https://doi.org/10.1021/acs.macromol.5b02594.

CHAPTER I

STATE OF ART

This first chapter exposes the literature tools, making it possible to undertake the study work. The literature review is organized into three parts. The first part presents the context of the thesis project. In this first part, the physiology of the skull will be introduced with a macroscopic presentation of the bones forming the skull, then with a more microscopic description of the composition, the mechanisms of remodelling and consolidation of the bone tissue processes.

This first part also presents the common bone defects which damage the skull. The second part of the review describes the importance of bone reconstruction by developing cranial prostheses. A brief history of the bone substitutes used in cranioplasty and the parameters to be considered for developing prostheses are presented. This part insists on the importance of the cell/biomaterial interface by outing the different types of responses of an implant following its implantation, the adhesion mechanisms of bone cells on the implant and the properties needed for a good implant/cell interface. The second part of the bibliographic review justifies the choice of titanium as a bone substitute for the development of cranial prostheses. This second part gives a non-exhaustive description of the inherent properties of titanium, the functionalization strategies, and the interest in designing hybrid structures called titanium sandwich structures. The third part, for its part, specifies the choice of the use of polymers based on phosphonic acid to improve the bioactive properties of titanium surfaces.

I.1. The skull: macroscopic to microscopic description

1.1. Physiology of the skull

1.1.1. Role of the skull

The skull is the strongest bone in the human body. It contains two parts: the cranial box (neurocranium) and the facial bone (viscerocranium). Each part of the skull plays a precise role. The cranial box ensures the protection of the encephalon (brain, cerebellum, brainstem), central nervous system, and sensory organs. The facial bone endorses the oral and pharyngeal cavities [1]. Skull has the specificity of being an attachment point for the muscles of the face and neck. It also has the particularity to regroup a sound box for the voice and a temperature regulator cavity. Thermoregulation of the skull is done by the skin of the scalp [2].

1.1.2. Anatomy of the skull

The human skull is made up of eight flat bones juxtaposed together by sutures: at the front: the frontal bone and the ethmoid bone; at the top and on the sides: the two symmetrical parietal bones; below and to the sides: the sphenoid bone and the two right and left temporal bones and behind is the occipital bone (**Figure 1.1**) [3]

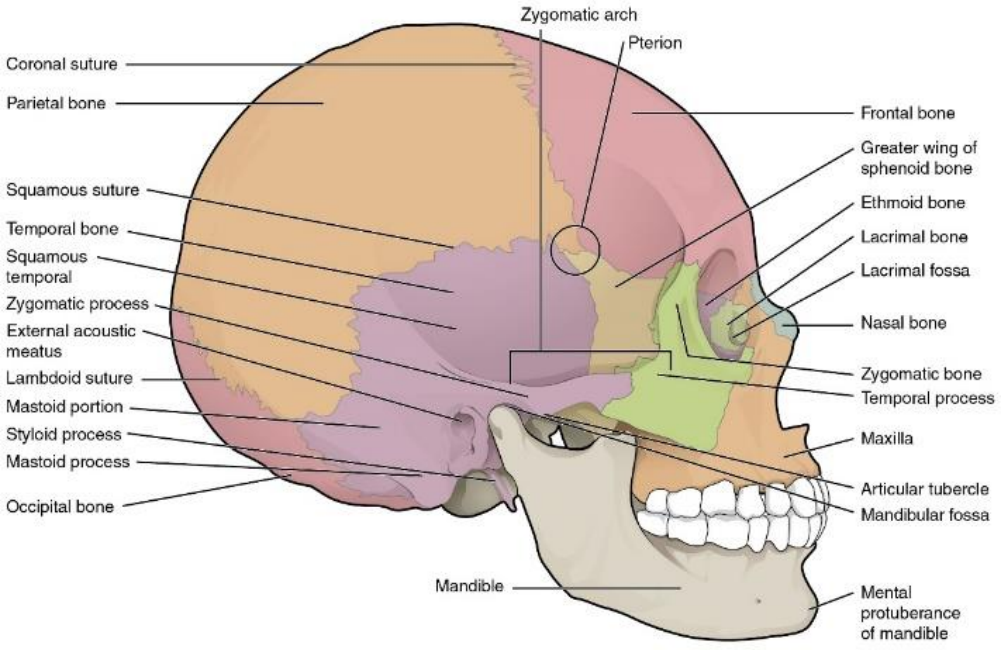

FIGURE 1.1 LATERAL VIEW OF THE SKULL [3]

The cranial box has a well-defined structure, constituted by the cranial vault (calvaria) and a lower part called the skull base [1]. The cranial vault is the upper part of the skull. It is composed of a set of bones: the frontal bone, which establishes the forehead, the parietal bones and the temporal bones form the entire side of the skull; the occipital bone, for its part, builds on the back of the skull. These convex bones are flat and are joined together by denticulate sutures. At birth, bone sutures are not welded and thereby contribute to the growth of the bones of the cranial box. The sutures that appear during growth (between the 5th and the 24th month) make it possible to freeze the skull's geometry and framework [4].

The base of the skull is limited by the frontal bone and the occipital bone of the vault. It is founded, from front to back, by the ethmoid, the sphenoid, and the occipital bone [5]. It is also made up of three cranial cavities: the anterior, middle, and posterior cranial fossae (**Figure 1.2**)

[6]. To allow nerve transmission and blood vascularization of the brainstem, the base of the skull is pierced with ten prominent foramina distributed over the three fossae.

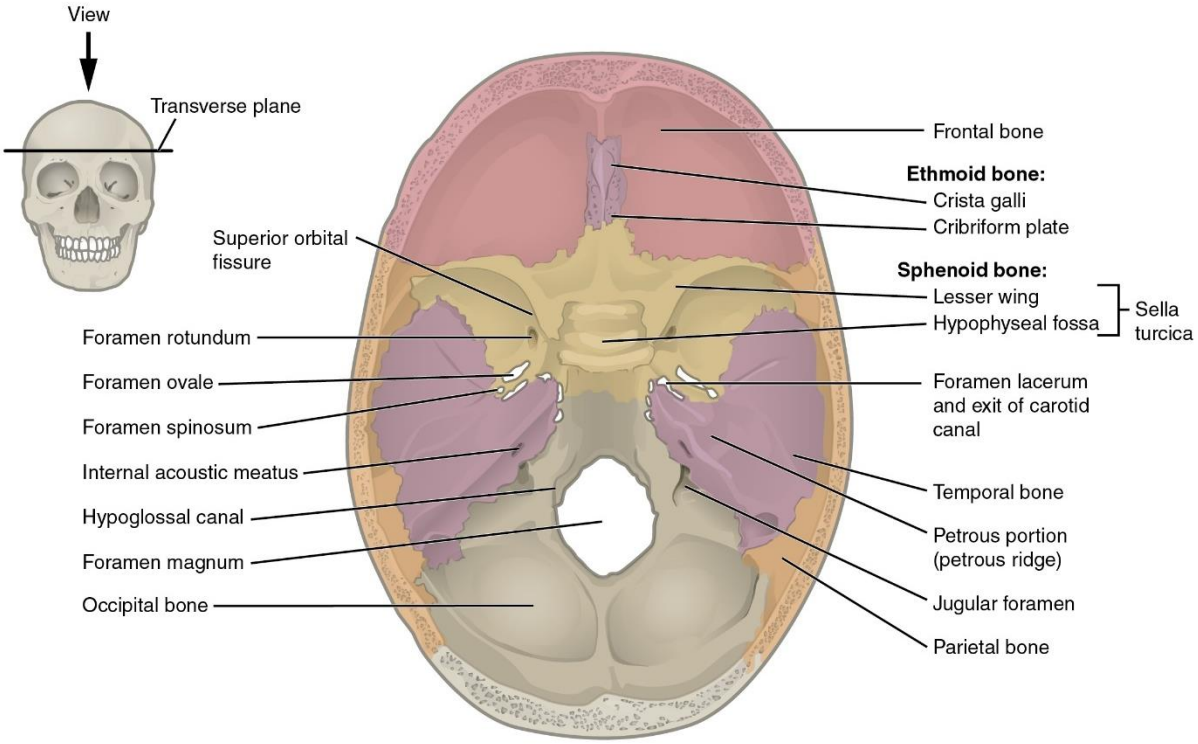

FIGURE 1.2 SUPERIOR VIEW OF THE SKULL [6]

The facial massif is made up of thirteen welded bones and the mandible. The maxillary bones and the mandible form the upper and lower dentitions (**Figure 1.3**) [6]. The facial bone contains air cavities called sinuses. The temporomandibular joints allow mandible articulation on either side of the skull [7].

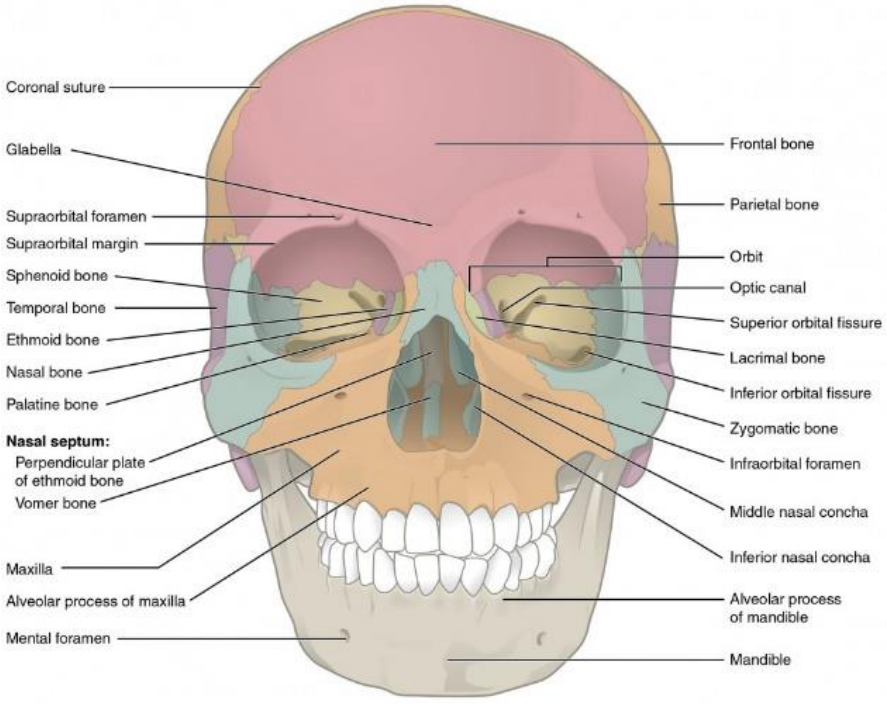

FIGURE 1.3 ANTERIOR VIEW OF THE SKULL [6]

The bones of the skull are robust. However, some areas are more fragile, mainly in the temporal regions, with reasonably thin bones traversed by vessels [8]. These vessels can be torn during a fracture, which is one of the major causes of haematomas.

Macroscopically, each of the bones of the skull is composed of 3 layers of bony tissue: two blades of compact bone called the table (internal table and external table) separated by a spongy tissue called the diploe [9] (**Figure 1.4**) [3].

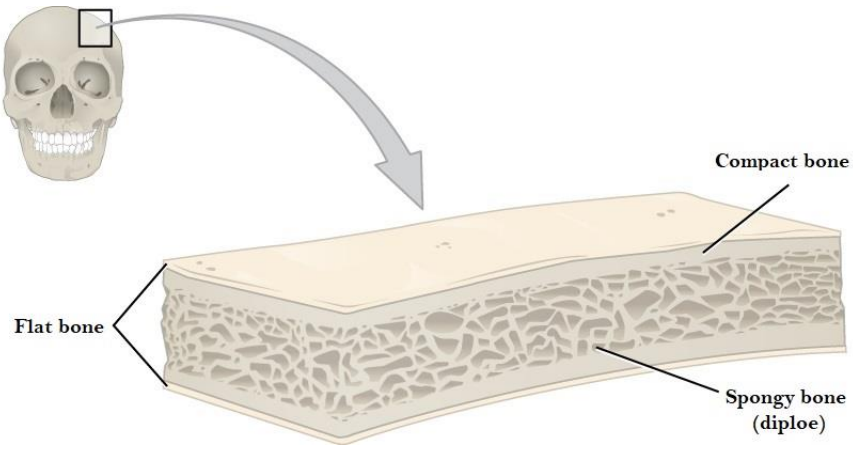

FIGURE 1.4 STRUCTURE OF THE BONES OF THE SKULL [3]

1.2. Structure of bones

1.2.1. Bone tissue

Bone tissue is one of the most interesting tissues in the human body. It is a connective tissue that contains cells separated by an extracellular matrix (ECM). It has two leading roles: a metabolic and a biomechanical role. As the bone tissue constitutes a reservoir of minerals (99% of the calcium and 90% of the phosphate in the body), its metabolic role consists of maintaining phosphor-calcium homoeostasis. The biomechanical role of the bone tissue is to allow locomotion, endorse the body, and protect vital organs [10].

Bone tissue is a composite material composed of 70% of a mineral phase – the mineralized, calcified, highly vascularized, and highly innervated ECM – and approximately 30% of organic phase: the organic ECM. ECM features type I collagen fibers, adhesion glycoproteins (osteopontin), and a ground substance of 50% water. Osteopontins bind together apatite crystals and build the mineral ECM [11]. Hence, the mineral phase is formed of calcium hydroxyapatite crystals, $Ca_{10}(PO_4)_2(OH)_2$. These crystals have the shape of a small needle 600 Å long and are the source of bone strength [12].

From an anatomical point of view, bone tissue is divided into three types [13]: non-lamellar primary bone tissue, lamellar secondary bone tissue, and periosteal bone tissue. Lamellar bone tissue of highly organized collagen fibers can be either cortical compact (10% porosity) or spongy (75 to 95% porosity). Periosteal bone tissue or periosteum is a fibrous, highly vascular connective tissue that surrounds the outer surface of the bone. The outer layer of the periosteum is very rich in type I collagen; its inner layer is the seat of osteoblasts. The periosteum consequently delimits the bone, the bone growth, and the tendons' insertion, making it possible to rectify fractures.

1.2.2. Bone cells

Microscopically, bone tissue is made up of many cells. Cells from the osteoblastic and osteoclasts lineages are those primarily involved in bone formation [14].

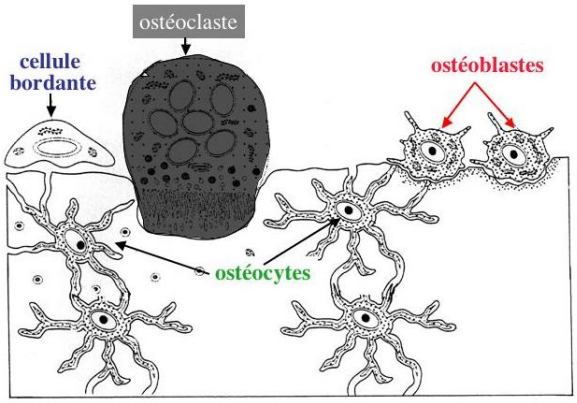

FIGURE 1.5 BONE CELLS [15]

The osteoblastic lineage includes three cell types [16]: osteoblasts, bone-lining cells and osteocytes. In the thickness of bone trabeculae, the osteocytes are connected to the cells of the bone surface, lining cells and osteoblasts by extensions which run in the canaliculi (**Figure 1.5**) [15].

Each osteoblastic cell has a specific role:

- **Osteoblasts** are responsible for forming bone tissue and are the main cellular component of bone. They synthesize the bone matrix and regulate its mineralization. The plasma membrane of osteoblasts contains alkaline phosphatase (ALP). The later releases the inorganic phosphate, which gives calcium phosphate by binding to calcium. Mature osteoblasts are distinguished by a cubic or polygonal cell body (15–30 µm in diameter), a rounded nucleus containing a bulky nucleolus, rinsed in a cytoplasm rich in organelles that provides fundamental cellular functions. These cells are on growing bone tissue's outer and inner surface [17].

- **Osteocytes** are osteoblasts in the last phase of differentiation, wholly imprisoned in the mineralized bone lattice. Fine cellular extensions allow them to be connected to cells on the surface of the bone trabeculae [18]. This network allows them to spread biochemical signals and mechanical stimulation. Osteocytes are also genuine mechanoreceptors sensitive to the stresses applied to the bone.

- **Bone lining cells** come from the same precursors as osteoblasts. They are osteoblasts that have gradually flattened to form an aligned cell layer along the bone surfaces. Lining cells line the bone matrix. In the process of bone resorption, they prevent access to osteoclasts involved in bone resorption. In extension, they create a reserve of osteoblastic cells, which, under the action of various factors, are capable of becoming active osteoblasts [19].

⇒ **The osteoclasts lineage** includes pre-osteoclasts which fuse to form mature osteoclasts. Mature osteoclasts are giant cells (100 µm in diameter) responsible for the resorption of bone tissue. They are rounded, prominent and contain several nuclei and cytoplasm [20].

1.2.3. The bone remodelling cycle

Bone is a living tissue in constant renewal. This phenomenon is called bone remodelling. It is regulated by hormonal factors, local factors, and mechanical stresses. Bone remodelling results from the activity of multiple cellular teams called BMU (Basal Multicellular Unit) [21]. In these units, two types of bone cells act coordinated: the osteoclasts, which resorb the old bone tissue and the osteoblasts, which form a new bone matrix. The processes of resorption and formation consequently ensure the stability of the bone tissue.

During the growth of a human being, bone formation is more significant than resorption, which allows the enlargement of the skeleton, while during old age, bone resorption accelerates. The bone then becomes less dense and more brittle. The renewal of adult bone tissue releases mineral salts that meet other tissues' calcium and phosphorus needs. It also makes it possible to reorganize the internal architecture of the skeleton by adapting it to the new mechanical constraints to which it is subjected during its life.

⇒ **The bone remodelling cycle** comprises several phases (**Figure 1.6**) [22]:

- **An activation phase** in which the osteocytes continuously send information signals to the adjacent cells of the bone surface die by apoptosis. The exchanges of signals from the osteocytes to the adjacent cells are then interrupted [23]. The lining cells then retract to expose the bone surface that needs to be shaped. The stromal cell and mesenchymal

stem cell differentiation into pre-osteoblasts. The stromal cells and pre-osteoblasts then express a ligand called RANKL. Afterward, the pre-osteoclasts from the medullary environment expressing the RANK receptors are attracted and bind to the osteoblastic lineage cells thanks to the RANK/RANKL bond [24,25]. This step led to the multiplication and fusion of pre-osteoclasts into a plurinucleate cell: a mature osteoclast.

- During the phase of resorption of bone tissue, this osteoclast has a wrinkled border, thanks to which it adheres to the surface of the bone. In three weeks, it creates a resorption gap of about 40 µm. The osteoclast is capable of secreting acids that will decalcify the bone and enzymes that will digest the collagen of the bone [26].

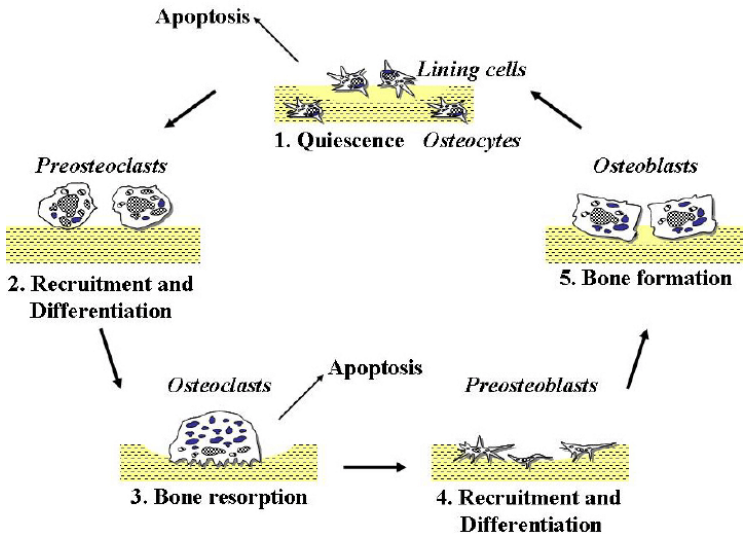

FIGURE 1.6 THE BONE REMODELLING CYCLE [22]

- Then comes the inversion phase, in which the osteoclast dies by apoptosis after having finished digging into the resorption gap. By digesting the bone, the osteoclast unearths growth factors buried during a previous remodelling cycle by the osteoblasts. Pre-osteoblasts multiply and differentiate into osteoblasts due to growth factors unearthed by osteoclasts [27].

- During the bone tissue formation phase, the osteoblasts then release a protein, osteoprotegerin, which binds to the RANK ligand, thus preventing the activation of osteoclasts differentiation [28]. As its name suggests, this protein protects the bone from excessive resorption. The osteoblasts thus line the bottom of the resorption gap. They

are then linked together by electrochemical junctions, allowing them to synthesize the bone matrix harmoniously. Osteoblasts release collagen microfibrils and alkaline phosphatase, an essential mineralization enzyme in the bone matrix. During filling, some osteoblasts (about 1/40) are immured in the bone matrix then differentiate into osteocytes. The bone formation phase lasts about 120 days. The remaining osteoblasts differentiate into bordering cells, thus completing the osteoblast life cycle. The osteocytes reconstitute their connection networks and the mineralization process takes its course and can last for several years. The osteoblastic lineage plays a key role early throughout the bone remodelling cycle.

- Once the volume of bone formed is equal to the one resorbed, the remodelling process stops. Then begins a quiescence phase, which is a phase of rest before a new start of a new cycle of bone remodelling.

A remodelling cycle lasts approximately 4 months in adults, the formation phase being more extended (3 months) than the resorption phase (1 month).

I.2. Bone reconstruction of the skull

2.1. Types of skull fractures

2.1.1. Simple linear skull fractures

Before introducing the most common type of fracture, it is essential to define a fracture. A break in the skull greater than 3 mm in width is qualified as a fracture. Often caused by a fall,

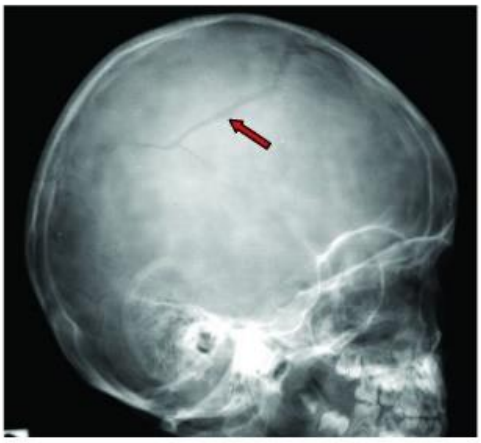

FIGURE 1.7 X-RAYS OF LINEAR RIGHT PARIETAL SKULL FRACTURE [29]

linear skull fractures are single fractures that extend through the thickness of skull bones (**Figure 1.7** [29]). They involve the temporal, parietal, frontal, or occipital bones.
If the linear fracture does not run through a suture of the skull, no interventions are necessary. In this case, the bone is capable of activating its natural regenerative process. This paragraph will describe the natural process of bone reparation at the fracture level. A fracture leads to both: the destruction of bone tissue and haemorrhage. If the lesions at the fracture site are small in volume, the bone can repair itself naturally. The regeneration/repair process of bone tissue is divided into three phases: the inflammatory phase, the repair phase, and the remodelling phase (**Figure 1.6**). The duration of this process depends on the injured person's age and state of health, and the injury's extent.

Here is a description of the bone fracture natural repair timeline illustrated in **Figure 1.8** [30]:

(A) In the first days following the fracture, the rupture of the blood vessels leads to the formation of a blood clot (haematoma) which is also quickly colonized by macrophages and reabsorbed. Then mesenchymal cells will form a secondary cartilaginous tissue in the center of the fracture.

(B) During the second process phase (the inflammatory phase), inflammatory cells are set up. Neovascularization is then stimulated at the periphery of the blood clot colonized by blood vessels. It thus contains signalling molecules that will initiate the formation of connective tissue and cartilaginous tissue, forming a "callus" and thus filling the fracture site. Different molecules are then secreted by immune cells (monocytes and lymphocytes) to stimulate the remodelling of the matrix [31].

(C) About a week later, the fracture repair phase allows stem cells at the fracture site to differentiate into fibroblasts and osteoblasts [32]. The provisional matrix then evolves into a fibrin-rich granular tissue. The whole of this structure evolves into a more organized structure called a calcified "callus". It is then gradually replaced by new cartilage.

(D) Several weeks after the fracture, remodelling occurs. In this phase, the bone is reorganized to restore the original site. An alternation of phases of resorption by

osteoclasts and formation by osteoblasts follows. This final phase of the process can take several months [33].

In practice, the repair of a minor fracture is favoured by immobilizing the bone fragments using plaster or surgical osteosynthesis. This repair requires 6 to 12 weeks, depending on the extent of the fracture.

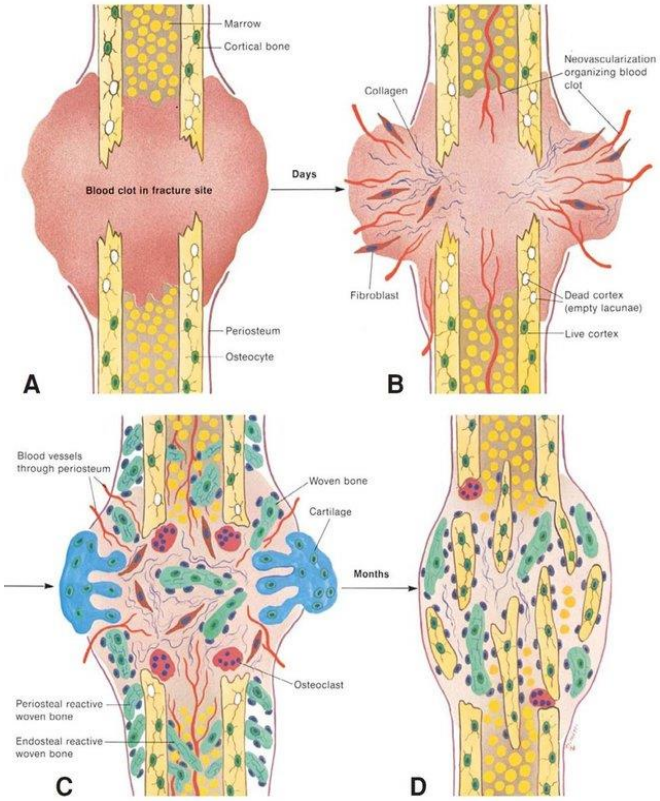

FIGURE 1.8 BONE FRACTURE HEALING TIMELINE [30]

Under certain circumstances, this natural self-healing process is ineffective. This is the case when biological or infectious problems prevent the fracture's consolidation. This process is also not applicable for losses of the bone substance of several centimeters (removal of tumors or cysts).

2.1.2. Skull fractures requiring surgical intervention

In the previous section, the linear skull fractures were described and did not require surgical intervention. However, other types of skull fractures, such as depressed, diastatic and basilar ones, require surgeons' intervention. In this case, the reconstruction of the bone must be assisted by bone implants. The whole issue of biomaterials rests on the skills of biologists, surgeons and

material specialists who will call on their knowledge to propose alternative techniques for reconstructing bone tissue. In the context of our study, it is therefore important to design cranial prostheses with good biological and mechanical properties for cranial repairs.

2.2. Craniofacial prostheses

2.2.1. A brief history of cranioplasty

The insertion of a prosthesis on the skull to fill a bone defect is a procedure that appeared back in the dawn of the history of medicine. Many materials were used for the design of cranial prostheses. This part describes the history of the various cranioplasty attempts made over time, from coconut to gold prostheses.

In pre-Columbian South America (3000 BC), the Aztecs, Mayans and Incas used different materials to fill the holes made during the skull trepanation [34]. Research on some pre-Inca mummies has revealed using gold, silver, coconut shells, or calabash (tropical tree fruit) for cranioplasty. Several old prostheses are preserved in museums; specifically, the most famous one (a gold plate on the skull) is kept in the Museum of Oro in Peru.

In Ancient Greece, this surgery was condemned by Hippocrates (460 BC – 370 BC) and Galen (129 BC – 216 BC). The practice of cranioplasty was discontinued until the 17th century, when Italian surgeons and anatomists Gabrielle Falloppio and Petronius commonly used gold plates to fill in bony defects [34].

In 1668, Dutch surgeon Job Hanszoon Van Meekeren performed the first dog skull xenograft to fill in the bone structure of a Russian soldier. The patient was cured but excommunicated due to animal bone transplantation. Then in 1742, the French physicist, botanist, and agronomist Henri Louis Duhamel Du Monceau discovered the osteogenic role of the periosteum. This discovery expanded knowledge to new avenues of bone reconstruction research.

It was only when the 19th century that the clinical utility of bone grafting was recognized. The German surgeon Philip Von Walther thus performed the first bone autograft in 1821. Then, in 1859, the clinician from Lyon, Louis Leopold Ollier was one of the pioneers in bone regeneration and joint surgery studies. He demonstrated the importance of the periosteum in

grafts. He also distinguished the notions of autograft, allografts and xenograft. A graft can be differentiated into:

- Autograft or autologous graft, when bone tissue is removed then re-implanted into the same body
- Allografts or homologous graft, when the tissue is removed from a donor, living or not, belonging to the same species as the recipient
- Heterograft or xenograft is when the tissue comes from a donor of a living species other than the recipient.

Louis Leopold Ollier formulated in 1897 his book *Experimental and Clinical Treaty of Bone Regeneration*, the first methodology of bone transplantation [35].

During the war period, the implantation of bone or cartilage tissue by another individual was intensively used. The French surgeon Henry Delagenière thus performed 104 cranioplasties with excellent results. During this period, the concept of sterility was developed with procedures such as boiling the bone or protecting it with alcohol and mercury. In 1945, L.F. Bush declared that bone could be kept sterile for up to 3 weeks at 2–5°C down to -25 °C [36].

Finally, at the end of the 19th century, the metallic bone substitutes (gold, aluminium, silver, lead, platinum, etc.) were gradually replaced by more modern and better-tolerated biomaterials (polymer, titanium, bioceramic).

2.2.2. Bone reconstruction techniques

Several bone reconstruction techniques are used in craniofacial surgery: grafts (allograft and autograft), osteogenic distraction and fillings using bone implants.

The autograft is the first-line cranial reconstruction technique, but its use is not always possible for two main reasons: the quantity of bone is limited and there is high morbidity (pain, blood loss and infection) linked to the engraftment [37]. Bone autografts have some limitations [38]. Indeed, depending on the bone replaced, the graft does not act immediately: for the cortical bone graft, there is an immediate loading and rapid restoration. However, for cancellous bone grafting, taking the graft is more complex and the risk of non-healing is not negligible [39]. On

the other hand, the allograft can cause the transmission of viral diseases and bacterial infections [40].

Osteogenic distraction is a surgical technique that aims to regenerate bone tissue under mechanical stimulation. This technique is very effective in the case of tissue defects. However, it is particularly long compared to other reconstruction techniques.

Research has thus focused on the chemistry of materials for developing cranial implants. This use is ideal in the case of hard tissue loss because the implants will immediately functionalize the injured bone with minimal risk of disease transmission. Implants can be classified into three categories based on the material used to manufacture them. Materials widely manufactured for cranial prostheses are polymers like poly (methyl methacrylate) (PMMA), ceramics (hydroxyapatite), and metals like titanium (Ti) [41,42].

Implants made of polymer materials are less fragile than ceramic substitutes. However, the mechanical strength of some polymers is insufficient to allow them to be mechanically loaded. They can be degraded by biological fluids and be toxic to the body [43]. Polymer bone substitutes are therefore manufactured to reconstruct non-mechanically loaded bone gaps (for example, to repair part of an injured skull).

Ceramic implants are essentially made of hydroxyapatite (HaP), tricalcium phosphate (TCP), or a mixture of these two materials [44]. The advantage of these bone substitutes is that they are bioresorbable. The bone will thus be able to replace the bone substitute. The resorption time of the implant is estimated at 1 year for TCP and between 2 and 5 years for HaP [45]. The disadvantage of ceramic implants is their fragility which can be dangerous in the event of a shock to the skull. In addition, the manipulation of these implants by surgeons can be very delicate.

Metal implants made of stainless steel or titanium are biocompatible and have very high strength, unlike ceramic and polymer substitutes. The main disadvantage of metallic materials is that they are not biodegradable [46-48]. Compared to the three materials, the metallic materials offer high mechanical resistance and can thus withstand the mechanical loads applied to the bone.

2.2.3. Specifications of craniofacial prostheses

The craniofacial skeleton is subjected to many mechanical stresses (compressive stresses, gravity, tensile stresses with mobilization of the head, masticatory muscle forces with intracranial muscle contractions, and shock stresses caused by trauma). Craniofacial bone reconstruction, therefore, involves a specific approach due to the polymorphism of the cranial bone structure and the stresses experienced by the craniofacial skeleton.

Thus, the design of prostheses must consider three fundamental points of view:

- The mechanical point of view: Due to the bone remodelling cycle described above, the reconstruction of the bone strongly depends on the mechanical environment in which the bone tissue evolves. During the placement of a cranial implant, the mechanical signals will be modified and affect the differentiation of bone cells. Thus, the elastic properties of the substitute must be close to those of the surrounding tissues to avoid the phenomenon of "stress shielding" which regularly leads to the detection of too rigid prostheses. The resistance of the implant is essential and must be at least equal to that of the bone it replaces to allow the restoration of the missing function.
- The physico-chemical point of view: The chemical properties of the implant's surface are essential. It is essential that the implant be bioactive so that it can establish chemical bonds with the surrounding tissues. The bone/implant interface interactions will be detailed in paragraph 1.3.
- The biological point of view: The implant must be biocompatible so that the substitute's durability is maximized and the bone cells can develop there.

I.3. Elaboration of functional craniofacial prostheses

3.1. Titanium

Titanium (Ti) is a non-magnetic material, occupying the 22nd position of the periodic table. It has an atomic mass of 47.9 g and is the fourth most abundant metal in the earth's crust. Ti was discovered in 1790 and its first use was as an additive paint to obtain white color paints. It was not until 1940 that American aeronautical specialists began to take an interest in the properties of this metal. After the second half of the twentieth century, Ti and its alloys began to be widely used in industry and the biomedical field, especially for replacing hard tissues.

Titanium is considered a material of choice for its intrinsic properties (Young's modulus, resistance to rupture, fatigue, resistance to corrosion and biocompatibility). Therefore, Ti plates are used mainly to build craniofacial prostheses. The intrinsic characteristics of titanium can be explained by the spontaneous formation of a superficial oxide layer that grows with its exposure to air. This amorphous layer 3 nm to 7 nm thick, mainly composed of Ti oxide (TiO_2), chemically stabilizes the material's structure [49–51].

Moreover, unlike some metallic materials, titanium does not experience corrosion that results in the release of ions. This is due to the formation of a very resistant protective oxide layer, with a thickness of the order of a few nanometers. This layer of TiO_2 protects the metal from chemical attacks, corrosion from chloride ions and biological fluids. **Figure 1.9** shows the structure of the oxide layer in contact with biological fluids [52].

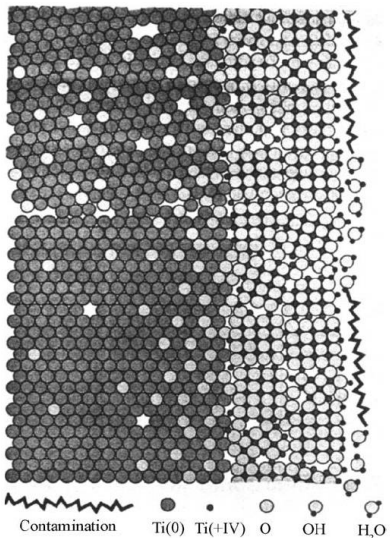

FIGURE 1.9 STUCTURE OF THE OXIDE LAYER [52]

Once titanium comes into contact with the biological medium, chemical and biochemical interactions occur: first, there is hydroxylation and hydration of the oxide, then adsorption of calcium and phosphate ions, for example, followed by adsorption of macromolecules such as proteins. This last step induces the formation of a biofilm which promotes the attraction of osteoblastic cells and consequently leads to tissue formation.

3.2. Bone/Implant interface

Our application must expose the biochemical aspect encountered at the bone/implant interface. Indeed, for the implant to be fully integrated into the human body and for its longevity to be as long as possible, it must be able to bond with the surrounding living tissues.

3.2.1. The different types of biological responses to implantation

Depending on the nature of the implanted material, the biological response will be different. Consequently, when surgeons' implants, there are 3 types of biological responses that classify the implants according to 3 categories (**Figure 1.10**):

1) A bio-tolerant implant = an inflammatory process resulting in the development of a fibrous capsule. The implant is surrounded by fibrous tissue, detaching it from the bone tissue and causing the implant to loosen [53]. This is the case for materials that release toxic products. This is also the case when the mechanical loads between the bone and the implant are not well distributed. The micro-movements prevent the anchoring of the implant, and the cells fail to recognize it. The cells disconnect the implant from the surrounding tissue by creating a fibrous capsule around it. This is why an implanted bone area must be perfectly inactive during the first months following the implantation of the prosthesis (immobilization of the area).

2) A bioinert implant = direct contact between the bone and the implant's surface. This is the case for untreated titanium and its alloys.

3) A bioactive implant = bone bond between the implant and the bone tissue. This is the case with hydroxyapatite and the different strategies used to functionalize titanium surfaces (modification of surface morphological properties / physical and chemical modifications).

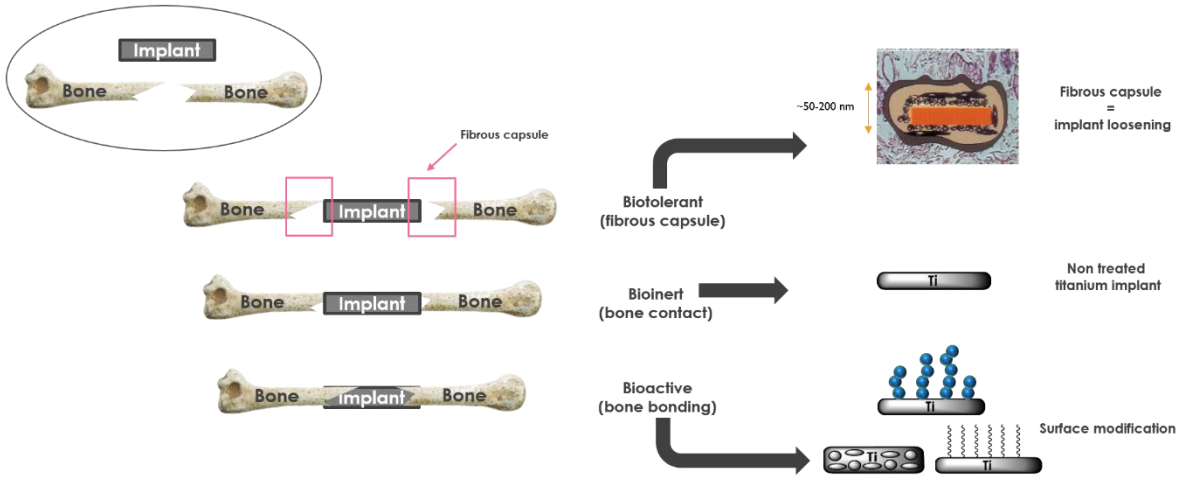

FIGURE 1.10 TYPES OF IMPLANTS' BIOLOGICAL RESPONSES — ADAPTED FROM [53]

3.2.2. Mechanisms occurring at the bone/implant interface

When bone cells are brought into contact with a material, they must adhere then spread out on its surface. A good understanding of the adhesion of osteoblasts to the material is essential to optimize the interface. Indeed, the first biological reaction which takes place after the implantation of a foreign body is the adsorption of the proteins present in the physiological fluid of the tissue. Knowing the extracellular matrix (ECM) composition secreted by the cells is important. This matrix is made up of several proteins (elastin, osteopontin), proteoglycans and glycoproteins (collagen, fibronectin, vitronectin, thrombospondin). All these molecules are deposited directly on the implants and interact with the surface of the implant and the cell membrane receptors.

The adhesion process takes place in several stages [54]:

1) The rapid adsorption of serum proteins on the surface forms a layer 2–5 nm thick. This step is fundamental because it represents the accurate contact between the living system and the material, and the nature of the interactions that will develop between the protein and the material will have consequences on the subsequent evolution of the cell ;

2) Cell contact with the protein layer ; this attachment phase appears quickly and generates short-term processes such as physico-chemical links between cells and material, which bring into play ionic forces, Van der Waals forces.

3) Cell attachment to the protein layer, which leads to long-term adhesion. At this stage, organic matrix proteins (EMCs), cell membrane proteins, and cytoskeletal proteins interact to induce a transcription signal and consequently modify the expression of the genes involved.

The interactions developed between proteins and the surface of materials are of the ionic, hydrophobic and hydrogen types.

Thus, the first phase of cell attachment, adhesion and distribution depend on the initial adhesion of proteins from bone tissue. The quality of this first step will determine the morphology of the cells and their ability to proliferate and differentiate. This is why the choice of the surface of the material and the characteristics of the surface thereofore must be judicious.

3.3. Titanium functionalization strategies

3.3.1. Surface modifications techniques and their recent development

To obtain an implant system that meets the human body's requirements, the physical and chemical properties of the materials of the outer layer of the materials must be controlled. As mentioned earlier, titanium-based materials can create a protective oxide layer in contact with oxygen. Unfortunately, this spontaneously formed passive film is not entirely ideal for biomedical uses. It is very thin and has a heterogeneous formation tending to disappear when rubbed. In this case, it causes the diffusion of the Ti oxide towards the biological medium, which will then act as abrasive elements. All these phenomena prevent the chemical adhesion of the implant to the biological material [49–52], which can even cause loosening of the implant years after implantation.

Thus, the surface properties of an implant are an essential element for its performance in the body. This, therefore, results in functionalization strategies to create conditions favourable to cellular activity on the titanium surface to integrate the implant into the body while retaining the material's intrinsic properties.

There are 4 leading families of surface modifications:

- Morphological modification (roughness, porosity) involves mechanical treatments [55].
- Chemical modification is a field that is very broad and uses different methods. For instance, acid and alkaline treatments make it possible to obtain an oxide layer of variable thickness on the surface and increase the quantity of $Ti-OH$ groups. Electrochemical treatments (anodic oxidation) also lead to obtaining a chemical oxide layer on the surface, but with the advantage of controlling the thickness. Deposition by chemical vaporization [56] gives rise to chemical reactions between entities in the gaseous state and the surface of the titanium, thus obtaining a deposit of a non-volatile compound on the surface.
- The biochemical modification groups together the methods that will make it possible to graft peptide sequences or proteins, hydroxyapatite, onto the titanium surface.
- Modification of a physical nature such as heat treatment, electron beam [57], laser [58], shock [59] or plasma treatment [60].

The covalent grafting method is preferable because the materials are more stable and there is less risk of releasing molecules.

3.3.1.1. Covalent grafting techniques

The modification of titanium surfaces by a thin layer of polymer is a particularly interesting technique for modulating the surface properties of the substrate. This technique makes it possible to introduce new functions on the surface that will improve certain properties of titanium. This modification of the Ti surface can be done either directly by using the "grafting from" method or indirectly by using the "grafting to" method.

Biocompatibility and biointegration on implanted prosthetic materials represent a major problem of public health. To combat these problems, solid surfaces modification is required. An alternative that is becoming more and more recurrent nowadays is the physisorption or the grafting of biomolecules or/and bioactive polymers. The use of bioactive polymers has been shown to be an excellent solution. Tethering of bioactive polymers to a surface has emerged as promising tool to tailor surface properties. Polymer brushes can be immobilized on appropriate surfaces using either a physisorption (chain attachment mainly through van der Waals interactions) or a covalent strategy (anchoring by chemical bonds). Although the physisorption

technique has been used to modify polymers and metallic surfaces, they suffer from the drawbacks inherent to their non-permanent nature: the release of polymers from such modified surfaces and the subsequent loss of activity potentially makes them unsuitable for most biomedical applications. So, it is important for polymers to be covalently immobilized on the surface. Covalent grafting [61-63]. (**Figure 1.11**) is one type of surface modification that offers the strongest link between the biomaterial and its coating, producing a more durable interface. Several techniques for covalently grafting of biomolecules and/or bioactive molecules onto titanium surfaces were developed, including covalent attachment of end-functionalized polymers incorporating an appropriate anchor ("grafting to") [63] or in-situ polymerization initiated from the surface ("grafting from"). [61,62].

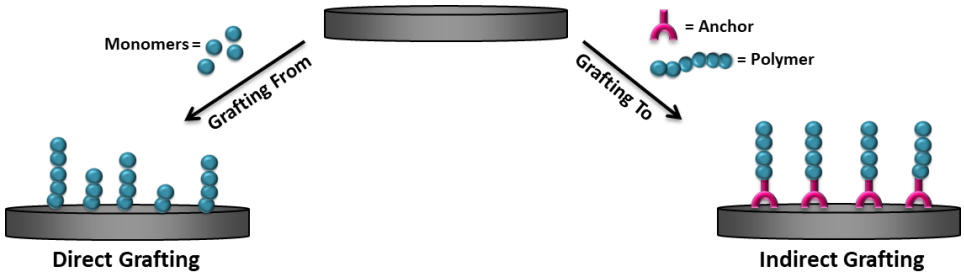

FIGURE 1.11 SCHEMATIC DESCRIPTION OF THE "GRAFTING FROM" AND "GRAFTING TO" PROCESSES

The "grafting to" method (**Figure 1.11**) involves reaction of (end)-functionalized polymer molecules with complementary functional groups located on the surface, resulting in the formation of tethered chains. If a surface that is to be modified does not possess the necessary functionalities, several techniques can be used for initial surface functionalization or immobilize anchors onto the solid surface, including plasma treatments, self-assembled monolayer (SAM) deposition or chemisorption of thin layer of reactive polymers. End-functionalized polymers with a narrow molecular weight distribution can be synthesized by living anionic, cationic, radical, group transfer and ring opening metathesis polymerizations. Afterwards, the functional groups of polymers can be involved in further chemical reactions to attach polymers on anchors.

The "grafting from" (**Figure 1.11**) approach has attracted considerable attention in recent years in the preparation of tethered polymers on a solid substrate surface. The initiators are immobilized onto the surface followed by *in situ* surface-initiated polymerization (non-controlled or controlled polymerization) generate tethered polymers. The immobilization of

initiators on the substrate surface can be achieved with plasma, UV irradiation or ozone treatment of the surface.

Previous studies carried out in the LBPS laboratory have shown that the grafting of bioactive polymers such as polyNaSS was successful by using radicals issued from titanium peroxides able to initiate the radical polymerization of sodium styrene sulfonate (NaSS) monomer. [61,62] Oxidation of titanium creates titanium peroxides at the surface; which, under heating, produce radicals to initiate the polymerization of ionic monomer NaSS (**Figure 1.12**). The drawback of this method is the long polymerization times (15 hrs). To this end, this study demonstrates the use of UV irradiation to decrease the polymerization time.

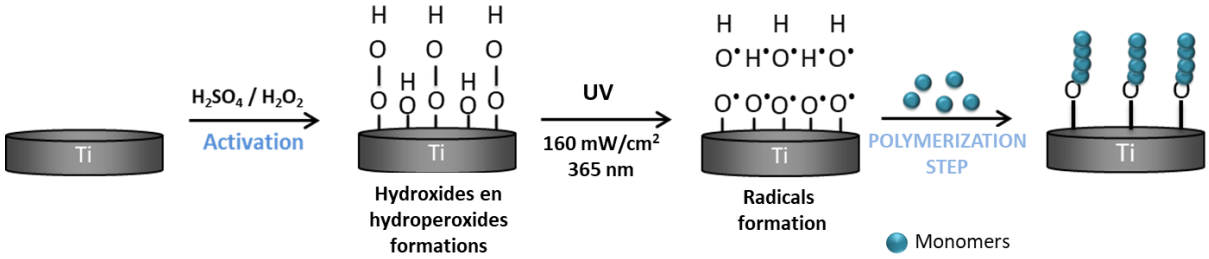

FIGURE 1.12 "GRAFTING FROM" APPROACH USING UV IRRADIATIONS

UV irradiation has been used to initiate radical graft polymerization of bioactive compounds on polymer surfaces [64]. When exposed to UV light, polymer surfaces generate reactive sites which can be used to initiate graft polymerization. For example, UV irradiation has been used to introduce carboxylic acid functionality to PMMA [65], as well as to activate polystyrene surfaces for cell tissue [66]. Chemical modification using UV irradiation is an easy process that can also be used as a suitable alternative due to its low cost and fast reaction rate.

3.4. Innovative Titanium/Polymer hybrid materials

In the biomedical field, the significant difference in the mechanical properties between the implants and the surrounding tissues results in stress shielding which is detrimental for load-bearing tissues [67]. The current study aimed at developing new layered sandwich materials able to attenuate this stress shielding effect. Sandwich materials, composed of two metallic skin sheets and a polymer core can be an interesting alternative to design innovative biomedical prostheses [68]. They are employed in the aircraft, automotive and naval industry because of

their high acoustic and damping capacity [69,70], high stiffness and strength, good formability and lightweight [71]. In these systems, an epoxy resin is commonly used as adhesive agent to stick the polymer core onto the metal skinsheets ensuring the bonding between the two components. The toxicity of this adhe-sive layerevidently prevents their application in the biomedical field. Nevertheless, in previous work [72], it was shown that, following the rule of mixtures, the mechanical properties of the whole sandwich can be tailored according to the skin and core thickness achieving structures able to decrease the bio-mechanical impairment existing between the bone and the implant. Moreover, they possess a good formability which is essential to build up complex shape, as required in the fabrication of prostheses. Thus, in order to extend the applications of sandwich materials in the biomedical field, the challenge of this work was to incorporate a polymer component between two metal substrates in order design innovative epoxy resin-free sandwich materials able to attenuate stress-shielding effects. In addition, recently grafted polymers (i.e., polymer chains with an extremity covalently bound to a substrate) were proposed as adhesives to be inserted between a metal substrate and a polymer coating requiring to be linked in order to improve the metal-polymer adhesion strength [73-79].

In this context, the idea was to employ surface-confined polymers to fabricate biocompatible resin-free sandwich materials by sticking the polymer core of the structure on the metallic skins previously coated with grafted polymer chains. As proof of concept, titanium (Ti) and poly methyl meth-acrylate (PMMA), the most extensively materials used for biomedical applications, were employed and Ti/PMMA/Ti sandwiches produced. Therefore, surface-confined PMMA chains replaced the epoxy resin layer and the adhesion between thetethered chains and those of the adhering PMMA foil (used as core material) was established by exploiting their miscibility, through the formation of entanglements. In particular, the PMMA chains were grown on ad-hoc activated Ti surfaces, by usinf the grating to or the “grafting from” method. In this way, PMMA chains were grown on Ti surfaces and resin-free sandwiches were prepared by hot-pressing. A PMMA foil (0.5 mm thick) was inserted between two PMMA-coated Ti surfaces by pressing togetherall the three components above the glass transition temperature of the polymer.

So, the solution proposed within the ANR DFG with our Strasbourg and German partners is to functionalize the titanium and the polymer to overcome the use of epoxy glue. For this, the IPCMS team has developed Ti/polymer interfaces in which a covalent bond links the titanium and the polymer. In this project, our team works on the functionalization of the external part of the sandwich to confer biological properties (**Figure 1.13**). The objective is to design a material that meets the two problems = mechanical properties and properties aimed at improving the bone grip of the implant.

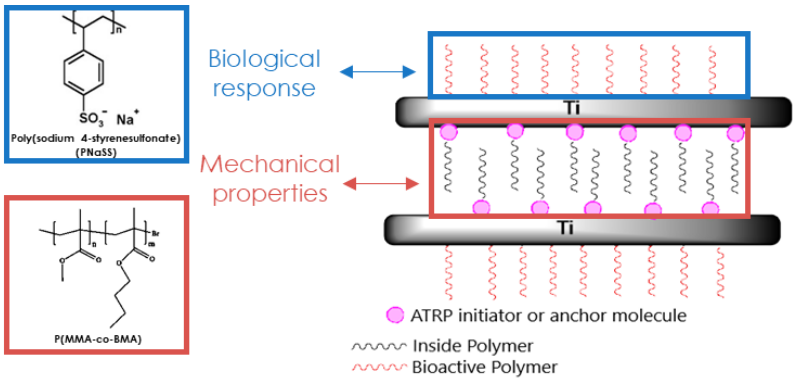

FIGURE 1.13 ELABORATION OF BIOACTIVE SANDWICH STRUCTURE TI/PMMA/TI

3.4.1. Functionalization of the external part: grafting phophonic acids

Before presenting the characteristics of phosphonic acids, it is important to remember that phosphorus is an element that constitutes approximately 0.04% of the atomic composition of the earth's crust [80]. Lipids, nucleic acids or even bone tissues are composed of phosphorus. Phosphorus therefore arouses great interest in the chemistry of living organisms.

Organophosphorus compounds have at least one phosphorus atom bonded directly to a carbon atom. In solution, these compounds exist as a balance of two tautomeric forms: a tetra-coordinated pentavalent form (phosphonate form) and a tri-coordinated trivalent form (phosphite form). The phosphonic acid function is characterized by a phosphorus atom bearing 3 oxygen atoms (1 P=O double bond and two hydroxy OH groups) as well as a PC bond. The length of the P=O double bond is shorter than the PO and PC bonds. For example, for methylphosphonic acid, the P=O bond is 1.4993 Å long, while the PO bonds are 1.5441 Å and 1.5442 Å long. The PC link, on the other hand, has a length of 1.7586 Å [81]. The bond energies are respectively 586 kJ/mol for the P=O bond, 360 kJ/mol for the PO bonds and 272 kJ/mol for the PC bond [82].

By analogy to sulphonic acids, phosphonic acids are strong acids. They have two acid protons presenting, for example when the R group is an aromatic, a first acidity with a pKa between 1.1-2.3 and a second acidity whose pKa is between 5.3-7.2 [83]. The pKa values strongly depend on the electronic properties induced by the R substituent. The phosphonic acid derivatives are more acidic (about 1.9 to 2.9 pKa units below) than those derived from the carboxylic acid. Due to its acidity, the phosphonic acid function is present in its ionized form over a wide pH range in an aqueous medium. The acidic nature of phosphonic acids makes it possible to increase the water solubility of organic compounds [84,85], polymers [86,87] or ligands for coordination chemistry [88].

The second interesting characteristic of phosphonic acids is their facility to create hydrogen bonds. Phosphonic acids are thus able to generate self-assembled supramolecular structures [89]. This supramolecular behavior allows the development of organic materials exhibiting proton conduction [90]. The third important characteristic of phosphonic acids comes from their coordination properties. Indeed, the three oxygen atoms can be engaged in coordination or iono-covalent bonds. These coordination properties allow the design of hybrid molecular materials.

Furthermore, the phosphonic acid function has the particularity of mimicking the phosphate group which is omnipresent in nature. The main difference between phosphate and phosphonic acid stems from the greater stability (resistance to enzymatic degradation) of the PC bond compared to the PO bond present in phosphate [91]. Thus, phosphonic acids are used in many applications in biology and medicine to mimic the phosphate group.

I.4. Bibliographical summary

Chapter I provided an update of the state of the art in the field of craniofacial bone reconstruction.

At the end of this bibliographic study, the following points can be summarized and noted:

- The difficulty of self-healing of the cranial bones.
- Although the autograft currently represents the gold standard for the rupture of a bone, the major disadvantages are the morbidity of the sampling site and a rehabilitation that can be long and expensive.
- Many synthetic implants with different designs and materials have been developed since the 1950s. Titanium stands out from all materials – sandwich structure. The chapter I shows the

importance to develop the functionalization by different bioactive polymers carrying sulfonate and phosphonate groups in order to improve the biological response of sandwich structures.

I.5. References

[1] C. Mabit Cours d'anatomie tête et cou. Faculté de Médecine de Limoges; 2003.

[2] P. Bonfils, J-M. Chevalier Anatomie ORL. 2ième ed. Médecine-Sciences Flammarion; 2005.

[3] J. Godon Betts Anatomy and Physiology; 2013.

[4] PH. Lefevre, J.P. Beauthier, M. Meunier, R. Orban, C. Polet, M. Rooze « Comparaison et fiabilité de la région du ptérion par rapport aux sutures ectocrâniennes classiques dans l'estimation de l'âge osseux ». Biom. Hum. et Anthropol., 2005, vol. 23, N° 1-2, pp. 15-22.

[5] B. Autuori "Modélisation par éléments finis de la face humaine en vue de la simulation de sa réponse au choc". Thèse en génie mécanique. Lyon: Institut National des Sciences Appliquées de Lyon, 2004, 268 p.

[6] http://amar-constantine.e-monsite.com/pages/cours-pour-autres-specialites/anatomie-physiologie/osteologie.html

[7] E. Rollet Anatomie des sinus de la face. 1902nd ed. Hachette Livre; 2013.

[8] https://aftc-gironde.org/site/anatomie/les-os-du-crane/

[9] M. Kutz, Bone Tissue. In: Biomedical Engineering and Design Handbook. MacGraw Hill. 2nd edition, vol.1. 2009.

[10] M.H. Ross, W. Pawlina Bone. In: Hostology, a Text and Atlas. Lippincott Williams & Wilkins: Wolters Kluwer. 6th edition. p.202-237.

[11] T. Thomas, A. Martin, M.-H. Lafage-Proust Physiologie du tissu osseux. EMC, Appareil locomoteur 2008 , 14-002-B-10.

[12] A.H.R.W Simpson,. The Blood Supply of the Periosteum: Plast. Reconstr. Surg. 1986, 78, 548.

[13] J.Y. Wu, D.T. Scadden, H.M. Kronenberg Role of the osteoblast lineage in the bone marrow hematopoietic niches. J Bone Miner Res. 2009 May;24(5):759-64.

[14] B. Clarke, Normal Bone Anatomy and Physiology. Clin. J. Am. Soc. Nephrol. 2008, 3, S131–S139.

[15] R.D. Chapurlat L'ostéoporose. J. Libbey Eurotext; 2003

[16] P.G. Robey, N.S. Fedarko, *et al.* Structure and molecular regulation of bone matrix proteins. J Bone Miner Res. 1993;8:483-487.

[17] L.F Bonewald, M.L. Johnson, Osteocytes, Mechanosensing and Wnt Signaling. Bone 2008, 42, 606–615.

[18] R. Civitelli Cell-cell communication in the osteoblast/osteocyte lineage. Arch Biochem Biophys. 2008 May 15;473(2):188-92.

[19] B.R. Troen Molecular mechanisms underlying osteoclast formation and activation. Exp Gerontol. 2003 Jun;38(6):605-14.

[20] N. Kohli, S. Ho, S.J. Brown, P. Sawadkar, V. Sharma, M. Snow, *et al.* Bone remodelling in vitro: Where are we headed?: -A review on the current understanding of physiological bone remodelling and inflammation and the strategies for testing biomaterials in vitro. Vol. 110, Bone. Elsevier Inc.; 2018. p. 38–46

[21] R.L. Jilka Biology of the basic multicellular unit and the pathophysiology of osteoporosis. Medical and Pediatric Oncology [Internet]. 2003 Sep 1 [cited 2020 Jun 18];41(3):182–5. Available from: http://doi.wiley.com/10.1002/mpo.1033

[22] T. Negishi-Koga, M. Shinohara, N. Komatsu, H. Bito, T. Kodama, R.H. Friedel, *et al.* Suppression of bone formation by osteoclastic expression of semaphorin 4D. Nat Med. 2011;17(11):1473-80.

[23] S. Khosla, Minireview: The OPG/RANKL/RANK System. 6.

[24] M. Pérez-Sayáns, J.M. Somoza-Martín, F. Barros-Angueira, J.M.G. Rey, , A. García-García RANK/RANKL/OPG Role in Distraction Osteogenesis. Oral Surg. Oral Med. Oral Pathol. Oral Radiol. Endodontology 2010, 109, 679–686, doi:10.1016/j.tripleo.2009.10.042.

[25] R. Baron, L'ostéoclaste et les mécanismes moléculaires de la résorption osseuse. médecine/sciences 2001, 17, 1260–1269.

[26] P. Marie, P. Halbout OPG/RANKL : implication et cible thérapeutique dans l'ostéoporose. Med Sci (Paris) 2008; 24 : 105–10.

[27] M. Cohen-Solal, M.-C. de Vernejoul, Remodelage osseux, Therapies. 58 (2003) 391–393.

[28] A. Ciurea, M. Gorgan, A. Tascu, A. Sandu, R. Rizea, Traumatic brain injury in infants and toddlers, 0–3 years old, Journal of Medicine and Life. 4 (2011) 234–43.

[29] S. D. Strayer, E. Rubin, J. E. Saffitz, A. L. Schiller. Rubin's Pathology: Clinicopathologic Foundations of Medicine [Internet]. 7th edition. Available from: https://books.google.fr/books/about/Rubin_s_Pathology.html?id=jS2MAwAAQBAJ&redir_esc=y

[30] L. Claes, S. Recknagel, A. Ignatius Fracture healing under healthy and inflammatory conditions. Vol. 8, Nature Reviews Rheumatology. 2012. p. 133–43.

[31] L. Marzona, B. Pavolini Play and Players in Bone Fracture Healing Match. Clinical Cases in Mineral Bone Metabolism. 2009;6(2):159–62.

[32] A. Ho-Shui-Ling, J. Bolander, LE Rustom, AW Johnson, FP Luyten, C. Picart Bone regeneration strategies: Engineered scaffolds, bioactive molecules and stem cells current stage and future perspectives. Vol. 180, Biomaterials. Elsevier Ltd; 2018. p. 143–62.

[33] D.W. Murray, J. Wilson-MacDonald, E. Morscher, BA Rahn, M. Käslin Bone growth and remodelling after fracture. J Bone Joint Surg Br. 1996 Jan;78(1):42-50.

[34] Sanan A, Haines SJ. Repairing holes in the head: a history of cranioplasty. Neurosurgery. 1997 Mar;40(3):588–603.

[35] L. Ollier Traité expérimental et clinique de la régénération des os et de la production artificielle du tissu osseux. Victor Masson et fils; 1897.

[36] G.M. Calori, E. Mazza, M. Colombo, C. Ripamonti The use of bone-graft substitutes in large bone defects: Any specific needs? Injury: International Journal of the Care of the Injured. 2011. 42(2): S56-S63.

[37] M.E. Elsalanty, D.G. Genecov Bone grafts in craniofacial surgery. Craniomaxillofac Trauma Reconstr. 2009 Oct;2(3):125-34.
[38] R. Betz, Limitations of Autograft and Allograft: New Synthetic Solutions. Orthopedics. (2002). 25. s561-70.
[39] T.C. Origitano et al., Skull base surgery, 5 (2), 109 , (1995).
[40] Y. Ducic, Journal of Oral and Maxillofacial Surgery, 60 (3), 272, (2002).
[41] D. Puppi, F. Chiellini, A.M. Piras, E. Chiellini Polymeric materials for bone and cartilage repair. Progress in Polymer Science. 2010. 35(4): 403-440.
[42] G. Hannink, JJC. Arts Bioresorbability, porosity and mechanical strength of bone substitutes: What is optimal for bone regeneration? Injury: International Journal of the Care of the Injured. 2011. 42(2):22-25.
[43] M. Peroglio, L. Gremillard, J. Chevalier, L. Chazeau, C. Gauthier, T. Hamaide Toughening of bio-ceramics scaffolds by polymer coating. Journal of the european Ceramic Society. 2007. 27(7): 2679-2685.
[44] P. Lichte, H.C. Pape, T. Pufe, P. Kobbe, H. Fischer Scaffolds for bone healing: Concepts, materials and evidence. Injury: International Journal of the Care of the Injured. 2011. 42(6): 569-573.
[45] Branemark P.-I., Hansson B., Adell R., Breine U., Lindstrom J., Hallen O. and Ohman A., "Osseointegrated implants in the treatment of the edentulous jaw. Experience from a 10-year period.", Scandinavian journal of plastic and reconstructive surgery, 1977, 11, 1-132.
[46] Albrektsson T., Brånemark P.-I., Hansson H.-A. and Lindström J., "Osseointegrated Titanium Implants: Requirements for Ensuring a Long-Lasting, Direct Bone-to-Implant Anchorage in Man.", Acta Orthopaedica, 1981, 52, 155-170.
[47] Albrektsson T. and Johansson C., "Osteoinduction, osteoconduction and osseointegration", European Spine Journal, 1-10-2001, 10, 0, S96-S101.
[48] Schuler M., "Morphology and Motility of Osteoblast Cells on Peptide- Modified Titanium Surfaces", thèse de l'Université de Zurich, 2003, 1-55.
[49] Textor M., Sittig C., Frauchiger V., Tosatti S. and Brunette D.M., "Properties and biological significiance of natural oxide films on titanium and its alloys",Titanium in Medecine, 2001, Springer's, chapter 7, 171-230.
[50] D.G. Castner, B.D. Ratner, Surf. Sci. 500 (2002) 26-60.
[51] Ratner BD, Hoffman AS, et al. Biomaterials science: an introduction to materials in medicine. In: Elsevier Academic Press. 2nd edition. 2004.
[52] Elias C.N., Oshida Y., Lima J.H.C. and Muller C.A., "Relationship between surface properties (roughness, wettability and morphology) of titanium and dental implant removal torque", Journal of the Mechanical Behavior of Biomedical Materials, 2008, 1(3), 234-242.
[53] Das K., Bose S. and Bandyopadhyay A., "Surface modifications and cell-materials interactions with anodized Ti", Acta Biomaterialia, 2007, 3(4), 573-585.
[54] Casaletto M.P., Ingo G.M., Kaciulis S., Mattogno G., Pandolfi L. and Scavia G., "Surface studies of in vitro biocompatibility of titanium oxide coatings", Applied Surface Science, 2001, 172(1-2), 167-177.

[55] Heinl P., Müller L., Körner C., Singer R.F. and Müller F.A., "Cellular Ti-6Al-4V structures with interconnected macro porosity for bone implants fabricated by selective electron beam melting", Acta Biomaterialia, 2008, 4(5), 1536-1544.

[56] Huang H.H., Chuang Y.C., Chen Z.H., Lee T.L. and Chen C.C., "Improving the initial biocompatibility of a titanium surface using an Er,Cr:YSGG laser-powered hydrokinetic system", Dental Materials, 2007, 23(4), 410-414.

[57] Gotz H.E., Muller M., Emmel A., Holzwarth U., Erben R.G. and Stangl R., "Effect of surface finish on the osseointegration of laser-treated titanium alloy implants", Biomaterials, 2004, 25(18), 4057-4064.

[58] Den Braber E.T., Smits H.TJ., Ginsel L.A., von Recum A.F., Jansen J.A. and de Ruijter J.E., "Effect of parallel surface microgrooves and surface energy on cell growth", Journal of Biomedical Materials Research, 1995, 29(4), 511-518.

[59] Le Guehennec L., Soueidan A., Layrolle P. and Amouriq Y., "Surface treatments of titanium dental implants for rapid osseointegration", Dental Materials, 2007, 23(7), 844-854.

[60] Huang N., Yang P., Leng Y.X., Wang J., Sun H., Chen J.Y. and Wan G.J., "Surface modification of biomaterials by plasma immersion ion implantation", Surface and Coatings Technology, 2004, 186(1-2), 218-226.

[61] H. Chouirfa, D. M. Evans, P. Bean, A. Saleh-Mghir, A.-C. Crémieux, D. G. C. Castner, C. Falentin-Daudré and V. Migonney, ACS Appl. Mat. Interfaces 10, 1480 (2018).

[62] H. Chouirfa, V. Migonney, and C. Falentin-Daudré, RSC Adv. 6, 13766 (2016).

[63] H. Chouirfa, M. Evans, D. Castner, P. Bean, D. Mercier, A. Galtayries, C. Falentin-Daudré and V. Migonney, Biointerphases 12, 02C418 (2017).

[64] C. Falentin-Daudré, V. Migonney, H. Chouirfa, and J. S. Baumann, WO patent PCT/EP2016/068909 (August 7th, 2015).

[65] C. Situma, Y. Wang, M. Hupert, F. Barany, R. L. McCarley,S. A. Soper, Anal. Biochem., 2005, 340, 123-135.

[66] A. Welle, S. Horn, J. Schimmelpfeng, D. J. Kalka, Neurosci. Meth., 2005, 142, 243-250.

[67] M.I.Z.Ridzwan, S. Shuib, A.Y. Hassan, A.A. Shokri, M.N.M. Ibrahim, “Problem of Stress Shielding and Improvement to the Hip Implant Designs: A review”, Journal of Medical Sciences, vol. 7, pp. 460-467, 2007

[68] M. Harhash, A. Carradò, and H. Palkowski, “Lightweight titanium/polymer/titanium sandwich sheet for tech-nical and biomedical application,” Materialwissenschaft und Werkstofftechnik, vol. 45, no. 12, pp. 1084-1091, 2014.

[69] Y. S. Chen, T. J. Hsu, S. I. Chen, “Vibration damping characteristics of laminated steel sheet”, Metallurgical transactions A, vol. 22, no. 3, pp. 653-656, 1991.

[70] E. Bernd, J. Buhl, “Metal Forming of Vibration-Damping Composite Sheets”, Steel Research International, vol. 82, no. 6, pp. 626-631, 2011.

[71] B. Harris, “A perspective view of composite materials development,” Materials & Design, vol. 12, no. 5, pp. 259-272, 1991.

[72] G. D. Parfitt, Adsorption from solution at the solid/liquid interface. Academic Pr, 1983.

[73] L. Librescu and T. Hause, “Recent developments in the modeling and behavior of advanced sandwich constructions: a survey,” Composite structures, vol. 48, no. 1, pp. 1-17, 2000.

[74] O. A. Sokolova, A. Carradò, and H. Palkowski, “Metal–polymer–metal sandwiches with local metal rein-forcements: A study on formability by deep drawing and bending,” Composite Structures, vol. 94, no. 1, pp. 1-7, 2011.

[75] C. Sun, F. Zhou, L. Shi, B. Yu, P. Gao, J. Zhang, and W. Liu, “Tribological properties of chemically bonded polyimide films on silicon with polyglycidyl methacrylate brush as adhesive layer,” Applied Surface Science, vol. 253, no. 4, pp. 1729-1735, 2006.

[76] Y. Shaulov, R. Okner, Y. Levi, N. Tal, V. Gutkin, D. Mandler, A. J. Domb, “Poly (methyl methacrylate) grafting onto stainless steel surfaces: application to drug-eluting stents”.ACS applied materials & interfaces, vol. 1, no. 11, pp. 2519-2528, 2009.

[77] K. Shimizu, K. Malmos, A. H. Holm, S. U. Pedersen, K. Daasbjerg, and M. Hinge, “Improved adhesion between PMMA and stainless steel modified with PMMA brushes,” ACS Applied Materials & Interfaces, vol. 6, no. 23, pp. 21308-21315, 2014.

[78] K. Shimizu, K. Malmos, S. A. Spiegelhauer, J. Hinke, A. H. Holm, S. U. Pedersen, K. Daasbjerg, and M. Hinge, “Durability of peek adhesive to stainless steel modified with aryldiazonium salts,” International Journal of Adhesion and Adhesives, vol. 51, pp. 1–12, 2014.

[79] O. Alageel, M.-N. Abdallah, Z. Y. Luo, J. Del-Rio-Highsmith, M. Cerruti, and F. Tamimi, “Bonding metals to poly (methyl methacrylate) using aryldiazonium salts,” Dental Materials, vol. 31, no. 2, pp. 105-114, 2015.

[80] R. Dubrisay, P. Pascal, Nouveau traité de chimie minérale, 10, 715-717,(1956).

[81] H. Reuter, M. Reichelt, Methyl-phospho-nic acid, CH3PO(OH)2. Acta Crystallogr., Sect. E: Struct. Rep. Online 2014, 70, o353.

[82] S. Maiti, S. Banerjee, S.R. Palit, Phosphorus-containing polymers. Prog. Polym. Sci. 1993, 18, 227–261.

[83] R. G. Franz, Comparisons of pKa and log P values of some carboxylic and phosphonic acids: synthesis and measurement. AAPS PharmSci 2001, 3, 1–13.

[84] S. R. LaBrenz, H. Bekele, J. W. Kelly, Tetrahedron 1998, 54, 8671–8678.

[85] J. Jiang, E. Yang, K. R. Reddy, D. M. Niedzwiedzki; C. Kirmaier; D. F. Bocian; D. Holte; J. S. Lindsey, “Synthetic Bacteriochlorins Bearing Polar Motifs (Carboxylate, Phosphonate, Ammonium and a short PEG). Water-Solubilization, Bioconjugation, and Photophysical Properties,” New J. Chem. 2015, 39, 5694–5714.

[86] B. L. Rivas, E. Pereira, P. Gallegos, D. Homper, K. E. Geckeler, J. Appl. Polym. Sci. 2004, 92, 2917–2922.

[87] F. Lebouc, I. Dez, M. Gulea, P.-J. Madec, P.-A. Jaffrès, Phosphorus, Sulfur Silicon Relat. Elem. 2009, 184, 872–889.

[88] T. L. Schull, J. C. Fettinger, D. A. Knight, Inorg. Chem. 1996, 35, 6717–6723.

[89] G. B. Hix, V. Caignaert, J.-M. Rueff, L. Le Pluart, J. E. Warren, P.-A. Jaffrès, Cryst. Growth Des. 2007, 7, 208–211.

[90] L. Jiménez-García, A. Kaltbeitzel, V. Enkelmann, J. S. Gutmann, M. Klapper, K. Müllen, Adv. Funct. Mater. 2011, 21, 2216–2224.

[91] J.-M. Rueff, M. Poienar, A. Guesdon, C. Martin, A. Maignan, P.-A. Jaffrès, J. Solid State Chem. 2016, 236, 236–245.

CHAPTER II

Double functionalization for the design of innovative craniofacial prostheses

II.1. Chapter II overview

This second chapter deals with the elaboration of functional and bioactive sandwich materials composed of titanium and polymer sheets (Ti/P or Ti/P/Ti) to build innovative craniofacial protheses.

The main goal of this layered sandwich materials is to attenuate the stress shielding effect that often occurs when there is a significant different in the mechanical properties between the implant and the surrounding tissues.

For this purpose, the potential of carboxylic acid and sulfonate functions, was used as a tool for functionalizing titanium implants. To fulfil this aim, the main objectives were:

- To develop a direct UV grafting technique to graft two polymers onto Ti surfaces selectively: one that will modulate the mechanical properties (poly (MMA)) and one that will improve biocompatibility (poly (NaSS)).
- To characterize the effect of the grafted polymer uniformity on surface properties by the use of physico-chemical characterizations such as surface wettability and attenuated total reflection-Fourier-transformed infrared (FTIR).

To build-up this layered sandwich materials, several covalent grafting techniques have been developed to graft PMMA chains onto Ti. Two different ways of linking PMMA chains onto Ti surfaces are reported: (i) the “grafting to” technique using an anchor molecule to which PMMA chains of various lengths synthesized by RAFT polymerization are covalently attached and (ii) the “grafting from” technique including the direct polymerization of PMMA by surface oxidation and UV irradiations. Moreover, to confer biological properties to the Ti/PMMA hybrid surfaces, a UV grafting technique that permits to selectively graft the PMMA onto one side of the Ti surface and PNaSS onto the opposite side of the surface has been developed.

II.2. Article 1:

Double Functionalization for the Design of Innovative Craniofacial Prostheses, JOM. 74 (2022) 87–95. https://doi.org/10.1007/s11837-021-04997-0

JOM
The Journal of The Minerals, Metals & Materials Society (TMS)

Double functionalization for the design of innovative craniofacial prostheses

CAROLINE PEREIRA[1], JEAN-SEBASTIEN BAUMANN[1], PATRICK MASSON[2], GENEVIEVE POURROY[2], ADELE CARRADÒ[2], VERONIQUE MIGONNEY[1], CELINE FALENTIN-DAUDRE[1*]

[1]Université Sorbonne Paris Nord, Institut Galilée, LBPS/CSPBAT, CNRS UMR 7244, Villetaneuse, France.

[2]Université de Strasbourg, Institut de Physique et Chimie des Matériaux de Strasbourg (IPCMS), CNRS UMR 7504, Strasbourg, France.

Abstract

Titanium (Ti) is the most commonly used material for cranial prostheses. However, this material does not exhibit the same mechanical properties as the bone. Incorporating polymers onto Ti by combining both their properties is a solution to overcome this issue. Thus, sandwich materials made of two Ti skin sheets and poly (methyl methacrylate) (PMMA) core are promising structures to design biomedical prostheses. The “grafting to” and “grafting from” procedures to functionalize the Ti/PMMA interface are described in this paper as two strategies for chemically connecting PMMA chains on Ti surfaces. The advantage of the first approach is the capacity to control the architecture of the grafted PMMA on Ti. Moreover, a method for selectively grafting a bioactive polymer such as poly (sodium styrene sulfonate) (PNaSS) on one side of the Ti and PMMA on the other side is developed. This contribution presents efficient ways of functionalizing Ti for biomedical applications.

1. Introduction

Cranioplasty is a surgical procedure used for the reconstruction of craniofacial bone substances losses. These bone losses are mainly due to skull injuries such as head traumas, infections, or pathologies requiring the removal of tumors. Therefore, it is necessary to develop cranial devices to replace part of the removed bone flap. However, tailoring the optimal interaction of craniofacial implants with bone tissues is a challenge. Consequently, there is a great interest in

creating composite designs with mechanical and biological properties nearer to the surrounding tissues.

The materials widely manufactured for cranial prostheses are polymers such as poly (methyl methacrylate) (PMMA), ceramics (hydroxyapatite), and metals such as titanium (Ti) [1,2]. Ti remains the most used material for cranioplasty due to its acceptable biocompatible properties. The spontaneous formation of a superficial oxide layer that grows with its exposure to air explains its numerous characteristics. This amorphous layer of 3 to 7 nm thickness, mainly composed of Ti oxide TiO_2, chemically stabilizes the material's structure. [3–5]. Currently, custom-made Ti implants are manufactured on the market. These prostheses are fabricated using a laser beam additive technology called selective laser melting (SLM). It is a relevant example of building light Ti skull and mandible prostheses [6–9]. Moreover, PMMA also is mainly used in cranioplasty due to its interesting biocompatibility, low cost, and strength [10,11]. The first PMMA cranioplasty was performed by Zander in 1940 [12].

However, these materials have many disadvantages, such as their lack of mechanical properties with bone or density [13]. In addition, unmodified Ti-based materials tend to initiate the development of a fibrous layer following several years of implantation, prompting continuous loss of osseointegration [14,15]. Since these materials alone cannot optimally solve these discrepancies, the strategy proposed is to combine two different materials: polymers and metals, to design innovative hybrid structures called sandwich structures. Indeed, those structures exploit the high-bending resistance of the metals [16] and the lightweight of polymers [17]. For non-biological applications, the bonding between polymer and metal is accomplished utilizing an epoxy resin which is cytotoxic and, therefore cannot be considered for biological applications [18]. On the other hand, the bonding between metals and polymers is usually a mechanical interface since neither material does chemically bound spontaneously. In this circumstance, procedures guaranteeing a robust covalent bond between a thick polymer layer and the Ti are needed [19]. Indeed, these techniques would allow structures that can handle mechanical properties, such as the Young's modulus, for better implants/bone interface.

Furthermore, the prosthesis must be biocompatible to be well integrated by living bone tissues. In this regard, various strategies have been created to advance osseointegration between the implant and the surrounding bone [20,21]. Previous works carried out by our laboratory exhibited that the long-term response of implants can be improved by the grafting of bioactive

polymers such as poly (sodium styrene sulfonate) (PNaSS), PMMA, and poly (methacryloyl phosphate) [22,23]. *In vitro* and *in vivo* studies were conducted to follow the interactions between the bioactive materials and living tissues. It has been shown that the functional groups of PNaSS are biologically active in osteoblasts cells since the cell adhesion proteins adopt a conformation more conducive to the adhesion and then to the osteoblast cells' development. [24,25]. The grafting of PNaSS presents a biocompatibility interest, as it makes the implant surface hydrophilic, charged, and bacteriostatic. Recently, the grafting of PNaSS was successfully established using radicals under ultraviolet (UV) irradiation [26,27].

In general, two unique methodologies have been used to interface polymer chains on metal surfaces: the covalent connection of end-functionalized polymers joining an anchor molecule ("grafting to") and the *in situ* polymerization started from the surface ("grafting from") [28]. It is in this perspective that in their previous investigations [29], Reggente *et al.* have designed innovative epoxy resin-free sandwich materials composed of Ti and polymer sheets (Ti/PMMA/Ti) by developing the "grafting from" method [30]. This technique involves the grafting of PMMA using atom transfer radical polymerization (ATRP) [31–33]. ATRP is a form of living radical polymerization used to carry out controlled radical polymerization (CRP). Another example of the CRP method is the reversible addition-fragmentation transfer (RAFT) polymerization that can control the polymer structure. Both techniques allow grafting covalently chosen polymers and controlling their architecture, thicknesses, and compositions.

Several covalent grafting techniques can thus be used to graft PMMA chains onto Ti. Referring to the previous work developed by our team [34,35], here two different ways of linking PMMA chains onto Ti surfaces are reported: (i) the "grafting to" technique using an anchor molecule to which PMMA chains of various lengths synthesized by RAFT polymerization are covalently attached and (ii) the "grafting from" technique including the direct polymerization of PMMA by surface oxidation and UV irradiations. Moreover, to confer biological properties to the Ti/PMMA hybrid surfaces, a UV grafting technique that permits to selectively graft the PMMA onto one side of the Ti surface and PNaSS onto the opposite side of the surface has been developed.

In this article, the polymers synthesized by RAFT polymerization were characterized by conventional methods (nuclear magnetic resonance (NMR), size exclusion chromatography (SEC), and attenuated total reflection-Fourier-transformed infrared (FTIR)). In addition, the

functionalized surfaces were characterized by FTIR, water contact angle measurements (WCA), Oxford energy dispersive spectroscopy (EDS), and the toluidine blue colorimetric method (TB).

2. Materials and Methods

a. Materials

All chemical products were acquired from commercial providers and were utilized as received. One and half-centimeter diameter commercially pure, grade 2 Ti was purchased from Goodfellow. The two faces of the Ti were polished consecutively with 500 and 1200 grit SiC papers. After the polishing process, the Ti disks were successively cleaned twice in an acetone bath, once in cyclohexane bath, once in isopropanol bath, and once in distilled water (dH_2O) bath with sonication for 15 min. Ti disks were then dried in an oven at 50 °C. Afterward, Ti surfaces were chemically etched with Kroll's reagent (2% hydrofluoric acid, Sigma; 10% HNO_3, Acros, and 88% dH_2O) for 1 min with stirring followed by 15 min of sonication cleaning in five consecutive water baths.

The dopamine acrylamide (DA) anchor group synthesis was performed based on the protocol established by Chouirfa *et al.* [34]. In a two-neck round bottom flask balloon, dopamine hydrochloride (3 g, 15.8 mmol, 1 equiv) was introduced with a magnetic stirrer bar and 3 vacuum-argon cycles were done. Then, in a round bottom flask, sodium tetraborate decahydrate ($Na_2B_4O_7.10H_2O$; 14.44 g, 37.9 mmol, > 2 equiv) was dissolved in 400 mL of water and the solution was bubbled under argon for 30 min under magnetic stirring. The solution of $Na_2B_4O_7$ was added to the two-neck round bottom flask balloon containing the dopamine hydrochloride. Then the flask was put in an ice bath before adding sodium carbonate (Na_2CO_3, 11 g, 103.8 mmol) and acryloyl chloride (8 mL, 98.5 mmol) over one hour. Then, the ice bath was removed and the reaction was carried out overnight at room temperature under magnetic stirring. The following day the solution pH was ~8 and hydrochloridric acid (HCl 37%) and was added until the pH equaled ~2 to remove the borate protection. Then the solution was washed twice with ethyl acetate (400 mL then 150 mL). The organic phase was collected and washed twice with HCl 37% (once with 500 mL (1%) and then with 200 mL (1%)). The collected organic phase was dried over magnesium sulfate ($MgSO_4$) and filtered. The ethyl acetate was removed under reduced pressure and the crude product was purified by silica gel column chromatography, a mixture of dichloromethane (DCM)/methanol (MeOH) 97/3 *v/v* and then with DCM/MeOH 95/5 *v/v*) to give after drying under vacuum at 50°C a light brown powder (Yield: 1.63 g, 50%).

The methyl methacrylate (MMA) was purified over a basic alumina column to remove the stabilizer. The description of the synthesis procedures used to prepare the PMMA via RAFT polymerization and thiolation of PMMA are provided in the **supplementary material (annexe 1, at the end of the Chapter 2)**. The additional material also describes experimental details for the nuclear magnetic resonance (NMR) and size exclusion chromatography (SEC) methods used to characterize the synthesized PMMA samples.

Sodium styrene sulfonate (NaSS, Sigma) was purified by recrystallization in a mixture of ethanol/water (Carlo Erba) (10: 90 v/v) overnight at 70 °C. The purified NaSS was dried under atmospheric pressure at 50 °C overnight and then stored at 4° C [27,37].

The UV source used for the grafting procedure comes from a Lot Quantum Design UV lamp with a generated power from 200 W to 500 W, at 365 nm under average temperature and pressure conditions.

b. Methods: The grafting processes

i. Indirect grafting of MMA process

Activation: After Kroll's treatment, Ti samples were activated according to the protocol established by Reggente *et al.* [29, 36]. The Ti disks were immersed in 1 h into a 2M sodium hydroxide (NaOH) solution heated at 80 °C in a Teflon beaker. Ti disks were suspended in the reactive media with a Ti wire during the activation step to avoid contact. Afterward, the alkali-activated Ti samples were suspended in a flask containing dH_2O water for 1h at 60 °C. This cleaning procedure was established to remove any traces of concentrated 2M NaOH solution.

Indirect grafting of MMA onto Ti: The surface functionalization with the catechol derivative was described in detail by Chouirfa *et al.* [34]. This process consists of a three-step methodology (**Figure 1**). Well-defined molecular weight (10, 16, and 50 kDa) RAFT synthetized PMMA bearing thiol end group (PMMA-SH) were covalently grafted via thiol-ene click reaction onto Ti substrates modified with the DA. More details about the dopamine adhesion and the coupling reaction of the polymer are provided in the supplementary material.

ii. Direct grafting of MMA process

The methyl methacrylate (MMA) with a concentration of 1.5 M – purified from its stabilizer by column chromatography on basic aluminum oxide – was added to a 100 mL round bottom flask containing dimethyl sulfoxide (DMSO) solvent. First, the solution was degassed with

argon for 30 min, and then the activated Ti surfaces (with the procedure described above (i)) were rapidly introduced within the solution. Next, the round bottom flask containing the MMA/DMSO solution and the Ti surface was irradiated with UV light (365 nm, 160 mW/cm ^{2}) at ambient temperature with stirring for 1 h. (**Figure 1**). The grafted surfaces were then rinsed for 48 h with dH_2O and dried overnight at 37 °C before any characterization.

iii. Double face functionalization

The selectivity of this functionalization method was made possible due to UV irradiation and the set-up implemented. Indeed, only the Ti surface directly exposed to the UV beam of the mercury lamp was able to graft the chosen polymer through the grafting process. Therefore, as a part of our study, this protocol was established strictly following the PMMA grafting protocol using the "grafting from" procedure, followed by the "grafting from" process of PNaSS.

Ti-PMMA-Ti-PNaSS procedure: Ti samples were activated according to the protocol established by Reggente *et al.* [29, 36]. The Ti disks were immersed in 1 h into a 1M sodium hydroxide (NaOH) solution, heated at 80 °C in a Teflon beaker. Ti disks were suspended in the reactive media with a Ti wire during the activation step to avoid contact. Afterward, the alkali-activated Ti samples were suspended in a flask containing dH_2O for 1 h at 60 °C. Then, Ti samples were immersed in a degassed DMSO solution of MMA (1.5M). The round bottom flask, containing the MMA/DMSO solution and Ti surfaces, was irradiated with UV light (365 nm, 160 mW/cm ^{2}) at ambient temperature with stirring for 1 h. For this first grafting, the face A has been exposed under UV irradiations. The grafted surfaces were then rinsed for 48 h with dH_2O. After the washing step, Ti samples were immersed in a degassed and aqueous solution of NaSS monomer (0.7 M). The round bottom flask containing the samples, the solution, and the face B of Ti samples were placed under UV irradiations (365 nm, 160 mW/cm ^{2}) at room temperature with stirring for 1h. Finally, grafted surfaces were then rinsed for 48 h with dH_2O.

3. Surfaces characterizations

Each surface functionalization was followed by attenuated total reflection Fourier-transform infrared spectroscopy (ATR-FTIR) by water contact angle measurement (WCA). The grafting degree of PNaSS was evaluated by the toluidine blue colorimetric method.

Fourier-transform infrared spectroscopy (FTIR) The Fourier-transformed infrared (FTIR) spectra were acquired between 4000 and 600 cm^{-1} in attenuated total reflectance mode. Ti samples were pressed against a diamond crystal (4000-500 $cm^{-1)}$ for acquirements (512 scans). Each spectrum was then fitted and analyzed.

EDS element chemical analysis This analysis was performed through scanning electron microscopy (SEM, Hitachi TM300) combined with Oxford energy dispersive spectroscopy (EDS). The instrument operated at 5 kV to 15 kV.

Water Contact angle measurements (WCA) The wettability after each surface treatment step was analyzed by WCA measurements using the DAS10 goniometer from Kruss. For each measure, 2 ul of dH_2O were dropped onto the surface. The dropped image was taken 20 seconds after the water drop in contact with the surface. The software from the photo taken then measured the WCA. Three measurements were taken and averaged.

Toluidine blue (TB) colorimetry assay To characterize the quantification of PNaSS grafted onto Ti surfaces, toluidine blue (TB) colorimetric technique was carried out according to the protocol established by Helary *et al.* [37]. TB is a chromophore molecule that absorbs in the visible at 633 nm. This molecule has the particularity to complex *via* its $N^+(CH_3)_2$ groups with anionic groups (sulfonate SO_3^- group of the NaSS). First, PNaSS grafted and washed samples were immersed in the dye solution (0.5 mM at pH =10) for complexation for 6 h at 30 °C. The excess of TB was removed with 3 washings with a solution of NaOH (10^{-3} M, three times 5 min). Then, complexed TB sample surfaces were de-complexed by putting the samples in acetic acid/water solution (50/50 v/v) for 24 h. The concentration of TB was then quantified by UV-visible spectroscopy (PerkinElmer lambda 25 spectrometer). TB assays were carried out onto six samples for each condition. According to Ikada *et al.* [38], one mole of TB molecule complexes with one mole of sulfonate ($-SO_3^-$). Non-grafted Ti samples were used as controls and were found not to react with the TB solution. Therefore, three Ti samples were used per analysis.

4. Results and discussion

a. Activation of Ti surfaces

The activation procedure aimed to prompt active spots on the Ti surface to graft the polymer. In the past, our laboratory was using acidic oxidation to create a surface layer of Ti hydroxide (Ti-OH) and titanium peroxides (Ti-OOH). However, since these hydroperoxides groups are not stable enough, it has been decided to activate the Ti surface with basic oxidation.

Based on the literature, an alkali activation was performed to activate the surface. The characterizations work done by M. Reggente *et al.* have demonstrated that the layer generated by the sodium hydroxide solution onto Ti surfaces has pore size ranges between 50 to 200 nm and is uniformly spread on the whole Ti surface (20 mm in diameter and 3 mm thick of commercially pure grade 4 Ti) [29]. In our type of Ti surface (15 mm in diameter and 1.5 mm thick of commercially pure grade 2 Ti), it has been noticed that the surfaces do not exhibit the same color depending on the oxidation (acid or alkaline). A light yellow Ti surface color was observed with Piranha solution and dark blue color with alkaline oxidation (details and descriptions are provided in the supplementary material). The color varies with the thickness of the Ti oxide layer. According to the literature [38], as long as the oxide layer is thin (20 to 30 nm), it is transparent, and the Ti sample keeps its metallic luster. As soon as the oxide thickens and reaches 40 nm, the surface acquires a color due to light interference effects. By referring to the table of the colours of titanium oxide films as a function of the thickness of the oxide layer, established by N.P. Peksheva *et al*, it can be assumed that the oxide layer's thickness would be, respectively, around 35 nm for acid oxidation and about 50 nm for alkaline oxidation.

The EDS element chemical analysis revealed several atoms (C, O, Na, Ti), mainly Na and O, essential layer compounds formed by the basic activation (**Table 2.1**). Moreover, the hydrophilicity character of the surface after the activation was shown by the water contact angle measurement. For example, the contact angle of the control Ti surface (polished Ti disk, cleaned with Kroll's reagent and oxidized with Piranha solution) was around 66°. After the activation step, the surface gave a contact angle around 42° showing the presence of hydroxyl groups onto Ti (**Figure 2.3**).

b. Ti functionalization with “grafting to” and “grafting from” procedure

The grafted PMMA Ti surface prepared *via* the “grafting to” technique requires the addition of an anchoring molecule (dopamine acrylamide) to link the PMMA chains to the Ti surface (**Figure 2.1**). This procedure was done in four steps (**Figure 2.1**): 1. Ti surface was activated with NaOH. 2. The surface was functionalized with dopamine acrylamide. 3. PMMA was synthesized by RAFT polymerization to generate a thiol function. 4. The thiol-end polymer chains were attached to the Ti surface by a thiolene click reaction.

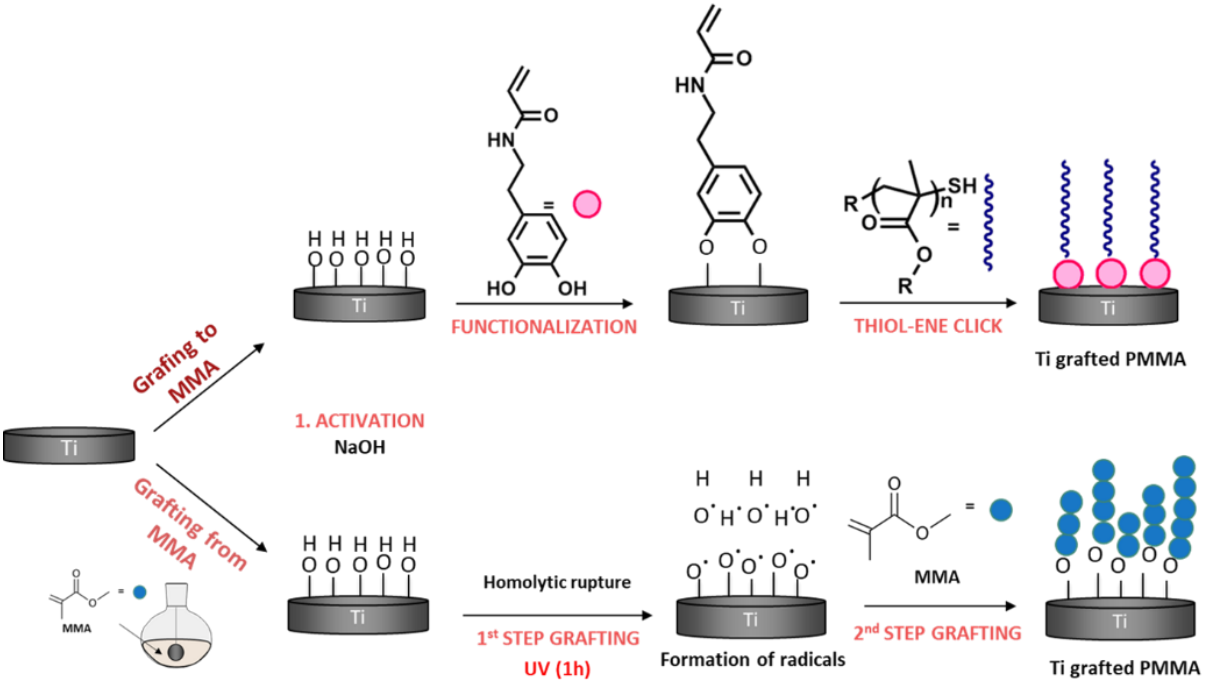

FIGURE 2.1 THE PMMA-GRAFTED TI SURFACES WERE DESIGNED USING THE FOLLOWING METHODOLOGY: "GRAFTING FROM" INCLUDES UV PMMA GRAFTING AND GIVES NON-CONTROL SIZED POLYMER CHAINS, WHEREAS THE "GRAFTING TO" ALLOWS THE GRAFTING OF POLYMER CHAINS OF CONTROLLED SIZE

FTIR spectra of the PMMA grafted Ti with this method (blue curve) and synthesized PMMA powders (yellow curve) are represented in **Figure 2.2.**

Both ranges contain the signal of the carbonyl group peak (C=O at 1725 cm^{-1}) and the α-methyl group vibrations (α-CH_3 at 2993 cm^{-1} and 2945 cm^{-1}), confirming that PMMA was successfully grafted onto the Ti surface. Other absorption bands were observed at 1438 cm^{-1} (-CH_2 bending vibration), 1060 cm^{-1} (C-O bond stretching), and 1380-749 cm^{-1} (α-methyl group vibrations).

The absorption bands around 800 cm^{-1} on the Ti grafted are attributable to Ti-O bonds. This observation through FTIR analyses indicates that the grafting of the controlled-sized PMMA chains is not homogeneous. Indeed, it has been observed that in the "grafting to" method, the grafted polymer on the Ti surface, polymerized by RAFT synthesis, results in a controlled architecture, but the surface coverage remains inhomogeneous.

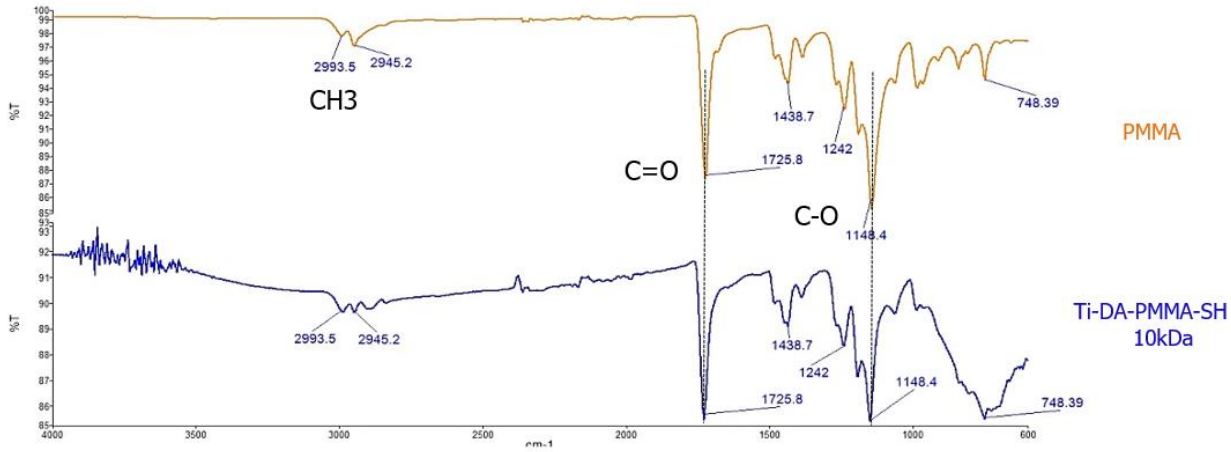

FIGURE 2.2 FTIR SPECTRUM FOR THE FUNCTIONALIZED TI WITH "GRAFTING TO" PROCEDURE

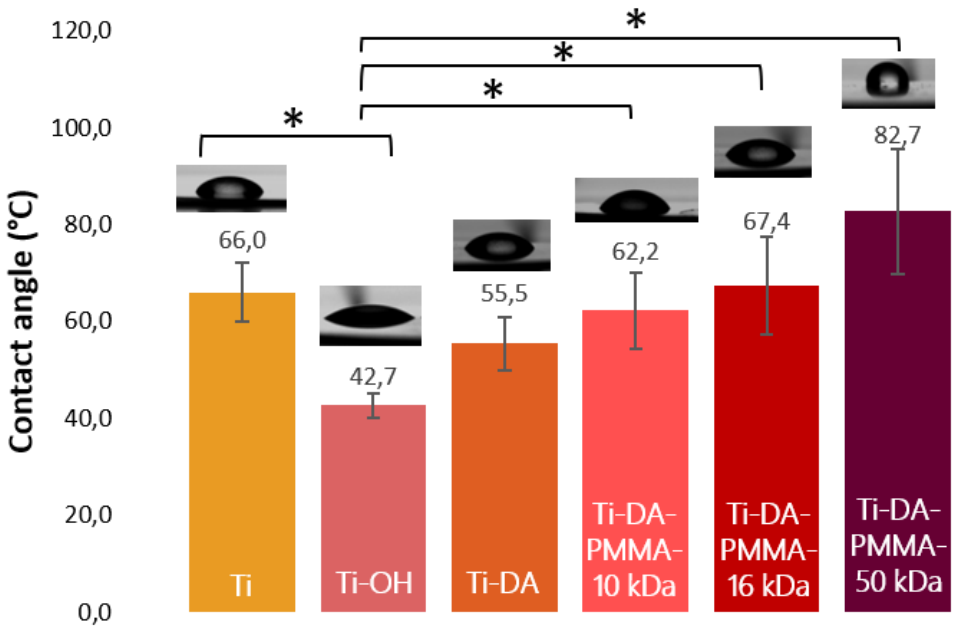

FIGURE 2.3 WCA MEASUREMENTS RESULT FOR THE FUNCTIONALIZED TI WITH "GRAFTING TO" PROCEDURE

In addition, the hydrophilicity/hydrophobicity of the surface was measured by the water contact angle (WCA) method (**Figure 2.3**). When the surface is functionalized with the anchor

molecule, the contact angle of the activated surface increases by about 13°. The surface becomes less hydrophilic with the presence of dopamine acrylamide. Ti surfaces grafted with 10kDa, 16 kDa, and 50 kDa PMMA-SH gave contact angles of 62°±8, 67°±10 and 83°±13, respectively. These contact angles increase with the grafting of PMMA which is a hydrophobic polymer. It is interesting to notice that as the size of the PMMA chains increases, the surface becomes more hydrophobic. On the other hand, the standard deviation also increases, showing that the surface coverage losses homogeneity with high-length PMMA chains. This technique, coupled with infrared spectra, demonstrates the same conclusions.

The second method proposed in this study is a direct grafting technique. First, the MMA monomer is directly placed in a solution in a solvent, which solubilizes it (DMSO). Then, the Ti surfaces activated by NaOH are introduced so that the grafting with UV occurs. The UV irradiation allows radicals on the Ti surface, which will then initiate the MMA polymerization. The direct grafting of MMA is very efficient since it will avoid the synthesis of the anchor molecule by allowing a direct grafting of the solubilized monomer in contact with the surface under UV.

FTIR spectra of the PMMA grafted Ti with this "grafting from" method (pink curve), and MMA monomer liquid (black curve) are represented in **Figure 2.4**. The principal proof of PMMA formation came from the vanishing of the signal due to the C=C stretching vibration mode of the vinyl group of the monomer (1601 cm^{-1}). The FTIR spectrum of the PMMA grafted Ti attests to the success of direct grafting. Other characteristic peaks of PMMA, described earlier, are present. The peaks are more defined, and the spectrum is more refined than the one obtained by the "grafting to" method.

In addition, the contact angle of a PMMA grafted surface is around 102.0°±0.8 (**Figure 2.5**). Furthermore, the standard deviation is acceptable, showing that the surface coverage homogeneity of PMMA is likely uniform on the Ti surface.

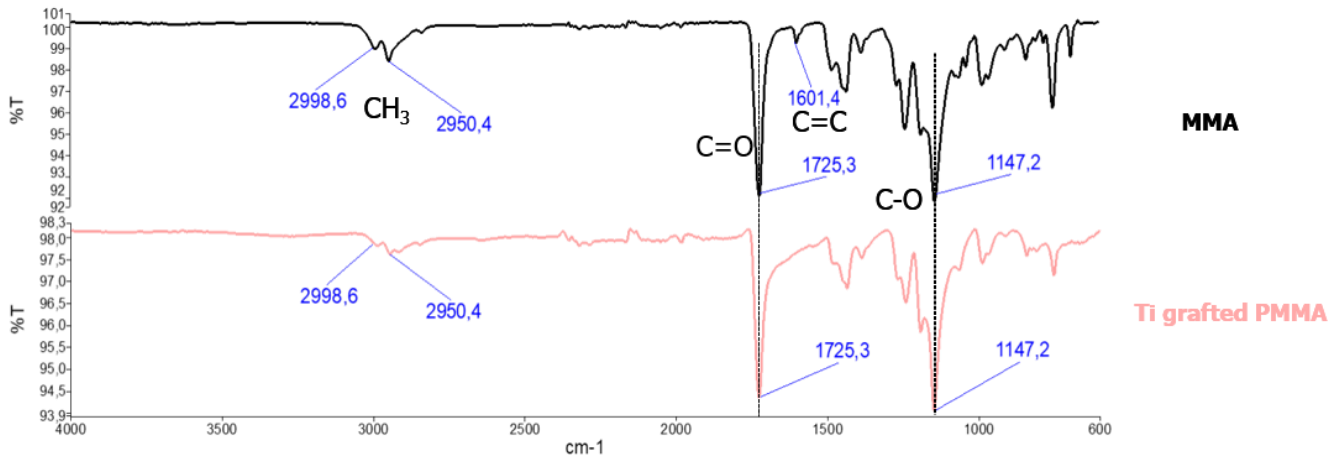

FIGURE 2.4 FTIR SPECTRUM FOR THE FUNCTIONALIZED TI WITH "GRAFTING FROM" PROCEDURE.

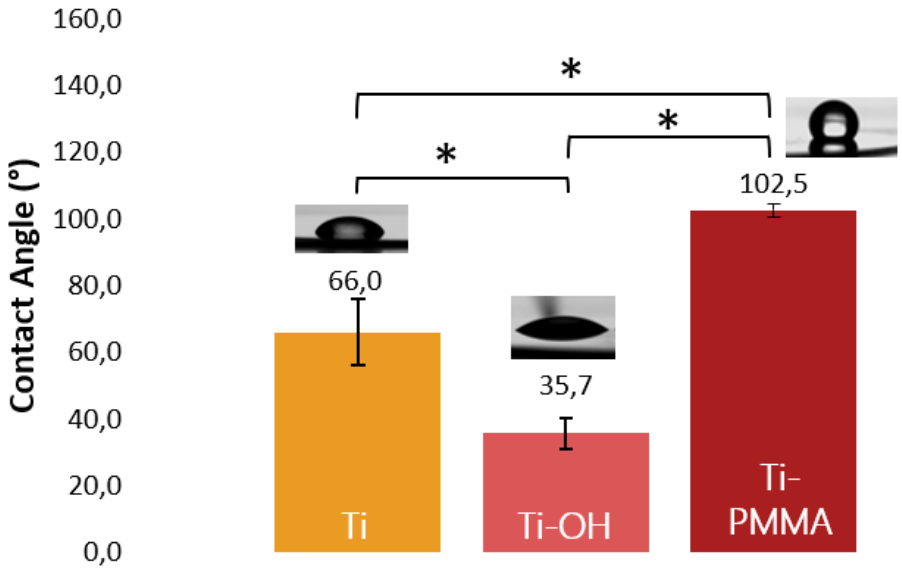

FIGURE 2.5 WCA MEASUREMENTS RESULT FOR THE FUNCTIONALIZED TI WITH "GRAFTING FROM" PROCEDURE

The results obtained by the FTIR spectrum combined with the contact angle result show that this direct grafting method is more efficient than the indirect grafting method. Therefore, direct grafting allows obtaining a better covering of the surface by the PMMA while having a straightforward grafting protocol.

c. Double-face functionalization

To confer bioactive properties to Ti surfaces, it has been decided to develop a method capable of grafting PMMA and PNaSS onto Ti. In this context, UV irradiation has been used, which produces a concentrated UV beam, to graft the Ti surfaces selectively. For this purpose, the Ti surfaces, suspended with Ti wires, were placed directly in contact with the UV beam (**Figure 2.6**). Thus, depending on the protocol used, the surface was able to graft the chosen polymer.

The double-face functionalization process was characterized by combining TB colorimetric assay, WCA measurements, FTIR and EDS.

The WCA measurement results (**Figure 2.6**) have attested to the presence of PMMA on the surface exposed to UV irradiation with PMMA grafting protocol ("grafting from" protocol), with the obtention of a contact angle of 102.0°±1.8. On the order hand, the surface exposed to UV with PNaSS grafting protocol showed a contact angle of 25.0°±1.2. PNaSS being an anionic and hydrophilic polymer, once grafted with PNaSS, the Ti surface should result in a low contact angle measurement. Thus, these results have demonstrated the presence of PMMA on one side of the Ti surface and PNaSS on the other side of the grafted Ti surfaces.

The TB results for the distinctive grafted surfaces were predictable with the contact angle results. Expecting 1 mol of TB complexes with 1 mol of sulfonate groups, TB provides data regarding the dispersion of the grafted PNaSS on Ti surfaces. As shown in Figure 4, the amount of PNaSS grafted (0.7 M 1 h at the UV power 160 mW.cm^{-2}) is 2.07±0.07 µg. cm^{-2}

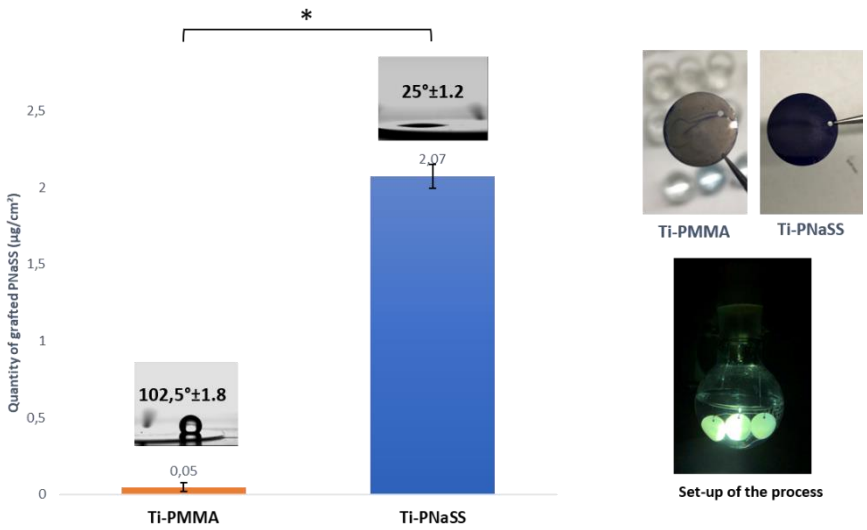

FIGURE 2.6 TB COLORIMETRIC ASSAY, TB IMAGES RESULTS, WCA MEASUREMENTS, AND SET-UP IMAGE OF THE "DOUBLE-FACE FUNCTIONALIZATION" PROCEDURE

(**Figure 2.6**). The surface grafted with PMMA has shown no presence of PNaSS as the grafting degree of PNaSS onto this surface is equal to 0.05 ±0.02 µg. cm^{-2}. Visually, the results of TB colorimetric assay are eloquent when comparing the surface grafted with PMMA and the surface grafted with PNaSS. The images (**Figure 2.6**) clearly show that the Ti-PNaSS surface gives a darker blue image due to the high concentration of sulfonate groups on the selectively grafted surface. Concerning the grafting degree of PNaSS, similar results have been obtained as Chouirfa *et al.* in the same condition with a power lamp at 160 $mW.cm^{-2}$, with 0.7 M of monomer concentration and a UV exposure of 1h [27].

Moreover, FTIR spectra of both sides of the grafted surface were done. The spectra (**Figure 2.7**) were assessed between 600 and 4000 cm^{-1}. Ti-PMMA FTIR spectrum showed the presence of all the characteristics band of the PMMA. In addition, the Ti-PNaSS spectrum also showed the presence of specific peaks of the PNaSS at the surface of the Ti disk (**Figure 2.7**).

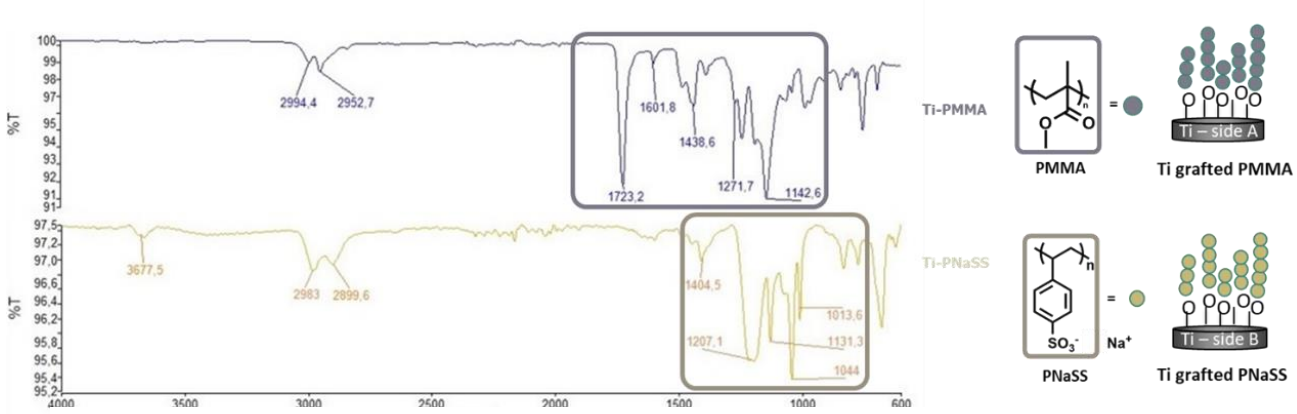

FIGURE 2.7 FTIR RESULTS OF THE SURFACE SELECTIVELY EXPOSED TO UV IRRADIATION FOR THE "DOUBLE-FACE FUNCTIONALIZATION" PROCEDURE

For instance, the FTIR spectrum of Ti-PNaSS shows the aromatic ring, and the symmetric vibrations of the SO_3^- groups generated a NaSS doublet (O=S=O) located at 1013 cm^{-1} and 1044 cm^{-1}. However, compared to the FTIR characterization work done for PNaSS [27], these two peaks are slightly shifted.

On the EDS analysis, the percentage of oxygen is more considerable after oxidation due to the oxide layer formation. The EDS element chemical analysis also showed Na and S atoms' presence, essential compounds of the PNaSS (**Table 2.1**) on the Ti-PMMA-Ti surface. In addition, a higher carbon percentage is observed; this result also confirms the grafting of the

PNaSS. The FTIR results combined with EDS results demonstrate the selectivity of this double functionalization.

TABLE 2.1 ANALYSIS OF ATOMIC (%) OF ELEMENTS AT THE TI SURFACE

Samples	C	O	Na	S	Ti
Ungrafted Ti	5.1±0.5	8.5±0.7	-	-	86.4±0.6
Activated Ti (NaOH)	9.1±0.4	24.6±0.2	0.4±0.1	-	65.9±0.7
UV PNaSS grafted Ti	20.7±1.3	19.8±1.5	0.9±0.2	1.0±0.4	57.6±2.2
UV PMMA grafted Ti	40.9±1.2	37.3±1.0	-	-	21.8±1.7

5. Conclusion and perspectives

Thanks to the study carried out and reported in this article, the two grafting methods, “grafting to” and “grafting from” previously developed for the NaSS monomer, have been successfully transposed to another monomer such as MMA. This polymer is particularly interesting since it aims at improving the mechanical properties of the targeted Ti / PMMA / Ti sandwich structure.

The originality of our study is based on the development of a double functionalization of Ti surfaces. It has been shown by different characterizations (TB colorimetric method, WCA, FTIR, EDS) that it is possible to selectively graft a polymer to the surface of Ti using UV irradiation.

The protocol developed will allow us to functionalize the external surface of our sandwich structure. In addition, the osseointegration properties of the structure will be assessed using biological tests on osteoblast cells (MTT, morphology, alkaline phosphatase, and calcium assay). Besides improving the grafting time and being easily industrialized, the UV irradiation technique opens the door to numerous studies.

Acknowledgments

This research was supported by the French Ministry of National Education, Higher Education, and Research. The materials used in this study were financed by the ANR-DFG project (ANR-18-CE92-0056-01). We especially thank the ANR DFG for their financial support.

III.3. Annexe 1: Supplementary file of article 1

Analytical Methods:

Nuclear Magnetic Resonance (NMR) spectroscopy (^{1}H NMR): Spectra were recorded on Bruker Avance III 400 spectrometer (400 MHz) at room temperature. Chemical shift values (δ) are reported in ppm. The residual proton signal of the NMR solvents were used as internal standard (D_2O: 4.79 ppm and DMSO-d_6: 2.50 ppm).

Calculation of $M_{n,\,th}$: The theoretical number average molecular weights ($M_{n,\,th}$) was calculated using the following **Equation (S1)**.

$$M_{n,\,th} = \frac{[\text{Monomer}]_0 p M_{monomer}}{[\text{RAFT agent}]} + M_{\text{RAFT}} \quad \text{(S1)}$$

$[\text{Monomer}]_0$ and [RAFT agent] are the initial concentrations (mol.L^{-1}) of the monomer and the chain transfer agent respectively.

p is the monomer conversion as determined by ^{1}H NMR.

$M_{monomrt}$ and M_{RAFT} are the molecular weights (g.mol^{-1}) of the monomer and the chain transfer agent.

Size exclusion chromatography (SEC): SEC analyses were performed on a Shimadzu Prominence instrument equipped with a SIL-20ACHT auto sampler and a Shimadzu RID-10A differential refractive index detector. The system was fitted with an Ultraphenoogel™ (Phenomenex) gel pre-column (6 × 40 mm) and two Ultraphenogel™ (Phenomenex) analytical columns (7.8 × 300 mm). The tetrahydrofuran (THF, Carl Roth) was used as the mobile phase, eluting at 1.0 mL.min^{-1} at 25 °C. Samples were dissolved in THF. Prior to injection, the samples were filtered through PTFE membranes (0.20 µm pore size). The molecular weights of the polymers (M_n) and the dispersity ($Đ$) were determined using LC solution GPC software by a conventional calibration obtained from PMMA standards (Agilent) ranging from ~500 to ~1.5 × 10^6 g.mol^{-1}.

Synthesis Procedures:

A) Preparation of the PMMA-SH

Preparation of polymethyl methacrylate (PMMA) *via* reversible addition-fragmentation chain transfer (RAFT) polymerization (Figure S2):

The methyl methacrylate (MMA, Sigma Aldrich) – purified from its stabilizer by column chromatography on basic aluminium oxide (Sigma Aldrich) was added to a 50 mL round bottom flask containing a stir bar, dimethyl sulfoxide (DMSO), 2,2'-azobis (2-methylpropionitrile) (AIBN) and 4-Cyano-4- (phenylcarbonothioylthio) pentanoic acid (ACP). Then argon was bubbled through the solution for 30 min. Then, the round bottom flask was sealed with a septum and placed in an oil bath thermostated at 80 °C overnight. The polymerization was stopped by soaking in an ice bath. An aliquot was taken to determine the final conversion by ^{1}H NMR. The PMMA-RAFT polymer was obtained by precipitation in cold distilled water. After being dried overnight in a vacuum oven at 50 °C, the polymers were analyzed by the SEC and by ^{1}H NMR.

Table S3. Quantitative information for the preparation of PMMA by reversible addition-fragmentation chain transfer (RAFT) polymerization.

Mn theoretical ($g.mol^{-1}$)	10 000	16 000	50 000
$[MMA]_0$ ($mol.L^{-1}$)	2.2	2.2	2.2
$[ACP]_0$ ($mol.L^{-1}$)	2.21×10^{-3}	7.41×10^{-3}	1.12×10^{-2}
$[AIBN]_0$ ($mol.L^{-1}$)	4.42×10^{-4}	1.48×10^{-3}	2.23×10^{-3}

ACP: chain transfer agent, 4-cyano-4- (phenylcarbonothioylthio) pentanoic acid.

SH end group formation of PMMA-SH by reduction reaction:

9 g of PMMA was dissolved in 10 mL of THF and degassed under argon for 20 min at 0 °C. Then, 30 mg of sodium dithionide and 3.2g hexylamine were added to the polymer solution and kept bubbling under argon for 15 min. The solution was stirred for at least 48 h at room temperature (RT) before the PMMA-SH was precipitated in the ice-cold hexane.(**see Figure S1**).

Table S2: Results of different RAFT polymerization and SH groups formation.

	Conv^{1}H NMR) (%)	Mn_{before} (g.mol^{-1})	$Đ_{before}$	Mn_{After} (g.mol^{-1})	$Đ_{after}$
$pMMA_{10k}$	51%	10637	1.10	11772	1.15
$pMMA_{16k}$	54%	16201	1.08	16638	1.17
$pMMA_{50k}$	72%	58165	1.11	51577	1.19

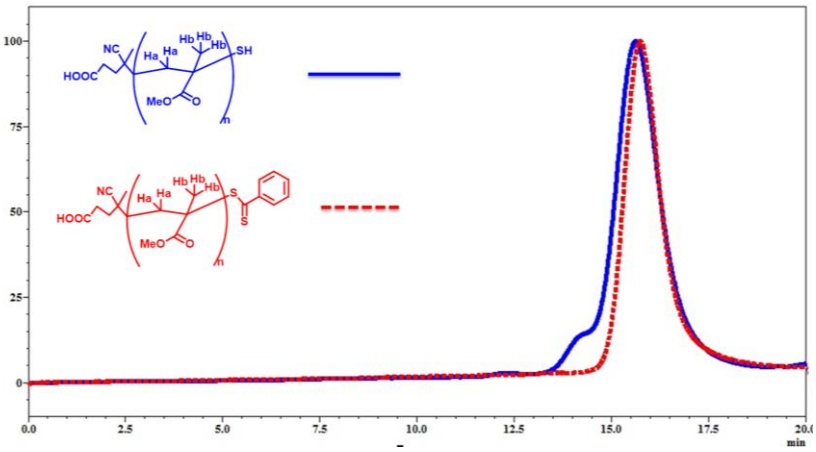

Figure S1. Size exclusion chromatograms (differential refractive index detector) of $PMMA_{10k}$ synthesized by RAFT polymerization and PMMA-SH in solid line after reducing.

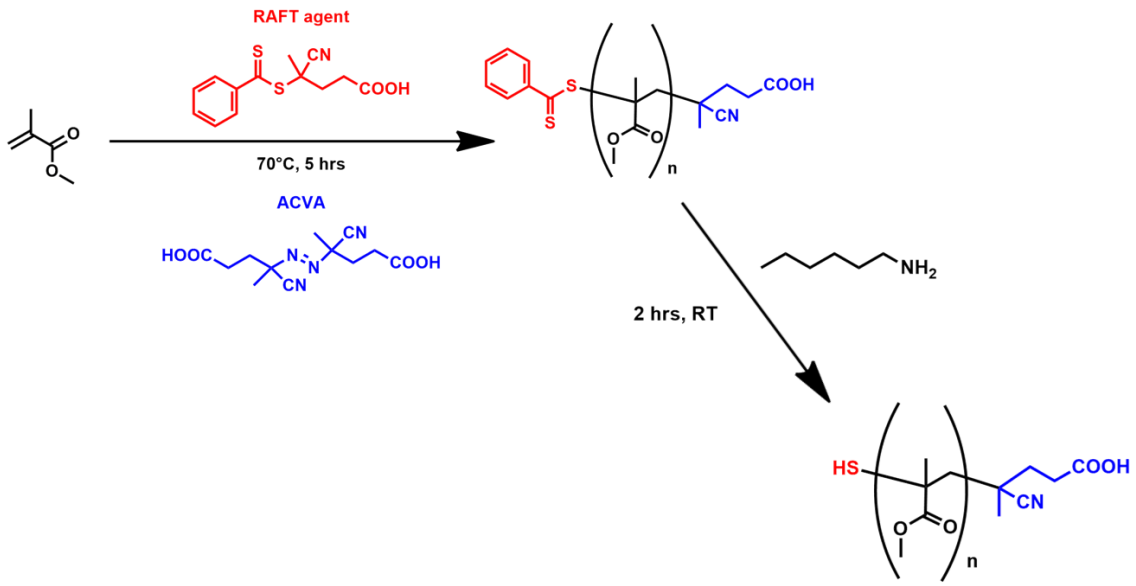

Figure S2: Preparation of thiolated PMMA.

B) Functionalization of the titanium surfaces

Activation of titanium (Ti) surfaces: It is possible to activate Ti surfaces with acidic oxidation based on our previous work. For this method, the Ti surfaces were immersed in a Piranha solution (H2SO4/H2O2 50:50 v/v) in a controlled and inert atmosphere (>99%argon). This type of oxidation allows the formation of hydroperoxide and hydroxide functions, as shown in Figure S3. For our study, the oxidation used was the alkali-activation (Figure S3).

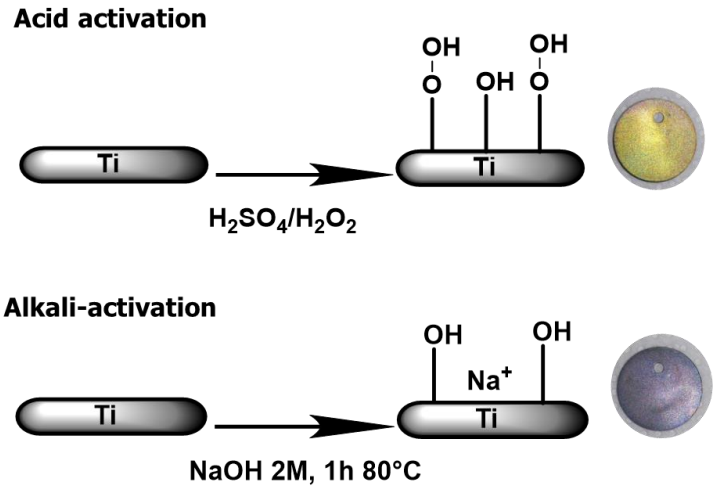

Figure S3: Comparison of the two Ti activation procedures and respective images of the color obtained after oxidation

Fixation of the anchor molecule, dopamine acrylamide (DA) to the Ti activated surfaces: 0.6 g of DA was dissolved in 14 mL of dimethyl sulfoxide (DMSO) in a round bottom flask. The flask was wrapped in aluminum foil, and the solution was degassed with argon for 30 min while stirring. The previously oxidized Ti surfaces were then added to the flask. The reaction was carried out for 24 h, under stirring and in the dark. Finally, the Ti surfaces were rinsed with distilled water for 24 h and dried overnight in a vacuum oven at 37 °C.

II.4. References

[1] T.C. Origitano, R. Izquierdo and L.B. Scannicchio, *Skull Base* 5, 109 (1995).
[2] Y. Ducic, *Journal of Oral and Maxillofacial Surgery* 60, 272 (2002).
[3] T.P. Queiroz, R.S. de Molon, F. Á. Souza, R. Margonar, A.H.A. Thomazini, A.C. Guastaldi and E. Hochuli-Vieira, *Clin. Oral Invest.* 21, 685 (2017).
[4] C. Debry, N.E. Vrana and A. Dupret-Bories, *N. Engl. J. Med.* 376, 97 (2017).
[5] A. Carradò, F. Perrin-Schmitt, Q.V. Le, M. Giraudel, C. Fischer, G. Koenig, L. Jacomine, L. Behr, A. Chalom, L. Fiette, A. Morlet and G. Pourroy, *Dent. Mater.* 33, 321 (2017).
[6] M. Szindler and T.G. Gaweł, *Porous selective laser melted Ti and Ti6Al4V materials for medical applications. Powder metallurgy-fundamentals and case studies.* (InTech.March 29th, 2017).
[7] S. Mueller, B. Hohlweg-Majert, R. Buergers, T. Steiner, T.E. Reichert, K.D. Wolff and K. Wolff, *Clin Oral Invest*. 19, 413 (2015).
[8] A.L. Jardini, M.A. Larosa, R. Filho, C.A. Zavaglia, L.F. Bernardes, C. Lambert, D. Calderoni and P. Kharmandayan, *J. Craniomaxillofac. Surg*. 42,1877 (2014).
[9] H. Rotaru, R. Schumacher, S.G. Kim and C. Dinu, *Maxillofac. Plast. Reconstr. Surg.* 37,12 (2015).
[10] G.J. Huang, S. Zhong, S.M. Susarla, E.W. Swanson, J. Huang andC.R. Gordon, *J. Craniofac. Surg.* 26, 64 (2015).
[11] A. Ridwan-Pramana, P. Marcian, L. Borak, N. Narra, T. Forouzanfar andJ. Wolff, *J. Craniomaxillofac. Surg.* 44, 34 (2016).
[12] A. Sanan andS. J. Haines, *Neurosurg.* 40, 588 (1997).
[13] M. Ridzwan, S. Shuib, A. Hassan, A. Shokri and M.M. Ibrahim, *J. Med. Sci.* 7,460 (2007).
[14] M. Esposito, J. M. Hirsch, U. Lekholm, and P. Thomsen, *Eur. J. Oral Sci.* 106, 527 (1998).
[15] A. M. Roos-Jansaker, S. Renvert, and J. Egelberg, *J. Clin. Periodontol*. 30, 467 (2003).
[16] B. Harris, *Mater. Des.* 12, 259 (1991).
[17] R.F. Landel and L.E. Nielsen, *Mechanical properties of polymers and composites.* (CRC Press; 1993).
[18] E. L. Kostoryz, P. Y. Tong, C. C. Chappelow, J. D. Eick, A. G. Glaros and D. M. Yourtee. *Dent Mater.* 15, 363 (1999).
[19] M. Reggente, M. Harhash, S. Kriegel, W. He, P. Masson, J. Faerber, G. Pourroy, H. Palkowski and A. Carradò, *Compos. Struct.* 218, 107 (2019).
[20] J. E. Raynor, J. R. Capadona, D. M. Collard, T. A. Petrie and A. J. García. *Biointerphases* 4, FA3 (2009).
[21] A. Michiardi, G. Hélary, P. C. Nguyen, L. J. Gamble, F. Anagnostou, D. G. Castner and V. Migonney. *Acta Biomater.* 6, 667 (2010).
[22] F. El Khadali, G. Hélary, G. Pavon-Djavid, and V. Migonney, *Biomacromolecules* 3, 51 (2002).
[23] F. Anagnostou, F. Debet, G. Pavon-Djavid, Z. Goudaby, G. Hélary, and V. Migonney, *Biomaterials* 27, 3912 (2006).
[24] H. Felgueiras, M. Evans, and V. Migonney, *Acta Biomater.* 28, 225 (2015).
[25] H. Felgueiras and V. Migonney, *IRBM* 37, 165 (2016).

[26] C. Falentin-Daudré, V. Migonney, H. Chouirfa, and J. S. Baumann, WO patent PCT/EP2016/068909 (August 7th, 2015).
[27] H. Chouirfa, V. Migonney, and C. Falentin-Daudré, *RSC Adv.* 6, 13766 (2016).
[28] S. Minko, *Polymer Surfaces and Interfaces*, edited by M. Stamm (Springer, Berlin, 2008), pp. 215–234.
[29] M. Reggente, P. Masson, C. Dollinger, H. Palkowski, S. Zafeiratos, L. Jacomine, D. Passeri, M. Rossi, N. E. Vrana, G. Pourroy and A. Carradò. *ACS Appl. Mater. Interfaces* 10, 5967 (2018).
[30] M. Kim, S. Schmitt, J. Choi, J. Krutty and P. Gopalan. *Polymers* 7, 1346 (2015).
[31] R. N. Foster, E. T. Harrison, and D. G. Castner, *Langmuir* 32, 3207 (2016).
[32] R. N. Foster, P. K. Johansson, N. Tom, P. Koelsh, and D. G. Castner, *J. Vac. Sci. Technol.* A 33, 05E131 (2015).
[33] R. N. Foster, A. J. Keefe, S. Jiang, and D. G. Castner, *J. Vac. Sci. Technol.* A 31, 06F103 (2013).
[34] H. Chouirfa, M. Evans, D. Castner, P. Bean, D. Mercier, A. Galtayries, C. Falentin-Daudré and V. Migonney, *Biointerphases* 12, 02C418 (2017).
[35] H. Chouirfa, D. M. Evans, P. Bean, A. Saleh-Mghir, A.-C. Crémieux, D. G. C. Castner, C. Falentin-Daudré and V. Migonney, *ACS Appl. Mat. Interfaces* 10, 1480 (2018).
[36] K. Zhang, J.A. Li, K. Deng, T. Liu, J.Y. Chen andN. Huang, *Biointerfaces* 108, 295 (2013).
[37] G. Helary, F. Noirclere, J. Mayingi and V. Migonney, *Acta Biomater.* 5, 124 (2009).
[38] N.P. Peksheva and V.M. Strukov, *Russ. Chem. Rev.* 48, 1092 (1979).

CHAPTER III

Ultraviolet irradiation modification of poly (methyl methacrylate) titanium grafted surface for biological purpose

III.1. Chapter III overview

This research theme is part of an ANR-DFG project, named BIOSMS and is multi-disciplinary, involving inorganic chemistry, polymer chemistry, surface physics, mechanics, biology and surgery. It therefore required the establishment of numerous collaborations with French partners such as “Institut de Physique et Chimie des Matériaux de Strasbourg” (ICPMS) in Strasbourg and European partners such as the Institut für Metallurgie (IMET) of the Technical University of Clausthal-Zellerfeld (Germany).

The idea of the project was to graft polymers (PMMA) onto the surface of the metal using the "grafting from" process to obtain a biocompatible interface. The proof of concept was carried out with poly(methyl methacrylate) (PMMA) in the form of a sheet inserted between two grafted titanium plates for the production of Ti/PMMA/Ti SMs. The grafted PMMA layers, as strong bonding adhesives between the polymer and Ti, are fundamental for the final shaping of the SMs without early delamination. The adhesion between the polymer and the titanium sheets was created using a grafting from strategy. Furthermore, as PMMA and Ti are biocompatible but biologically inert, it is possible to increase the biocompatibility and osseointegration of the SMs by incorporating sodium 4- styrene sulfonate (NaSS) units into the polymethacrylate alkyl chains by post-functionalization of the latter. Potentially easier to shape and presenting a priori a better osseointegration, these new SMs were designed and developed in this work and they constitute the second generation of SMs (PNaSS-Ti/P(MMA-ran-BMA)/Ti-PNaSS).

In this Chapter, we present :

1. The strategy to chemically modify PMMA chains previously grafted onto Ti surfaces *via* covalent grafting methods in order to graft bioactive polymers.
2. The evaluation of bone cells response on Ti-PMMA and Ti-PMMA-PNaSS.
3. The application of the chemically modify PMMA strategy and the biological response in the ANR BIOSMS context.

III.2. Article 2: Ultraviolet irradiation modification of poly(methyl methacrylate) titanium grafted surface for biological purpose, Colloids and Surfaces A: Physicochemical and Engineering Aspects.

655 (2022) 130295. https://doi.org/10.1016/j.colsurfa.2022.130295.

Contents lists available at ScienceDirect

Colloids and Surfaces A: Physicochemical and Engineering Aspects

journal homepage: www.elsevier.com/locate/colsurfa

Ultraviolet irradiation modification of poly(methyl methacrylate) titanium grafted surface for biological purpose

Caroline Pereira [a], Claire Semedo Da Moura [a], Adele Carradò [b], Celine Falentin-Daudre [a,*]

[a] Université Sorbonne Paris Nord, Institut Galilée, LBPS/CSPBAT, CNRS UMR 7244, Villetaneuse, France
[b] Université de Strasbourg, Institut de Physique et Chimie des Matériaux de Strasbourg (IPCMS), CNRS UMR 7504, Strasbourg, France

Abstract

The modification of the surface of pure titanium (Ti) implant by grafting biomimetic polymers offers the possibility of camouflaging the synthetic origin of the implant to bone cells. In our previous studies, we have shown that with ultraviolet irradiation (UV) technology, polymers such as poly (methyl methacrylate) (PMMA) and poly (sodium styrene sulfonate) (PNaSS) can be selectively grafted onto Ti surfaces. This technology offers the possibility to photochemically modify Ti-PMMA grafted surfaces by UV light with the formation of carboxylic acid groups that will allow the grafting of PNaSS. A biological study of functionalized Ti-PMMA-PNaSS surfaces in contact with bone cells was performed along with the physico-chemical characterizations of the functionalization. The Fourier-transformed infrared spectra recorded in an attenuated total reflection (FTIR-ATR) results confirmed that carboxylic acid sites (-OH, -C=O, -COOH) were incorporated into the surface during UV light exposure. Moreover, the morphological images obtained with environmental scanning electron microscopy (SEM), the differentiation and mineralization results showed an improvement of osteoblast cells spreading on Ti-PMMA-PNaSS grafted surfaces.

Graphical abstract

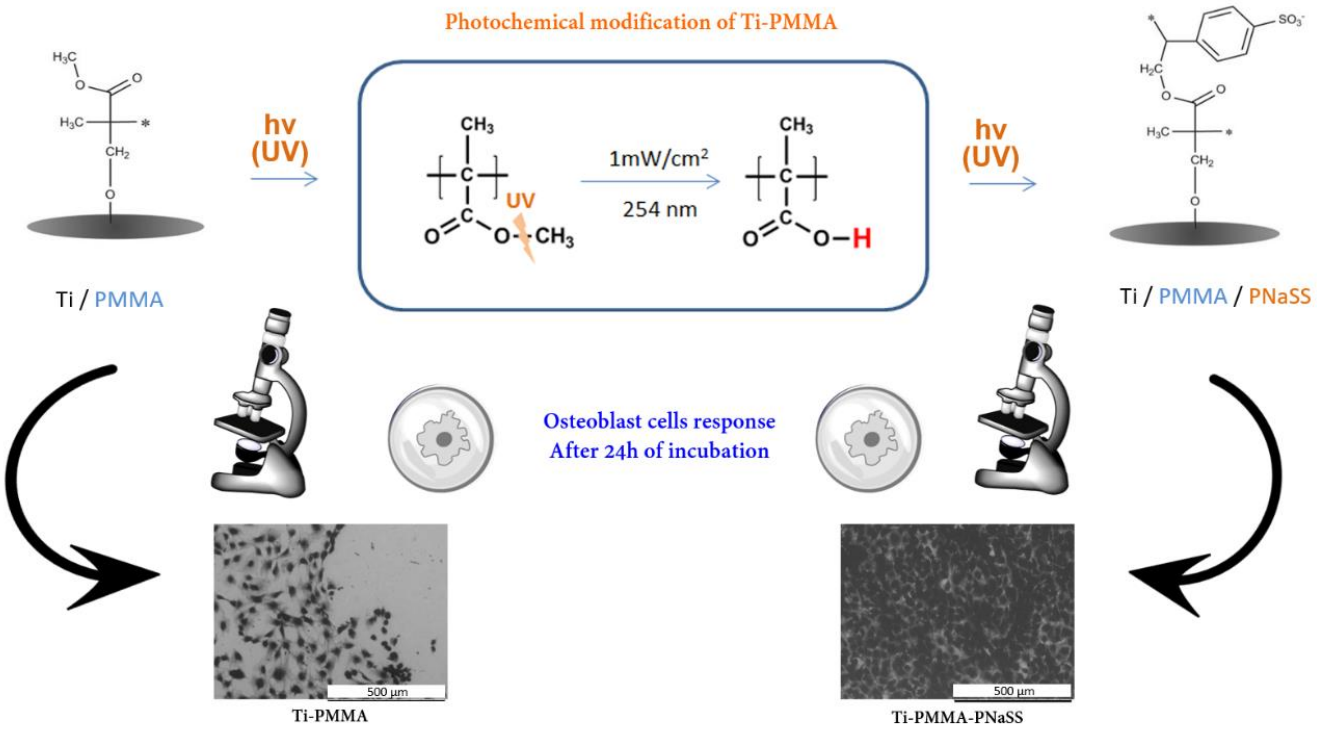

Keywords: Titanium, Poly (methyl methacrylate), Osseointegration, Photochemical Modification, Ultraviolet

1. Introduction

Titanium implants (Ti) are frequently used in the field of biomaterials. Their bio-inert character helps to avoid the encapsulation process encountered when a biomaterial is rejected by the cells [1,2]. In addition, their corrosion resistance and chemical properties make them particularly appealing for building bone substitutes. Another mainly used material in biomedical devices is poly(methyl methacrylate) (PMMA) which is an interesting thermoplastic polymer [3-5]. PMMA $(C_5O_2H_8)_n$ is a synthetic acrylic polymer based on a methyl methacrylate monomer. PMMA and Ti are the most used materials for building craniofacial prostheses. Combining PMMA and Ti in innovative hybrid structures such as sandwich materials is an interesting strategy to obtain functional biomaterials. Those structures often used an epoxy resin to link the polymer to the metal surfaces [6]. The use of epoxy resin cannot be considered for biological applications [7]. Although sandwich structures seem to be well adapted to mechanical properties required in biomaterials, the use of epoxy resin is a serious drawback for *in vitro* biological applications and consequently for *in vivo* applications. Kostoryz et al. [7] have shown

that cytotoxic responses was due to toxic leach. These leachables may arised from the unpolymerized resin components. Therefore, Reggente *et al* have designed epoxy resin-free sandwich materials by directly grafting of PMMA to Ti surfaces [8]. The main concern of the use of PMMA is its hydrophobic nature. Hydrophobic surfaces modify the conformation of certain plasmatic proteins, which causes bacteria to adhere to the surface [9-11]. Thus, it is necessary to modify the PMMA wettability to limit bacteria adhesion for biological ap plications.

The hydrophilic/hydrophobic character is a parameter that influences cellular interactions at the material/bone tissue interface. In fact, researchers have shown that bone tissue cells prefer to grow in contact with hydrophilic surfaces [12,13]. A large number of studies have been performed to modify the surface of polymer in order to obtain hydrophilic surfaces. These can be categorized as mechanical, chemical and physicochemical methods [14]. Some ways consist of the use of high-energy treatment such as plasma [15], irradiation with ion beam [16], or corona discharge [17]. These methods can introduce hydroxyl groups to the polymer surface, making the material hydrophilic. Another intriguing functionalization process is to attach hydrophilic polymers to the PMMA-grafted titanium surfaces. Wet chemical treatments offer the possibility to coat or graft some polar functionalities onto the polymer surface.

By referring to the literature, the photochemical surface modification protocol for PMMA has been developed to fabricate of biological devices [18]. It has been found that carboxylic acid groups are formed upon UV exposure to PMMA surfaces, and the resulting carboxylic acids functions allow for further functionalization of PMMA-based devices. Photo-induced modification appears to be a simple handling and low-cost technique. This method is advantageous for simply grafting a bioactive polymer such as poly(sodium styrene sulfonate) (PNaSS) that will improve the biological response of the Ti/PMMA/Ti sandwich material (Fig.1.). This strategy aims to obtain implants with good bone anchorage offering proper mechanical performance in a relatively short time [19, 20]. It is thus a question of optimizing the osseointegration of the implant from its implantation to avoid its fibrous encapsulation by the cellular tissue. Moreover, polymer grafting allows preserving the underlying solid substrate's geometry and mechanical characteristics.

The work described in this article uses a method to modify Ti-PMMA surfaces by chemically grafting PNaSS. The Ti surfaces before and after the functionalization were characterized by

applying Attenuated Total Reflection-Fourier Transform Infrared Spectroscopy (ATR-FTIR), Water Contact Angle measurements (WCA) and Toluidine Blue colorimetric method (TB). Furthermore, *in vitro* investigations on MC3T3-E1 osteoblast cells were assessed to evaluate how the grafted Ti-PMMA-PNaSS surfaces influenced cell adherence, spreading, and differentiation.

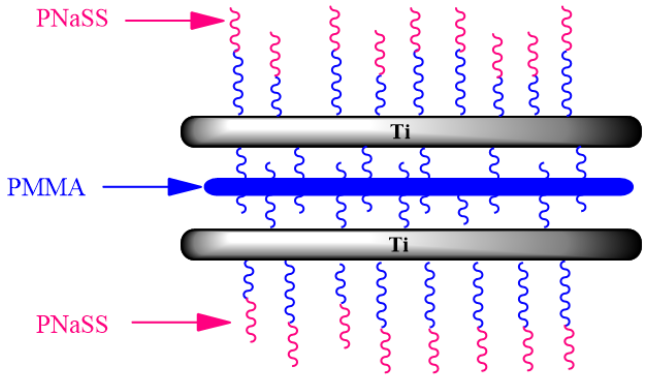

FIGURE 3.1 SCHEMATIC STRUCTURE OF TI/PMMA/TI STRUCTURES AND THE STRATEGY EMPLOYED TO GRAFT A BIOACTIVE POLYMER

By referring to the literature, the photochemical surface modification protocol for PMMA has been developed to fabricate of biological devices [16]. It has been found that carboxylic acid groups are formed upon UV exposure to PMMA surfaces, and the resulting carboxylic acid functions allow for further functionalization of PMMA-based devices. Photo-induced modification appears to be a simple handling and low-cost technique. This method is advantageous for simply grafting a bioactive polymer such as poly (sodium styrene sulfonate) (PNaSS) that will improve the biological response of the Ti/PMMA/Ti sandwich material (**Figure 3.1**). This strategy aims to obtain implants with good bone anchorage offering proper mechanical performance in a relatively short time [17,18]. It is thus a question of optimizing the osseointegration of the implant from its implantation to avoid its fibrous encapsulation by the cellular tissue. Moreover, polymer grafting allows preserving the underlying solid substrate's geometry and mechanical characteristics.

The work described in this article uses a method to modify Ti-PMMA surfaces by chemically grafting PNaSS. The Ti surfaces before and after the functionalization were characterized by applying Attenuated Total Reflection-Fourier Transform Infrared Spectroscopy (ATR-FTIR),

Water Contact Angle measurements (WCA) and Toluidine Blue colorimetric method (TB). Furthermore, *in vitro* investigations on MC3T3-E1 osteoblast cells were assessed to evaluate how the grafted Ti-PMMA-PNaSS surfaces influenced cell adherence, spreading, and differentiation.

2. Materials and Methods

2.1. Materials

All chemical products used to conduct this study were obtained from commercial suppliers.

One and half-centimeter diameter with one-millimeter thickness, commercially pure, grade 2 titanium (99.6% purity) was manufactured by the company Goodfellow (Lille, France).

The commercial methyl methacrylate (MMA) solution used was supplied by Sigma-Aldrich. This solution contains polymerisation inhibitors. MMA was purified over a basic alumina column to remove the stabilizer. The purified MMA was then stored at 4° C until it is used.

Sodium styrene sulfonate (NaSS, Sigma) was purified by recrystallization in a combination of ethanol/water (Carlo Erba) (10: 90 v/v) overnight at 70 °C. The product was filtered and then dried overnight at 50 °C under air pressure and kept at 4° C as described in our previous article [18–20].

2.2. Methods

2.2.1. Polishing, cleaning and stripping of titanium surfaces

To remove the metal thickness damaged by machining, mechanical polishing of both sides of Ti surfaces was carried out using a mechanical arm mounted on a rotary polisher (Struers). A first polishing was done with a 500 grit SiC paper (30 µm grit). The polishing was then refined using a lower grit paper of grade 1200 (15 µm grit).

The surfaces were then ultrasonically washed for 15 minutes at room temperature with solutions of acetone, cyclohexane, isopropanol, and distilled water (dH_2O) to make sure there was no sign of polishing inclusions.

Titanium has the particularity of forming a layer of titanium oxide very quickly in contact with air. To remove this oxide layer, the titanium surfaces were etched for 1 minute under agitation in a Kroll solution composed of 2% hydrofluoric acid HF, 10% nitric acid HNO_3, and 88% dH_2O. After stripping, the surfaces were cleaned 5 times in distilled water baths under ultrasound. The titanium samples were then dried in an oven at 50 °C during 2 hours and used immediately for the various grafting processes envisaged.

2.2.2. Procedure for activating titanium surfaces

Briefly, Ti substrates were chemically oxidized by immersion with an acidic solution (H_2SO_4/H_2O_2 50:50 v/v, Sigma) at room temperature. This step activates the surfaces with hydroxide groups and peroxide radicals. The first reagent (H_2SO_4) was first poured with the titanium surfaces for 1 minute with stirring, then the second reagent (H_2O_2) was introduced into the beaker for 3 minutes. The reaction was immediate and strongly exothermic with a gas release. Initially, the oxidation solution is colourless, then it turns yellow and orange. This colouring is explained by the reaction of sulphuric acid on the titanium and the formation of $Ti4^+$ ions. The Ti surfaces were then rinsed with distilled water to remove all traces of the oxidation solution. The surfaces were directly used for the next steps of chemical functionalization.

2.2.3. Grafting procedure of MMA onto titanium surfaces

Methyl methacrylate (MMA) with a concentration of 1.5 M – purified from its stabilizer by column chromatography on basic aluminum oxide – was added to 100 mL round bottom flask containing dimethyl sulfoxide (DMSO) solvent. The solution was degassed with argon for 30 min, and then the activated Ti surfaces were rapidly introduced in the solution. The round bottom flask containing the MMA/DMSO solution and the Ti surface was irradiated with UV light (365 nm, 160 mW/cm ^{2}) at ambient temperature with stirring for 1 h. The grafted surfaces were then rinsed for 48 h with dH_2O and dried overnight at 37 °C before any characterization.

2.2.4. Cleavage protocol and grafting of PNaSS onto Ti-PMMA surfaces

The methodology used for the protocol is outlined in **Figure 3.2** and is as follows. First, the PMMA-grafted Ti surfaces were placed in an isopropanol bath for 15 minutes under ultrasound. Then, the surfaces were exposed to UV light in an aqueous distilled water solution in order to cleave the -O-CH_3 bonds of the copolymer to form hydroxyl groups – OH. The lamp used in

this procedure was a thin layer chromatography (TLC) lamp (MilliporeSigma 254 nm, 1 mW/cm ^{2}). In the literature, the cleavage kinetics are adapted to the powers used. The higher the power of the UV lamp, the shorter is the exposure time required for cleavage. Two types of kinetics have been studied, for a UV exposure power of 15mW/cm ^{2}, only 30 min are needed to cleave the PMMA chains [20] and obtain the hydroxyl function on the surface. For lower powers of the order of 1mW/cm ^{2} [21], an exposure of at least 2h is required to obtain the cleavage of the PMMA and the hydroxyl functions on the surface. The kinetics of the exposure time of UV irradiation was evaluated. With a power of 1 mW/cm ^{2}, 2h of exposure is required to observe hydroxyl groups. The creation of hydroxyl groups then allows the grafting of NaSS. The grafting of NaSS is done according to the protocol of Falentin-Daudré *et al.* [18]. The surfaces were then immersed in a degassed and aqueous solution of NaSS monomers (0.7M). The round-bottomed flask containing the samples was placed under UV irradiation (365 nm, 160 mW/cm ^{2}) at room temperature with stirring for 1h. Finally, the grafted surfaces were then rinsed for 48h with distilled water.

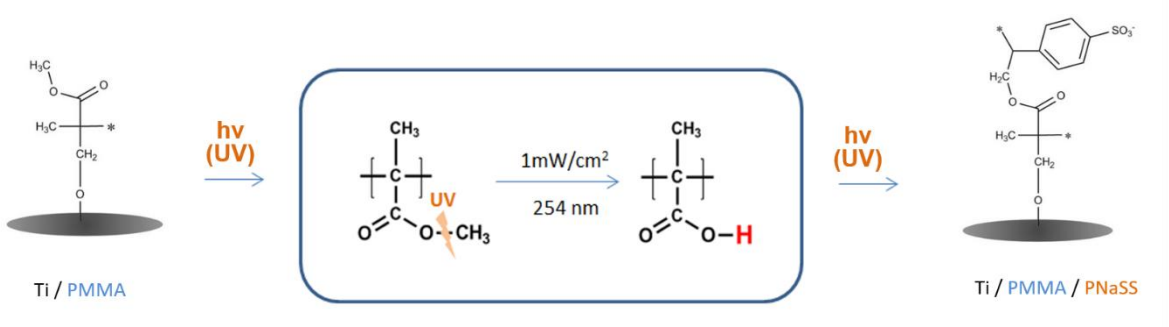

FIGURE 3.2 THE METHODOLOGY USED TO DESIGN THE TI-PMMA-PNASS GRAFTED SURFACES: PHOTOCHEMICAL MODIFICATION OF PMMA UNDER UV AND DIRECT GRAFTING OF PNASS

2.3. Surface characterization

To assess the functionalization of Ti-PMMA grafted surfaces with PNaSS, each step was followed by attenuated total reflection Fourrier-transform infrared spectroscopy (ATR-FTIR), water contact angle measurement (WCA), and the toluidine blue (TB) colorimetric method.

The Fourier-transformed infrared (FTIR) spectra were recorded between 4000 and 600 cm^{-1}, in attenuated total reflectance (ATR) mode. Ti samples were put in contact against a diamond crystal (4000-500 cm$^{-1)}$ for acquirements (512 scans). For the presentation of the spectrum, each one of them then fitted and analyzed.

The change in wettability after each step of the surface treatment was analyzed by WCA measurements, by using DAS10 goniometer from Kruss. For each measurement, 2 µl of dH_2O was dropped onto the surface. The image of the drop was taken 20 seconds after the water drops contact with the surface. The WCA was then measured by the software from the image taken. 3 measurements were taken and averaged.

To characterize the quantification of PNaSS grafted onto Ti surfaces, toluidine blue (TB) colorimetric technique was carried out according to the protocol established by Helary *et al* [19]. TB is a chromophore molecule that absorbs in the visible at 633 nm. This molecule has the particularity to complex *via* its $N^+(CH_3)_2$ groups with anionic groups (sulfonate SO_3^- group of the NaSS). PNaSS grafted and washed samples were immersed in the dye solution (0.5 mM at pH =10) for complexation for 6 hours at 30 °C. The excess of TB was removed with 3 washings with a solution of NaOH (10^{-3} M, three times 5 minutes). Then, complexed TB sample surfaces were de-complexed by putting the samples in acetic acid/water solution (50/50 v/v) for 24h at room temperature. The concentration of TB was then quantified by UV-visible spectroscopy (PerkinElmer lambda 25 spectrometer). TB assays were carried out onto six samples for each condition.

2.4. Preparation of titanium surfaces for biological assays

All substrates (non grafted Ti (Ti NG), oxidised Ti (Ti-OH), Ti-PMMA and Ti-PMMA-PNaSS grafted surfaces) were cleaned and sterilized before interaction with the osteoblast cells. Ti disks were washed for three hours with phosphate-buffered saline solution (PBS, Gibco), followed by 10-minute wash with ultra-pure water. This step will allow the removal of superficial impurities and the equilibration of the surfaces at physiological pH. The second step is followed by UV sterilisation: for 15 min, each side of the Ti substrates was sterilized using an ultraviolet germicidal lamp (UV, 30 W, 254 nm). Then, the samples were kept overnight on well-plates with Gibco's Dulbecco's Modified Eagle's Medium (DMEM). Finally, the samples were put in wells with enriched DMEM medium (1% penicillin, 1% glutamine, 10% fetal bovine serum) and kept until the experiments began. These steps will balance the surfaces in ions and proteins before the contact with the cells.

2.5. Osteoblastic cell culture

All the tests were conducted using pre-osteoblast MC3T3-E1 cells procured from the American Type Culture Collection. The cells were cultivated according to the protocol established by

Felgueiras *et al* [22]. The media was replaced twice per week. All of the investigations employed just early passage cells. To separate cells, trypsin-EDTA (Gibco) was used. All studies used a cell loading dose of 1 x 10^5 cells/ml, with 1 ml of cell suspension introduced onto each Ti surface. The analysis of variance was used to analyze the data.

2.5.2. Cellular spreading and morphology

Ungrafted, oxidized Ti-PMMA, and Ti-PMMA – after 1 hour, 4 hours, and 24 hours of incubation using environmentally controlled scanning electron micrographs (ESEM – Hitachi TM3000). The cell morphology on the surface of the PNaSS graft was analyzed. The Ti surfaces were cleaned in PBS after being withdrawn from the culture. The cells were fixed for 30 minutes at 4° C with 4% formalin (Sigma) in PBS.

2.5.3. Differentiation: Alkaline phosphatase activity

The ALP is a precursor to the development of osteoblasts. After seven and fourteen days of culturing, the activity of the sample was measured after it was converted to p-nitrophenol at 37 °C. Use a Triton x 100 to detach the enzyme from the cell membrane for 1 hr with agitation. The cell suspension was coupled in the same amount with 20 mM p-nitrophenyl phosphate substrates in 2-amino-2-methylpropanol buffer and kept at 37 °C for 30 min. UV-vis spectrometer set at 405 nm was used to measure the amount of p-nitrophenol generated (Perkin-Elmer). The enzyme activity was normalized to protein mass and expressed in nmol of p-nitrophenol generated per minute (expressed in mg.). A commercially available colorimetric assay was used to determine the amount of ALP in the sample (Bio-Rad protein kit assay).

2.5.4. Extracellular matrix mineralization: Calcium production

Calcium deposits were assessed for mineralization after 3 and 4 weeks of culture. The Ti surface was cleaned with PBS and then transferred to a fresh well containing 1 ml of 15% trichloroacetic acid solution to dissolve calcium-phosphate crystals. To test the calcium concentration, a small amount of the supernatant was added to a sample of arsenazo-III (0.2 mM in PBS) after 1 hour of gentle shaking. The calcium concentration was estimated by comparing the absorbance at 650 nm with a standard linear curve for $CaCl_2$ in trichloroacetic acid (15% w/v) from 50 to 1000 μg. ml^{-1}.

2.6. Statistical analysis

Each experiment was carried out three times and yielded the same findings. The data were provided as mean standard deviation with n = 9. The standard deviations are indicated by the error bars in the graphs. A one-way analysis of variance (ANOVA) was used to compare grafted and non-grafted samples, followed by a multiple comparison correction using the Tuckey test. A p-value < 0.05 was deemed significant.

3. Results and discussion

3.1. Kinetics studies of Ti-PMMA cleavage procedure and photochemical functionalization with PNaSS

In order to set up the cleavage protocol for Ti-PMMA surfaces, a kinetic study based on conditions found in the literature was established. For this purpose, the Ti-PMMA surfaces were exposed to UV with a power density of 1 mW/cm ^{2} in distilled water at three different times: 2h, 3h, and 4h. The preferred characterization to ensure efficient grafting of NaSS onto the cleaved Ti-PMMA surfaces is to determine the grafting density of NaSS by the toluidine blue colorimetric technique. The results of this study are presented in **Figure 3.3** The time of exposure of the surfaces to UV seems to play an important role. For 2h of UV exposure, the grafting density of PNaSS is 8 µg. cm ^{2}, then drops to 5.2 µg. cm^{-2} for 3h of exposure and finally 4 µg. cm^{-2} for 4h of UV exposure. The best grafting density was thus obtained for a 2h UV exposure time.

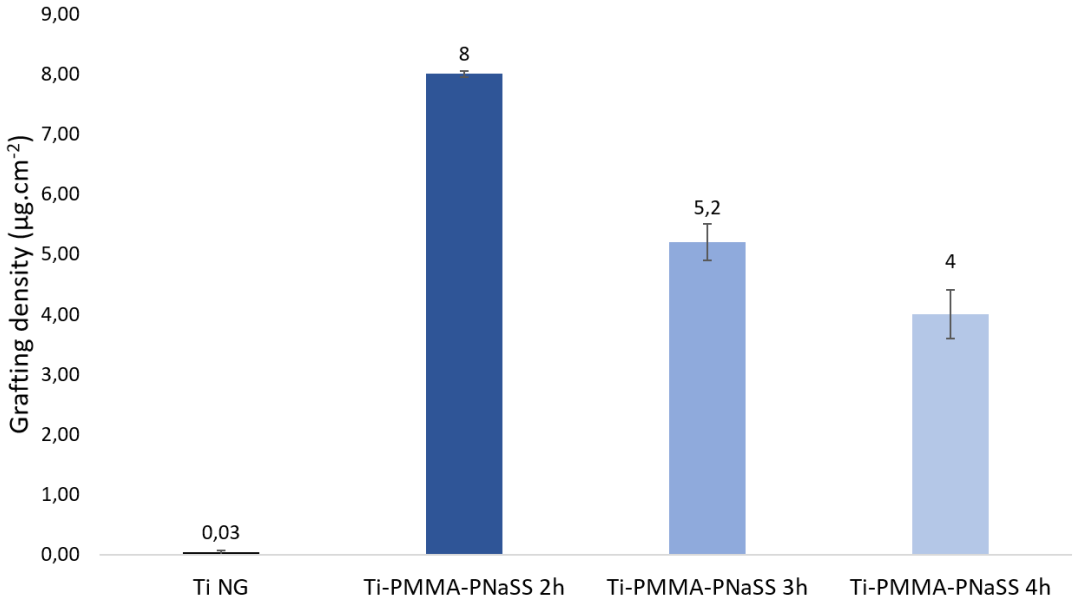

FIGURE 3.3 TB COLORIMETRIC ASSAY RESULTS AFTER UV EXPOSURE OF THE TI-PMMA SURFACES IN DISTILLED WATER WITH DIFFERENT KINETICS: 2H, 3H AND 4H

In a second step, another cleavage protocol was tested to promote the cleavage of the PMMA chains. The Ti-PMMA surfaces were washed with an ultrasonic bath in isopropanol. The isopropanol was chosen to exalt the PMMA chains to promote their cleavage. By exposing them for 2h to UV radiation, the result obtained after grafting with PNaSS is presented in **Figure 3.4** The ultrasonic isopropanol bath prior to cleavage significantly increased the graft density of PNaSS to 13.3 µg. cm^{-2}. Without the use of isopropanol, the grafting density was 8 µg. cm^{-2}. This protocol was therefore validated to allow a better grafting of PNaSS on cleaved Ti-PMMA surfaces. Ungrafted (Ti NG), and PMMA-grafted (Ti-PMMA) titanium surfaces were used as controls. The toluidine blue dye complexed via its $N^+(CH_3)_2$ groups with anionic groups. No coloration was observed on the control surfaces confirming that the coloration obtained on the grafted samples is only due to the decomplexation of the Toluidine Blue from the sulfonate functions. As for the cleaved Ti-PMMA surfaces, the grafting density obtained is around 0.5 µg. cm^{-2}. Theoretically, Toluidine Blue should be complex with the carboxylate groups. One of the hypotheses foreseen forward to explain this is that very few carboxylate groups are formed to quantify them by this method. On the other hand, it could also be explained by the fact that the dye molecule is not complex with the carboxylic acids because the carboxylic acids remain in their – COOH form instead of in the $-COO^-$ form.

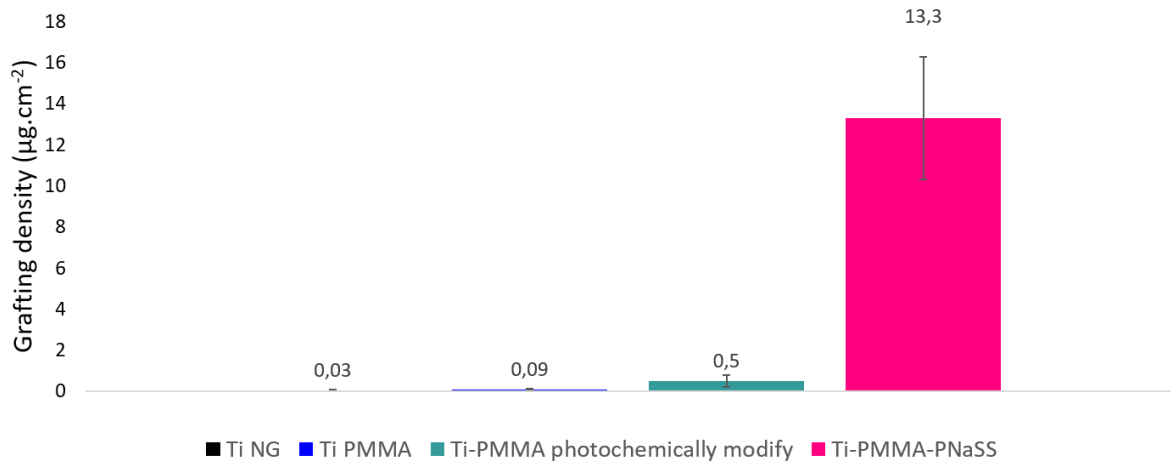

FIGURE 3.4 TB COLORIMETRIC ASSAY RESULTS OF THE TI-PMMA MODIFIED SURFACES WITH ISOPROPANOL PROTOCOL

The advantage of the colorimetric test result is that it allows us to report on the grafting efficiency of PNaSS on photo-modified Ti-PMMA surfaces. In conclusion, with this technique, the formation of a complex between TB and the sulfonate groups, apart from any other chemical group (TiO_2, TiOH), made it possible to demonstrate the grafting and the quantification of these groups on Ti-PMMA surfaces. The result of the grafting density of Ti-PMMA-PNaSS surfaces is promising and makes it possible to account for the grafting efficiency of PNaSS on photo-modified Ti-PMMA surfaces.

3.2. Chemical characterization of grafted Ti-PMMA surfaces with PNaSS

FTIR and WCA were assessed to verify the presence of PNaSS on Ti-PMMA photochemically modified surfaces.

Infrared spectroscopy is a fast and efficient method of determining the characteristic bands of surface-grafted polymers in a non-destructive manner. The infrared spectra of Ti NG, Ti-PMMA, Ti-PMMA photochemically modified, and Ti-PMMA-PNaSS are shown in **Figure 3.5**

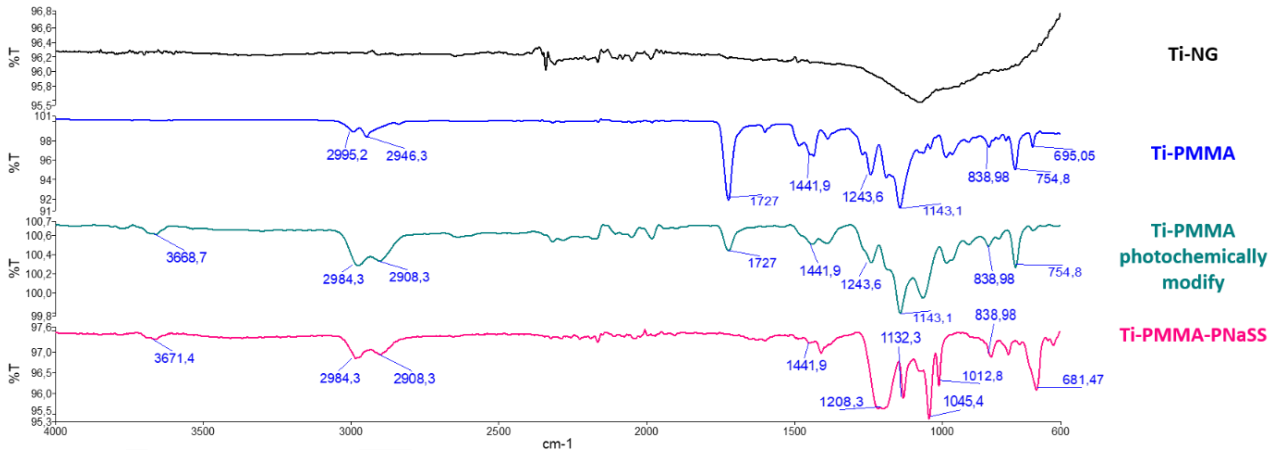

FIGURE 3.5 FTIR-ATR SPECTRA OF NON GRAFTED TI (TI NG), PMMA GRAFTED TI (TI-PMMA), TI-PMMA PHOTOCHEMICALLY MODIFY AND TI-PMMA-PNASS

Only a peak at about 1100 cm^{-1} is observed on the ungrafted Ti. This peak is attributable to the presence of an oxygen film which forms spontaneously in contact with air. The curve for Ti-PMMA shows the grafting of PMMA onto the previously oxidized titanium with the presence of the characteristic PMMA groups: the α-methyl group vibrations (C-CH_3) at 2995 cm^{-1} and 2946 cm^{-1} , the signal of the carbonyl group peak (C=O) at 1727 cm^{-1}, , O-CH_3 and C-CH_3

bending vibration at 1441 cm^{-1}, the C-O-C bending at 1243-1143 cm^{-1} and the C-O bond stretching at 1143 cm^{-1}. Most important changes in FTIR-ATR spectrum on the effect of the photochemical modification of Ti-PMMA occurred in the range of 3700-3100 cm^{-1}. The absorption peak at 3668 cm^{-1} is attributed to OH stretching vibrations and demonstrates an increase of oxygen functionalities on the surface. This peak is essential to allow the grafting of the PNaSS. In fact, the spectrum of Ti-PMMA-PNaSS attests the presence of PNaSS with the characteristic peaks found in the literature. The vibrations of the aromatic ring characterize PNaSS, and the symmetric vibrations of the SO_3^- groups generated a NaSS doublet (O=S=O) located at 1013 cm^{-1} and 1044 cm^{-1}. Moreover, there is the presence of asymmetric vibrations of the SO_3^- groups with peaks at 1200-1185 cm^{-1} and 1130 cm^{-1}. All the information revealed by the infrared analysis of the Ti surfaces attests to the success of the surface functionalization.

In addition, the hydrophilicity/hydrophobicity of the surface was measured by the water contact angle (WCA) method (**Figure 3.6**). The treatment of the titanium surface with the H_2SO_4/H_2O_2 acid mixture results in a decrease in the contact angle: from 53°±2 on non-grafted titanium to 25°±4 after oxidation. This oxidation thus increases the hydrophilic character of the Ti surface. Subsequently, the PMMA-grafted surfaces show a contact angle of 90°. This is easily explained because PMMA is a hydrophobic polymer (presence of the CH_3 type group). The Ti surface will therefore become hydrophobic after the grafting of PMMA. To overcome this hydrophobic character of PMMA, our study aimed to graft a hydrophilic polymer such as PNaSS. After grafting PNaSS onto the Ti-PMMA surfaces, it is satisfying to observe that the contact angle decreases by 57%. The surface goes from a contact angle of 90°±2 to 20°±5, which represents a decrease of 70°.

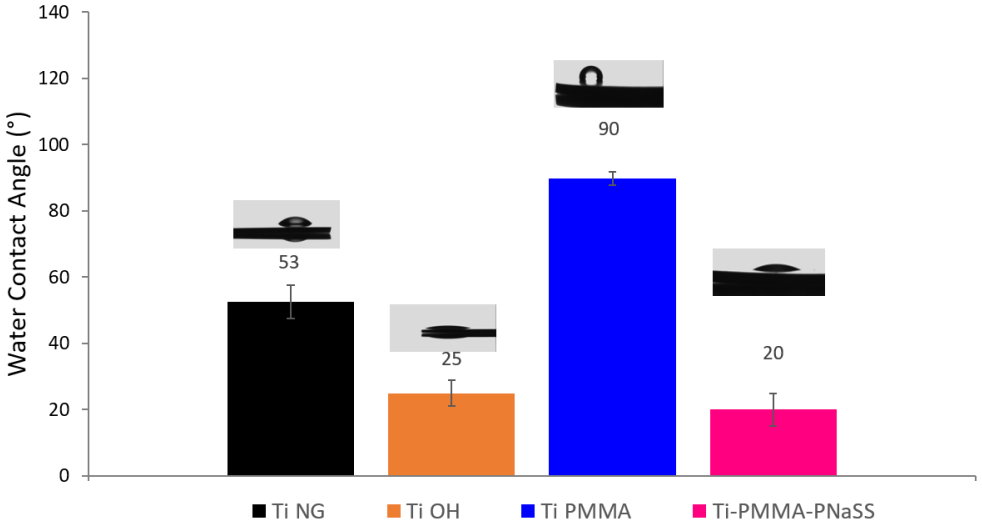

FIGURE 3.6 WCA MEASUREMENTS RESULT FOR IMPORTANT STEP OF THE PROCEDURE: TI-NG, TI-OH, TI-PMMA AND TI-PMMA-PNASS

Thanks to the results of the FTIR and WCA techniques described above, it was possible to show the implemented protocol's effectiveness. The presence of PNaSS on the Ti-PMMA surfaces was revealed by the presence of the characteristic groups of this polymer and its hydrophilic character. These results confirm those given by the toluidine blue assay. Thus, it is possible to obtain chemically modified Ti-PMMA surfaces to graft a bioactive polymer such as PNaSS onto them.

3.3. Cellular spreading and morphology

The second part of our study focused on the response of osteoblastic cells to the functionalization of Ti-PMMA surfaces by PNaSS. MC 3 T3-E1 cells were chosen for their ability to proliferate rapidly and express osteoblastic functions. Many authors have studied them regarding adhesion, proliferation, spreading, and differentiation.

Cell morphology and cytoskeletal organisation were observed by environmental scanning electron microscopy (SEM) at 1h, 4h and 24h incubation on Ti-NG, Ti-OH, Ti-PMMA and Ti-PMMA-PNaSS surfaces. The results obtained are presented in **Figure 3.7.**

The early osteoblast cells spreading and morphology were acquired 1h after incubation. The results at 1h shown round-shaped morphology for non-grafted, oxidized and PMMA grafted titanium surfaces. A more polygonal shape is observed for the Ti-PMMA surfaces grafted with

PNaSS. At 1h of contact, most of the cells are still initiating their interaction with the surface and therefore exhibit a round shape. Interestingly, PNaSS was seen to intensify cell spreading even at this early stage. Moreover, osteoblast cells appeared to be more confluent on Ti-PMMA-PNaSS surfaces. According to Kowalczynska [23] sulfonic acid groups improve the short-term adhesion of the cells. Our results confirm this observation at 1h of incubation.

After 4h of incubation, osteoblast cells were more prominent on Ti-PMMA-PNaSS surfaces. Moreover, the cells cover the entire area of the Ti-PMMA-PNaSS surfaces. The behavior of osteoblast cells on ungrafted Ti and Ti-PMMA surfaces was different. In fact, on these surfaces, the cells started to form some zones where they are grouped together, whereas there are areas where the cells do not spread. his observation can be explained by the fact that non-grafted Ti and Ti-PMMA surfaces are hydrophobic, so the cells do not entirely spread of these types of surfaces. In contrast, Ti-OH and Ti-PMMA-PNaSS are hydrophilic surfaces and therefore allow the growth of osteoblast cells.

After 24h of incubation, the same pattern as 4h of incubation is observed for Ti NG and Ti-PMMA surfaces. Their morphology is flattened and does not exhibit the polygonal shape usually observed on osteoblast cells. For the Ti-PMMA-PNaSS surfaces, the osteoblast cells appeared to cover the entire surface.

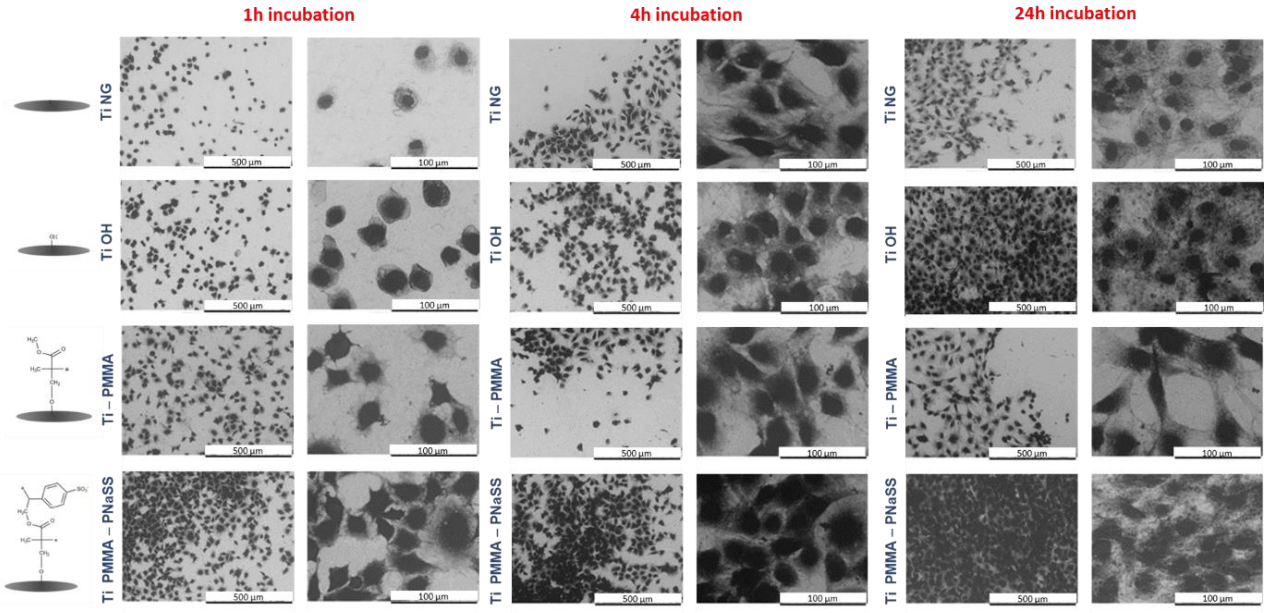

Figure 3.7. Morphological results with environmental scanning electron microscopy (SEM) at 1h, 4h and 24h of incubation on non-grafted, oxidized, Ti-PMMA and Ti-PMMA-PNaSS surfaces.

The main goal of this research was to illustrate the benefit of PNaSS grafting on Ti-PMMA surfaces on osteoblast cells. The osteoblast cell morphology and spreading through SEM were performed in this context. The SEM images obtained for Ti-PMMA-PNaSS surfaces with osteoblast cells showed an improvement in cell morphology and spreading. These results underline the importance of grafting a bioactive polymer to improve osseointegration.

3.4. Differentiation and mineralization

In the previous study, we described the morphology of MC3T3-E1 cells on ungrafted and functionalized titanium surfaces for short incubation times (1h, 4h and 24h). It is now necessary to study the behavior of these same cells over more extended periods (14 days and more), which will give us indications of their differentiation or their evolution into bone cells depending on the surface on which they are seeded. During osteoblastic differentiation, the cell goes through different states expressing specific markers. Two markers have been studied: alkaline phosphatase activity and the precipitation of calcium phosphate, to estimate osteoblastic cells' capacity to mineralize and to lead to bone formation (**Figure 3.8.**).

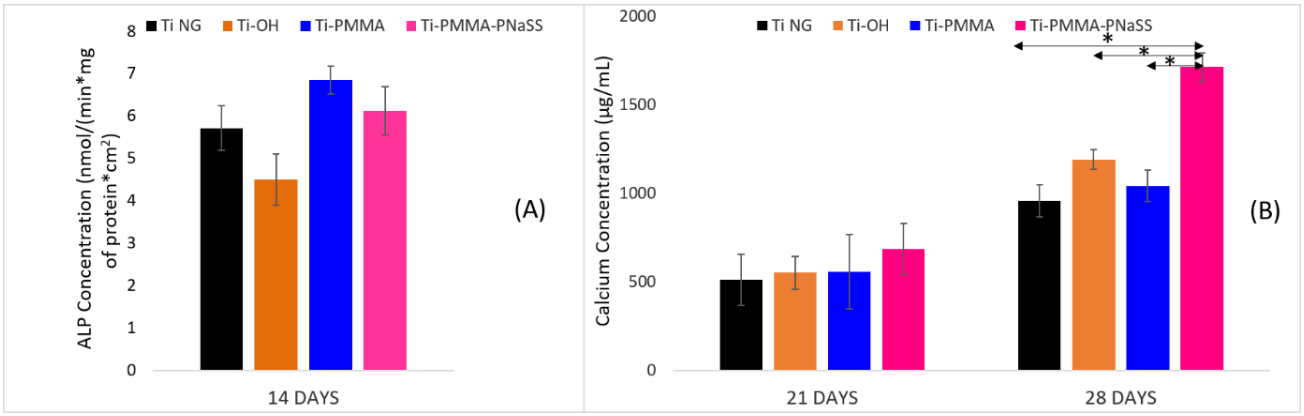

Figure 3.8. ALP activity (A) and mineralization assay (B) of MC3T3-E1 osteoblast cells onto titanium surfaces (Ti NG, Ti-OH, Ti-PMMA and Ti-PMMA-PNaSS) after 14, 21 and 28 days of culture.

The measurement of alkaline phosphatase is widely studied as a marker of cell differentiation and is usually performed after day 14 of culture once proliferation is complete and confluence is reached [17]. Therefore, the alkaline phosphatase activity of MC3T3-E1 cells was measured after 14 days regardless of the surface area. Alkaline phosphatase is an enzyme present in the cell membrane, capable of releasing phosphate into the extracellular matrix, leading to bone

mineralization by precipitation of calcium phosphate. The analysis of the results showed that the grafting of polymers, independent of the nature of the polymer bound to the titanium, improves the activity of ALP in comparison with non-grafted titanium. These results concord with previous work carried out in the laboratory indicating that the presence of sulphonate and carboxylate functions improves alkaline phosphatase activity. ALP concentration is around 6.9 nmol/min/mg protein*cm ^{2} for Ti-PMMA surfaces and around of 6 nmol/min/mg*cm ^{2} for Ti-PMMA-PNaSS surfaces. One hypothesis to explain this difference is related to the ability of PNaSS to enhance the second stage of the differentiation process.

The second marker of cell differentiation studied was the determination of calcium phosphate. Indeed, the calcification stage, which is the last phase of bone formation, corresponds to the precipitation of calcium phosphate, the last stage of MC3T3-E1 differentiation. When the phosphate released by alkaline phosphatase activity reaches a concentration threshold, it spontaneously precipitates with the calcium present in the medium to lead to the formation of nodules. The time after which calcium should be measured depends on the activity of alkaline phosphatase, which is the first stage of differentiation. Our choice to measure this first stage after 14 days of culture led us to choose a longer time for the determination of calcium. According to the literature, the study of the last stage of differentiation is usually carried out after 20 days of culture [24]. For this reason, the measurement of calcium was performed on days 21 and 28 of culture. Analysis of the results in **Figure 3.8.** showed an increase in the amounts of extracted calcium at 21 days of culture, regardless of the state of modification of the titanium surface. Cells grown on PNaSS grafted surfaces presented slightly better (683 µg/ml) mineralization than the non-grafted surfaces (509 µg/ml). The formation of calcium was favoured at 28 days for Ti-PMMA-PNaSS surfaces indicating that osteoblasts cells' maturation process is significantly improved with the grafting of PNaSS. An increase of 671 µg/ml of calcium concentration is observed for Ti-PMMA-PNaSS compared to Ti-PMMA surfaces. Those results revealed the ability of osteoblast cells to produce more calcium on Ti-PMMA-PNaSS surfaces than those on ungrafted, oxidized and Ti-PMMA surfaces.

ALP activity and calcium mineralization results were assessed to examine osteogenic differentiation of osteoblast cells. Surfaces grafted with PNaSS have been demonstrated to favor the process of the mineralization of osteoblast cells. These results are in accord with those obtained during the morphological study of cells.

4. Conclusion and perspectives

This study focuses on the surface modification of Ti-PMMA grafted substrates with a simple UV photochemical technique. During the modification of Ti-PMMA surfaces, a monolayer of carboxylic functional group formation occurs. This non-destructive surface process further leads to the grafting of bioactive polymers such as PNaSS. FTIR-ATR, WCA, and TB colorimetric method results proved that PNaSS was successfully grafted onto Ti-PMMA surfaces. Biological studies with osteoblast cells have shown that surface activity is enhanced by PNaSS grafting. The better cell spreading demonstrated by the morphological study and the improvement of cell differentiation at 28 days of culture indicate the usefulness of this surface functionalization procedure.

Our research perspectives will extend this process to graft phosphonate-based polymer onto Ti-PMMA surfaces and study the biological response. Moreover, an *in vivo* study in a rat model with mandibular and calvaria implants using this procedure of implant functionalization was performed and is currently under process.

Acknowledgments

This research was supported by the French Ministry of National Education, Higher Education, and Research. The materials used in this study were financed by the ANR-DFG project (ANR-18-CE92-0056-01). We especially thank the ANR DFG for their financial support.

III.4. Conclusion & Perspectives

In this Chapter, we have developed the strategy to chemically modify PMMA chains previously grafted onto Ti surfaces *via* covalent grafting methods in order to graft bioactive polymers. In the ANR context, the objective is to apply this strategy to the “grafting from” technique developed by the IPCMS group (**Figure 3.9**). The continuation of the project is to evaluate the *in vitro* and *in vivo* biological response of the modified sandwich structures (see Thesis Flavien Mouillard).

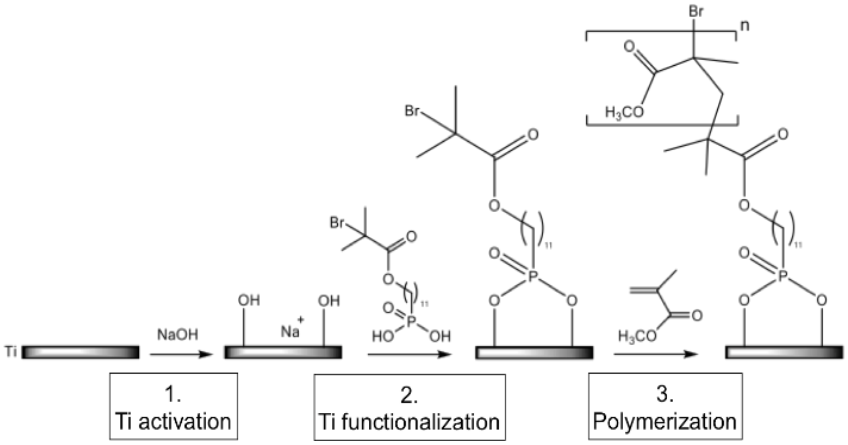

Figure 3.9. Ti-PMMA process developed by IPCMS [7].

III.5. References

[1] M. Esposito, J.-M. Hirsch, U. Lekholm, P. Thomsen, Biological factors contributing to failures of osseointegrated oral implants, European Journal of Oral Sciences. 106 (1998) 527–551. https://doi.org/10.1046/j.0909-8836..t01-2-.x.

[2] A.M. Roos-Jansaker, S. Renvert, J. Egelberg, Treatment of peri-implant infections: a literature review, J. Clin. Periodontol. 30 (2003) 467–485. https://doi.org/10.1034/j.1600-051X.2003.00296.x.

[3] S. A. Soper, S. M. Ford, S. Qi, R. L. McCarley, K. Kelly, M. C. Murphy, Peer Reviewed: Polymeric Microelectromechanical Systems., Anal. Chem. 72 (2000) 642 A-651 A. https://doi.org/10.1021/ac0029511.

[4] T. D. Boone, Z. H. Fan, H. H. Hooper, A. J. Ricco, H. Tan, S. J. Williams, "Plastic advances microfluidic devices", Anal. Chem. 74 (2002) 78A–86 A.

[5] H. Becker, L.E. Locascio, Polymer microfluidic devices, Talanta. 56 (2002) 267–287. https://doi.org/10.1016/S0039-9140 (01)00594-X.

[6] R.F. Landel and L.E. Nielsen, Mechanical properties of polymers and composites. (CRC Press; 1993).

[7] M. Reggente, P. Masson, C. Dollinger, H. Palkowski, S. Zafeiratos, L. Jacomine, D. Passeri, M. Rossi, N. E. Vrana, G. Pourroy and A. Carradò. ACS Appl. Mater. Interfaces 10, 5967 (2018).

[8] A.S. Hoffman, A general classification scheme for "hydrophilic" and "hydrophobic" biomaterial surfaces, J. Biomed. Mater. Res. 20 (1986) ix- xi

[9] H.E. Kaufman, J. Katz, J. Valenti, J.W. Sheets, E.P. Goldberg, Corneal endothelium damage with intraocular lenses: contact adhesion between surgical materials and tissue, Science 198 (1977) 525–527.

[10] B. Feng, J. Weng, B.C. Yang, S.X. Qu, X.D. Zhang, Characterization of surface oxide films on titanium and adhesion of osteoblasts, Biomaterials. 24 (2003) 4663–4670. https://doi.org/10.1016/S0142-9612 (03)00366-1.
[11] S. Takemoto, T. Yamamoto, K. Tsuru, S. Hayakawa, A. Osaka, S. Takashima, Platelet adhesion on titanium oxide gels: effect of surface oxidation, Biomaterials. 25 (2004) 3485–3492. https://doi.org/10.1016/j.biomaterials.2003.10.070.
[12] A. Kruse, G. Krüger, A. Baalmann, O. D. Hennemann, Surface pretreatment of plastics for adhesive bonding. J. Adhes. Sci. Technol. 9 (2012) 1611–1621. https://doi.org/10.1163/156856195X00248.
[13] A. Ridwan-Pramana, P. Marcian, L. Borak, N. Narra, T. Forouzanfar, J. Wolff, *J. Craniomaxillofac. Surg.* 44(1), 34–44 (2016).
[14] A. Sanan, S.J. Haines, *Neurosurg.* 40 (3), 588–603 (1997).
[15] V. D. Virgilio, S. Bermejo and L. Castañer, Wettability Increase by "Corona" Ionization, Langmuir 27 (2011) 9614–9620
[16] Liang C, Liu Y., Liu C., Li X, Chen L., Duan C, Li J, One-step selective wettability modification of PMMA microfluidic devices by using controllable gradient UV irradiation (CGUI), Sensors and Actuators: B. Chemical https://doi.org/10.1016/j.snb.2018.07.034 (2018).
[17] A. Michiardi, G. Hélary, P.-C.T. Nguyen, L.J. Gamble, F. Anagnostou, D.G. Castner, V. Migonney, Bioactive polymer grafting onto titanium alloy surfaces, Acta Biomaterialia. 6 (2010) 667–675. https://doi.org/10.1016/j.actbio.2009.08.043.
[18] H. Chouirfa, V. Migonney, C. Falentin-Daudré, Grafting bioactive polymers onto titanium implants by UV irradiation, RSC Adv. 6 (2016) 13766–13771. https://doi.org/10.1039/C5RA24497H.
[19] G. Helary, F. Noirclere, J. Mayingi, V. Migonney, A new approach to graft bioactive polymer on titanium implants: Improvement of MG 63 cell differentiation onto this coating, Acta Biomaterialia. 5 (2009) 124–133. https://doi.org/10.1016/j.actbio.2008.07.037.
[20] C. Falentin-Daudré, V. Migonney, H. Chouirfa, and J. S. Baumann, WO patent PCT/EP2016/068909 (August 7th, 2015).
[20] S. Pletincx, K. Marcoen, L. Trotochaud, L.-L. Fockaert, J.M.C. Mol, A.R. Head, O. Karslioğlu, H. Bluhm, H. Terryn, T. Hauffman, Unravelling the Chemical Influence of Water on the PMMA/Aluminum Oxide Hybrid Interface In Situ, Sci Rep. 7 (2017) 13341. https://doi.org/10.1038/s41598-017-13549-z.
[21] S. Wei, B. Vaidya, A.B. Patel, S.A. Soper, R.L. McCarley, Photochemically Patterned Poly (methyl methacrylate) Surfaces Used in the Fabrication of Microanalytical Devices, J. Phys. Chem. B. 109 (2005) 16988–16996. https://doi.org/10.1021/jp051550s.
[22] H.P. Felgueiras, M.D.M. Evans, V. Migonney, Contribution of fibronectin and vitronectin to the adhesion and morphology of MC3T3-E1 osteoblastic cells to poly (NaSS) grafted Ti6Al4V, Acta Biomaterialia. 28 (2015) 225–233. https://doi.org/10.1016/j.actbio.2015.09.030.
[23] H.M. Kowalczynska, Modulation of adhesion spreding and cytoskeleton organization of 3T3 fibroblasts by sulfonic groups present on polymer surfaces. Cell Biol Int 27 (2003) 101–14.
[24] J.Y. Lim, M.C. Shaughnessy, Z. Zhou, H. Noh, E.A. Vogler, H.J. Donahue, Surface energy effects on osteoblast spatial growth and mineralization, Biomaterials 12 (2008) 1776–1784.

CHAPTER IV

Biological properties of direct grafting by ultraviolet irradiation of vinyl benzyl phosphonic acid onto titanium surfaces

IV.1. Chapter IV overview

This chapter aims to develop active implant surface modifications to improve implant osseointegration. Several regenerative techniques to stimulate bone formation have been investigated through bone grafts and tissue engineering, but their widespread adoption remains limited because they are risky or have shown so far only limited effect, respectively. Acting on the implant side with the modification of its surface has been shown to affect bone growth and adhesion. For instance, grafting bioactive polymers represents a promising recent approach to improve osseointegration, as mastered by the LBPS team. The distribution of ionic groups (sulfonate and phosphonate) along the macromolecular chains of the polymer creates active sites, which can interact with extracellular proteins, such as fibronectin and collagen. Based on recent patents[26], the grafting of these anionic polymers was successful by using radicals from titanium peroxides able to initiate the radical polymerisation of ionic monomers. Applied to the bone-implant context, bioactive polymers grafting on titanium surfaces has been shown to prevent bacteria adhesion thus reducing infections, while enhancing osteoblasts (bone forming cells) adhesion and differentiation, *in vitro*[12-13] . However, if such results represent solid bases to use bioactive polymer bearing sulfonate groups, the use of phosphonate groups as a new therapeutic tool to improve implant anchorage represent a better solution.

In this chapter IV, our objectives are:

1. To develop, optimize and characterize the grafting of phosphonic-acid-based monomers mimicking the structure of the well-known bioactive monomer NaSS
2. To evaluate the impact of the phosphonic-acid-based polymer on pre-osteoblasts cell adhesion, spreading, and differentiation

IV.2. Article 3: Biological properties of direct grafting by ultraviolet irradiation of vinyl benzyl phosphonic acid onto titanium surfaces, Reactive and Functional Polymers.

173 (2022) 105215. https://doi.org/10.1016/j.reactfunctpolym.2022.105215

Contents lists available at ScienceDirect

Reactive and Functional Polymers

journal homepage: www.elsevier.com/locate/react

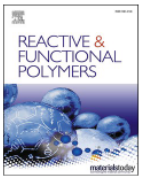

Biological properties of direct grafting by ultraviolet irradiation of vinyl benzyl phosphonic acid onto titanium surfaces

Caroline Pereira [a], Jean-Sébastien Baumann [a], Vincent Humblot [b], Céline Falentin-Daudré [a,*]

[a] LBPS/CSPBAT, UMR CNRS 7244, Institut Galilée, Université Sorbonne Paris Nord, 99 avenue JB-Clément, 93430 Villetaneuse, France
[b] FEMTO-ST Institute, UMR 6174 CNRS, Université Bourgogne Franche-Comté, 15B avenue Montboucons, 23030 Besançon Cedex, France

Abstract

Titanium (Ti) and its alloys are the most effective metals for structural implantable device applications. However, Ti-based materials are passively integrated into the bone, resulting in a purely mechanical attachment. Consequently, the loss of osseointegration often leads to implant failure. Therefore, enhancing bone formation surrounding the implant is primordial. In previous investigations conducted in our laboratory, grafting bioactive polymers with sulfonate groups, such as poly (sodium styrene sulfonate) (polyNaSS), was demonstrated to increase the adherence and differentiation of osteoblast cells. In this context, this contribution proposes to functionalize Ti with a phosphonic acid-based polymers, poly (vinyl benzyl phosphonic acid) (poly (VBP)). A two-step UV-initiated grafting polymerization was developed to covalently graft VBP into Ti surfaces. The surfaces were characterized using colorimetry, Fourier-transformed infrared spectra recorded in an attenuated total reflection (FTIR-ATR), X-ray photoelectron spectroscopy (XPS) techniques, and water contact angle (WCA) measurements. The Ti substrates were evaluated for cell viability, spreading, alkaline phosphatase activity, and calcium formation using MC3T3-E1 osteoblast cells. The interaction of Ti grafted samples with osteoblast cells was significantly improved as well as the cell/surface interaction. Together, these findings demonstrated that poly (VBP) grafted on Ti surfaces improved osteoblasts' early cell adhesion and spreading activities, crucial for osseointegration applications.

Graphical abstract

Keywords: Titanium, Poly (vinyl benzyl phosphonic acid) grafting, Osseointegration, bioactive, UV

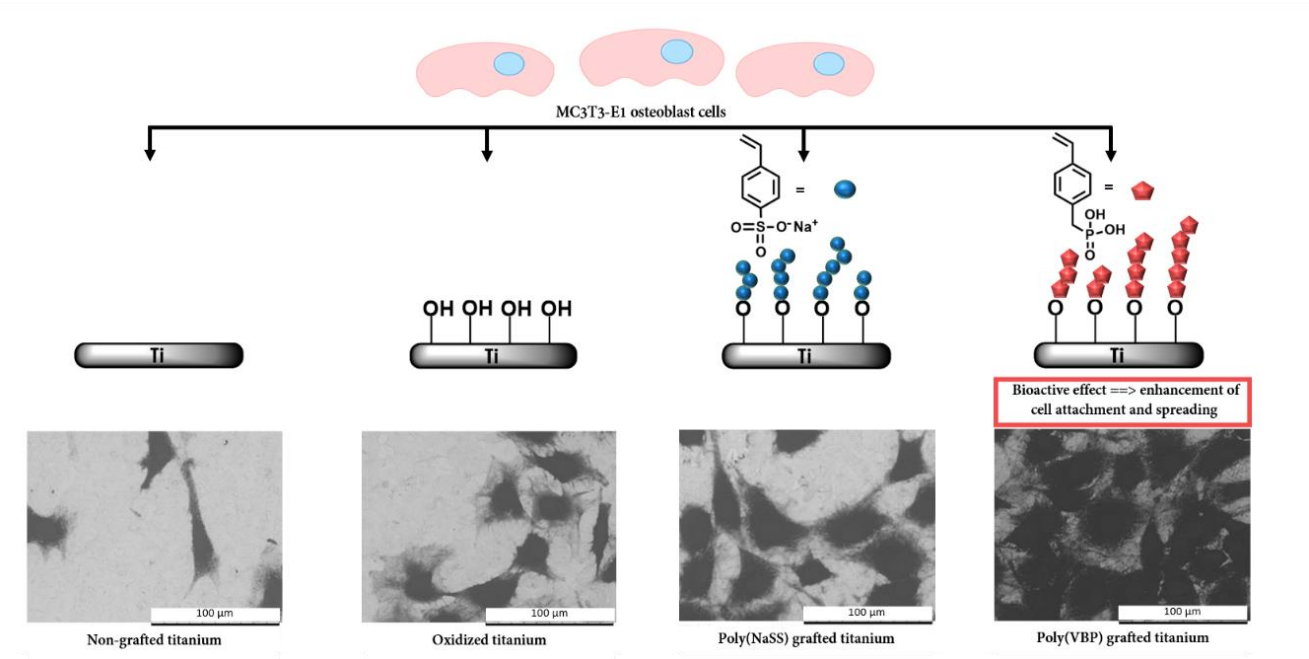

1. Introduction

Titanium (Ti) and its alloys, employed in the biomedical field since the early 1950s [1], have demonstrated the success of their mechanically-compatible properties as biomedical devices. However, despite their biocompatibility, titanium implants are not optimally osseointegrated, and an inflammatory process resulting in fibrous capsule development can ensue. As a result, implants are encased by fibrous tissue, isolating them from the bone tissue and causing implant loosening [2,3].

The success of implant surgery is primarily based on the complex osseointegration mechanisms involving both mechanical and biochemical aspects occurring at the contact between the bone tissue and the implant surface. The effectiveness of biomaterial placement is closely linked to the osseointegration phenomenon that occurs when the bone tissue adjusts to the presence of the implant through the bone remodelling mechanisms. Therefore, an exemplary bone/implant interface would consist of bone merged with the implant surface without a fibrous connective tissue layer in between.

To improve the bone uptake of the implant, researchers have developed different strategies. Modifications of the morphological surface properties (roughness, porosity) using various methods, essentially mechanical treatments, allow an essential range of roughness and textures that promote bone bonding [4]. Other approaches have been used to improve osseointegration, including physical modifications (thermal treatment, plasma treatment) [5–7], chemical modifications (silane treatments, protein coating) [8], and electrochemical treatments (anodic oxidation) [9,10]. Moreover, to improve osteoblast responses and bone-implant integration, chemical modifications were made to directly functionalize Ti surfaces with various chemical groups, like hydroxyl [11], carboxyl [12], sulfonic groups [13], and phosphate groups [14]. As a result of our prior research, polymers bearing ionic chemical functions have been found to modulate cell attachment and spreading [15,16]. The arrangement of these ionic groups throughout the polymer chains affords effective sites that operate with extracellular proteins vital in cell response, such as fibronectin [17]. Despite the effectiveness of the approaches described above, numerous limitations remain, such as poor coating-to-substrate adhesion and sophisticated and time-consuming chemical processes. Grafting polymerization induced by ultraviolet (UV) light is an easy, quick, and low-cost approach for introducing desired functional groups to the surfaces of materials without changing their bulk characteristics. Our laboratory has developed a direct UV grafting process of a bioactive monomer such as sodium styrene sulfonate (NaSS) [18]. By activating the Ti surface with hydroxyl, it is possible to generate active radicals under UV irradiation. The polymerization of functional monomers is induced by radical species, resulting in bioactive groups on the surface of Ti.

One interesting molecule to graft is a phosphonic acid-based monomer. Studies have shown that titanium and polymers functionalized with phosphate groups ($-PO_3H_2$) exhibit enhanced bioactivity due to their bone-like apatite-induced ability [19–21]. In recent years, vinyl phosphonic acid was used as a coating to manufacture bone graft replacements [22,23] and functionalize bone scaffolds [24] to stimulate regenerating bones. These findings suggested the beneficial influence of phosphonate groups on implant osseointegration.

The current work described a method for improving bone-implant integration by functionalizing Ti with a phosphonic-acid-based monomers: vinyl benzyl phosphonate (VBP). This study used a two-step UV-induced graft polymerization of VBP to functionalize Ti surfaces with phosphonate groups. Ti oxidation produces peroxides on the surface, which generate radicals when exposed to UV light, initiating the monomer VBP polymerization.

Various factors for optimizing poly (VBP) grafting on titanium substrates were investigated. The surface grafting effect was chemically characterized. Furthermore, *in vitro* investigations on MC3T3-E1 osteoblast cells were assessed to evaluate how the grafted Ti surfaces influenced cell adherence, spreading, and differentiation.

2. Materials and Methods

2.1. Materials

Grade 2, commercially pure Ti disks of 10 mm diameter and ≈ 1 mm thickness purchased from Goodfellow (supplier set in Lille, France) were used as raw surfaces. Both sides of the Ti were polished with 500 and 1200 grit SiC papers.

(4-Vinylbenzyl) phosphonic acid (VBP) was supplied by Specific Polymers (supplier set in Montpellier, France) and stored at 4° C. The monomer was used without further purification, as it is provided without polymerization inhibitors.

Recrystallization in a combination of ethanol/water (Carlo Erba) (10: 90 v/v) overnight at 70 °C was used to purify sodium styrene sulfonate (NaSS, Sigma). The product was then dried overnight at 50 °C under air pressure and kept at 4° C as previously described [18,25,26].

2,2'-azobis (2-methylpropionitrile) (AIBN) was refined by the same recrystallization described above for 1h at 30 °C. The purified AIBN was vacuum-dried at 30 °C and stored at 4°C.

The solvents used for the cleaning treatment, activation procedures and functionalization of titanium surfaces were used without further purification.

2.2. Methods

2.2.1. Cleaning treatment of titanium substrates

The surfaces were ultrasonically cleaned for 15 minutes following the polishing procedure with different solvents: acetone, cyclohexane, isopropanol, and distilled water (dH_2O). After that, Ti surfaces were then stripped for 1 min with stirring in Kroll's reagent (2% hydrofluoric acid (Sigma) ; 10% HNO_3 (Acros organics) and 88% dH_2O), followed by 15 min of ultrasonic washing in five successive distilled water baths. Ti substrates were then dried in an oven at 50 °C.

2.2.2. Activation procedure of titanium substrates

Briefly, Ti substrates were chemically oxidized by immersion with an acidic solution (H_2SO_4/H_2O_2 50:50 v/v, Sigma) to activate the surfaces with hydroxide and peroxide groups. Then, the Ti surfaces were rinsed with dH_2O to remove any traces of the Piranha solution.

2.2.3. Grafting procedure of VBP onto titanium surfaces

A 1 M VBP solution in dimethyl sulfoxide (DMSO) was poured into a flask with a circular bottom that contains 2% of 2,2'-azobis (2-methylpropionitrile) (AIBN). After degassing the solution with argon for 30 minutes, the oxidized Ti substrates were quickly added to the solution. The Ti surfaces immersed in the VBP/DMSO solution containing 2% AIBN were then irradiated with UV radiation (365 nm, 160 mW/cm ^{2} with a power of 38%) at ambient temperature for 2h while stirring (**Figure 4.1.**). The grafted surfaces were then washed with a mixture of DMSO/methanol (50:50 v/v, Sigma). Then the surfaces were washed with methanol for 48h to remove nonreacted monomers and non-grafted homopolymers. Finally, the poly (VBP) grafted Ti surfaces were dried overnight at 37 °C.

Under normal temperature and pressure conditions, UV sources for the grafting technique come from an LED lamp (Omnicure) with a produced power ranging from 200 W to 500 W at

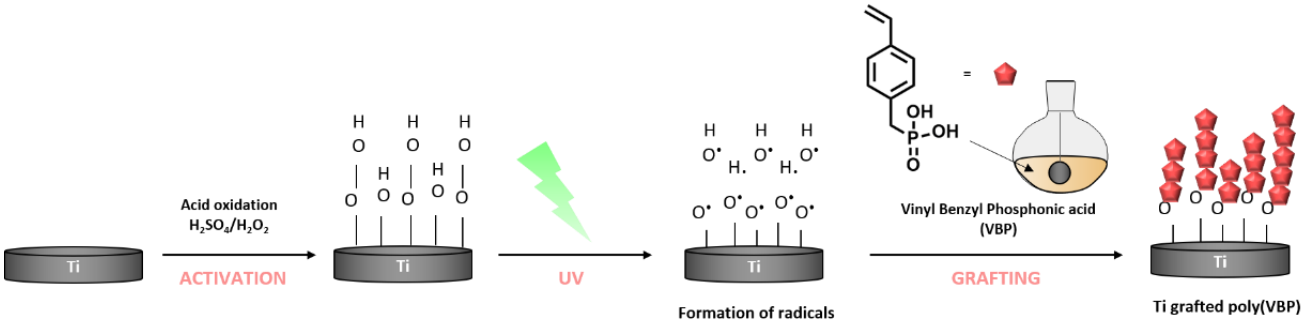

FIGURE 4.1 GRAFTING MECHANISM OF POLY (VBP) ON TITANIUM SURFACE

365 nm.

2.3. Surface characterization

Fourier-transformed infrared (FTIR) spectroscopy, X-ray photoelectron spectroscopy (XPS), water contact angle measurements (WCA), and the toluidine blue (TB) colorimetric technique were used to assess the existence of poly (VBP) on grafted Ti surfaces.

In attenuated total reflectance (ATR) mode, FTIR spectra were collected between 4000 and 600 cm^{-1}. Ti disks were pushed equally against a diamond crystal (4000-500 cm^{-1}) (512 scans). After that, each spectrum was fitted and examined.

Under ultra-high vacuum circumstances (≤10-10 Torr), photoelectrons emission was studied at a 90° take-off angle. The chemical contents of the surface were analyzed using XPS (from the Omicron Argus spectrometer in Taunusstein, Germany) with a monochromated Alkα radiation source (hv = 1486.6 eV) and a 300 W electron beam. The survey spectrum was captured with a pass energy of 100 eV and the high-resolution areas with 20 eV. The C1s binding energy of aliphatic carbon atoms, 284.8 eV, was used to calibrate the binding energies. Casa XPS v.2.5.15 software (Casa Software Ldt, UK) was used to profile high-resolution spectra, and the resultant peak regions were utilized to compute the elemental composition.

The wettability of the samples was measured after each surface treatment phase by measuring WCA with one drop (2 µl) of dH2O using a Kruss DAS10 goniometer at ambient temperature. Six samples from each group were examined, with three measurements made on each to determine the average contact angle 20 seconds after the water drop made contact with the surface. The contact angle was evaluated using the DSA drop shape analysis tool after photos of the droplet were obtained.

The TB colorimetric technique was used to evaluate the quantity of poly (VBP) grafted on Ti surfaces, following the methodology established by Helary et al [25]. To facilitate the complexation of TB with the PO_3^{2-} groups from the polymer, Ti surfaces were submerged in a TB aqueous solution (5 x 10^{-4} M, pH = 10) at 30 °C for 6 hours. To remove the non-complexed dye, the surfaces were washed with 5 x 10^{-3} M sodium hydroxide in dH2O. A combination of acetic acid/dH2O (50/50 v/V Sigma) was used to de-complex the disks for 24 hours. Finally, the concentration of de-complexed TB was determined using a Perkin-Elmer Lambda 25 spectrometer using visible spectroscopy at 633 nm. Three Ti samples of each condition (non-grafted, oxidized, poly (NaSS) grafted, and poly (VBP) grafted) were used per analysis.

2.4. Preparation of titanium disks for biological assays

All substrates (ungrafted, oxidized, poly (NaSS), and poly (VBP) grafted) were cleaned and sterilized before interaction with the osteoblast cells. Ti disks were washed three times for three hours in 1.5 M sodium chloride (NaCl, Fisher), 0.15 M sodium chloride, pure water, and phosphate-buffered saline solution, respectively (PBS, Gibco). For 15 min, each side of the Ti substrates was sterilized using an ultraviolet germicidal lamp (UV, 30 W, 254 nm). The samples were kept overnight on well-plates with Gibco's Dulbecco's Modified Eagle's Medium (DMEM). Finally, the samples were put in wells with enriched DMEM medium (1% penicillin, 1% glutamine, 10% fetal bovine serum) and kept until the experiments began.

2.5. Osteoblastic cell culture

All tests were carried out using MC3T3-E1 cells procured from the American Type Culture Collection (ATCC). The cells were cultivation was based on the protocol established by Felgueiras et al [17]. The cell culture media were replaced twice a week. All investigations employed just early passage (P2-P6) cells. To separate the cells, trypsin-EDTA (Gibco) was utilized. All studies used a cell loading dose of 1 x 10^5 cells/ml, with 1 ml of cell suspension introduced onto each Ti surface kept in a 24-well tissue culture polystyrene plate. Analysis of variances (ANOVA) was used to analyze quantitative data.

2.5.2. Cell viability

A MTT (3 – (4,5-dimethyl thiazolyl-2) – 2,5– diphenyltetrazolium bromide) test was used to determine the vitality of the cells. The Ti substrates were first seeded for 24 hours. The samples were then transferred to a fresh 24-well plate and washed twice with 1 ml of PBS per well after the culture. The wells were then filled with 50 µl of 5 mg/ml MTT in a DMEM medium without phenol red. The samples were incubated at 37 °C with 5% CO_2 for 4 hours. After incubation, all of the solutions were withdrawn from the wells, and the formazan crystals were dissolved in 1 ml of DMSO for 10 min during orbital stirring. A UV-Vis reader was used to measure the solution's absorbance (PerkinElmer lambda 25).

2.5.3. Cellular spreading and morphology

Environmental scanning electron microscopy pictures (ESEM – Hitachi TM3000) were used to analyze the cellular morphology on ungrafted, oxidized, poly (NaSS), and poly (VBP) grafted surfaces 1h, 4h, and 24h after incubation.

The Ti surfaces were first cleaned in PBS after being withdrawn from the cultures. The cells were then fixed for 30 minutes at 4° C with 4% formaldehyde (Sigma) in PBS.

2.5.4. Differentiation: Alkaline phosphatase activity

ALP is a precursor to the development of osteoblasts. After 7 and 14 days of culture, its activity was measured after p-nitrophenyl phosphate was converted to p-nitrophenol at 37 °C. The enzyme was isolated from cell's membrane for 1 hour under agitation using Triton x 100. The cellular suspension was coupled with 20 mM p-nitrophenyl phosphate substrates in a 2-amino-2-methyl-propanol buffer in the same quantities and kept at 37 °C for 30 minutes. A UV-vis spectrometer set to 405 nm was used to measure the amount of p-nitrophenol generated (Perkin-Elmer). The enzyme activity was normalized to the protein mass and expressed in nmol of p-nitrophenol generated per minute (expressed in mg). A commercially available colorimetric assay was used to determine the amount of ALP in the sample (Bio-Rad protein kit assay).

2.5.5. Extracellular matrix mineralization: Calcium production

After 3 and 4 weeks of culture, the mineralization of calcium deposits was assessed. The Ti surfaces and culture medium were removed, washed twice in PBS, and transferred to a fresh well containing 1 ml of 15% (w/v) trichloroacetic acid solution to dissolve calcium-phosphate crystals. To test the calcium concentration, 10 µl of the supernatant was added to 1 ml of arsenazo-III (0.2 mM in PBS) containing calcium reagent after 1 h of continuous gentle shaking. The calcium concentration was estimated by comparing absorbance at 650 nm to a standard linear curve of $CaCl_2$ in trichloroacetic acid (15% w/v) from 50 to 1000 µg. ml^{-1}.

2.6. Statistical analysis

Each experiment was carried out three times and yielded the same findings. The data were provided as mean standard deviation with n = 9. The standard deviations are indicated by the error bars in the graphs. A one-way analysis of variance (ANOVA) was used to compare grafted and non-grafted samples, followed by a multiple comparison correction using the Tuckey test. A p-value < 0.05 was deemed significant.

3. Results and Discussion

3.1. Functionalization of titanium surfaces with bioactive polymers

Free radical polymerization of vinyl benzyl phosphonic acid, initiated by the formation of radicals generated by titanium peroxide, was used to covalently graft phosphonate groups to titanium surfaces. The yields of the grafting procedure were computed after the grafting density of poly (VBP) was assessed using the TB colorimetric technique. Controls were titanium oxidized (Ti-OH) and UV-exposed samples. Control samples showed no blue staining, indicating that the coloring was attributable only to the dye being de-complexed from the bioactive polymer's monomer units and, as a result, the proof of poly (VBP) grafted on the titanium surface. However, toluidine blue complexation of the VBP monomer or poly (VBP) adsorbed on the titanium surface might generate the staining. To reject this hypothesis, poly (VBP) and VBP monomers at a concentration of 1 M were introduced with Ti-OH samples for 1 day. The polymerization of VBP monomers was induced by UV irradiation of the VBP aqueous solution containing titanium-oxidized samples, resulting in the formation of radicals of peroxide groups (**Figure 4.1**). There was no interaction with the dye beyond this period, confirming that the staining is only due to covalent bonding between the Ti surface and the polymer (results are shown in **Figure 4.3**).

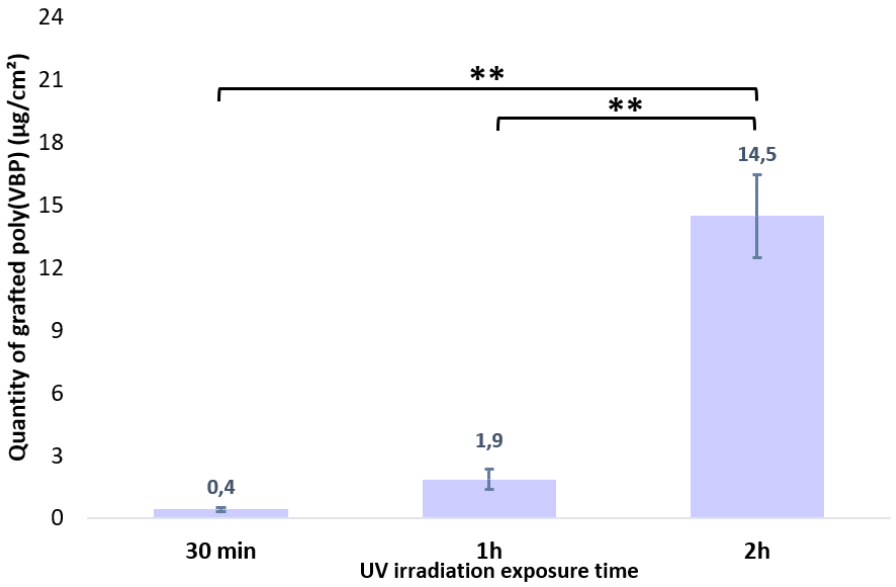

FIGURE 4.2 QUANTITY OF GRAFTED POLYMERS MEASURED AS A FUNCTION OF UV IRRADIATION EXPOSURE TIME AT A CONCENTRATION OF MONOMER [VBP] = 1 M

To identify the best grafting conditions, variables including polymerization time (UV irradiation exposure duration) and monomer concentration, were studied.

The quantity of grafted polymers assessed as a function of UV irradiation exposure duration (**Figure 4.2**) for a monomer concentration of 1 M revealed that the greatest value was attained after 2 hours of UV irradiation exposure (160 mW/cm ^{2} 38% power). Hence, this period was chosen for the investigation of additional characteristics. Furthermore, a concentration of 1 M of VBP monomer allows 14.5±2 µg. cm^{-2} of grafted polymer, whereas a concentration of 0.5 M of VBP monomer produces lower yields (**Figure 4.3**). To achieve high grafting degree yields, all polymerizations were carried out in an inert gas environment with 2 h of UV irradiation and a monomer concentration of 1 M.

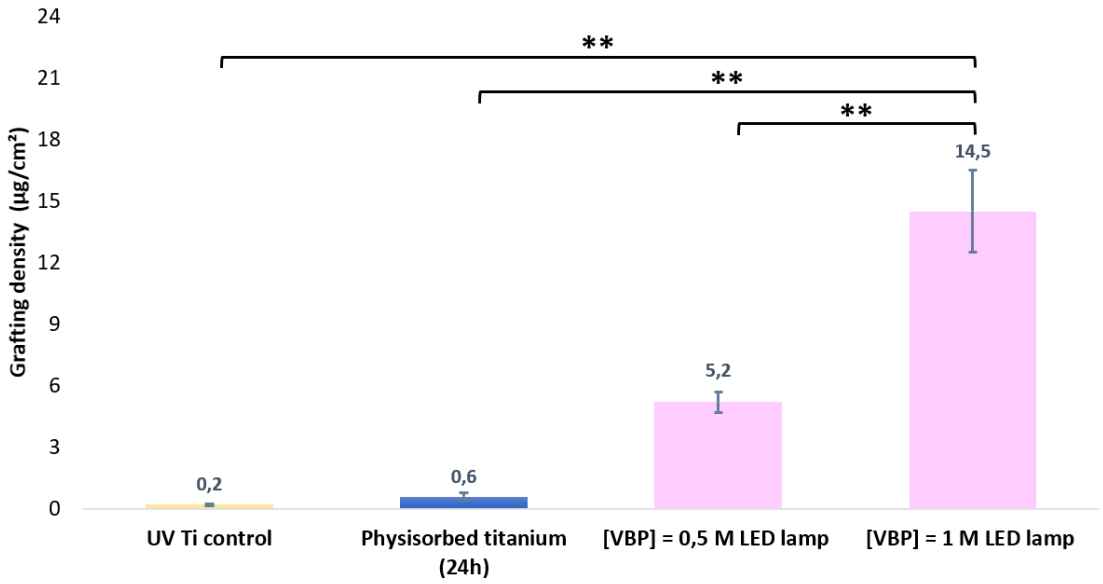

FIGURE 4.3 AMOUNT OF GRAFTED POLYMERS MEASURED AT TWO DIFFERENT MONOMER CONCENTRATIONS

This study aimed to investigate the potential benefit of a poly (NaSS)-mimicking polymer with a phosphonic acid moiety for improving osseointegration. For this purpose, it was necessary to find the optimal grafting conditions to obtain a good yield.

The exposure time to UV irradiation and the concentration of the monomer were tested to find the best grafting conditions. The colorimetric characterization technique revealed that the grafting of poly (VBP) on titanium surfaces could reach a grafting density of 14.5 µg. cm^{-2}, a

high value compared to the one found in the literature for the grafting of bioactive molecules [27–29]. Therefore, the method used in this study is appealing for industrial application since only 2 stages (surface activation then UV irradiation) are required to achieve a high yield of covalent grafting on titanium implants.

3.2. Chemical characterization of grafted titanium surfaces with poly (VBP)

FTIR, XPS, and WCA were used to verify the presence of poly (VBP) on grafted surfaces.

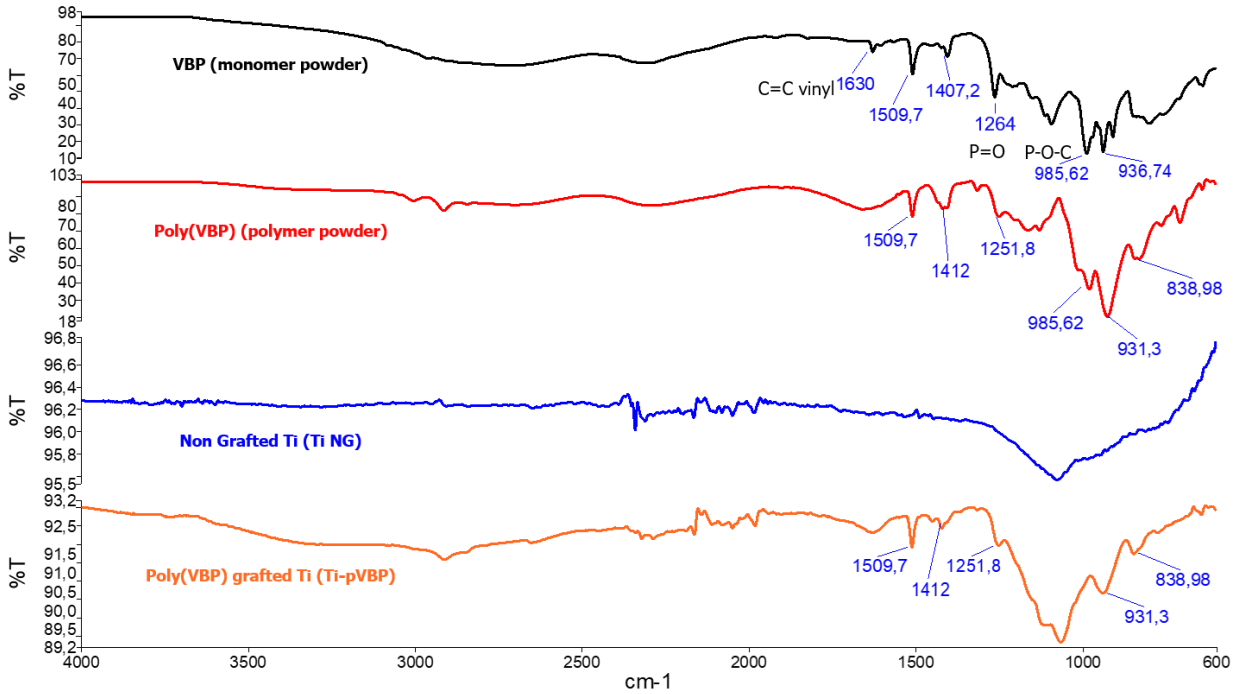

FIGURE 4.4 FTIR-ATR SPECTRA OF VBP MONOMER, POLY (VBP) POLYMER, NON GRAFTED TITANIUM, AND POLY (VBP) GRAFTED ON TITANIUM SURFACE.

First, FTIR-ATR spectra of grafted titanium revealed the existence of phosphonate groups' distinctive bands: the P=O stretching vibration mode at 1264 cm^{-1}, P-O-C stretching at 985 cm^{-1}, all related to the – PO (CH_2) group, and C=C stretching at 1509 cm^{-1} of the phenyl group (**Figure 4.4**). The absorption at 3050 cm^{-1} and 2915 cm^{-1} were attributed to C-H streatching in CH_2. The vibrational studies of organic and phosphonate compounds were used to assign these bands [30–33].

The elimination of the signal owing to the C=C stretching vibration mode of the vinyl group of the monomer was the most convincing proof of polymer formation (**Figure 4.4**). No specific poly (VBP) peaks were detected on non-grafted Ti surfaces and Ti oxidized samples. The peak observed on non-grafted Ti in 1100 cm^{-1} is attributed to the presence of a thin oxygen layer on the Ti surface. This observation is in agreement with XPS measurements, as shown in **Figure 4.5** and **Table 4.1.**

XPS studies were performed on materials under various settings: non grafted Ti (Ti NG), oxidized Ti (Ti-OH) and poly (VBP) grafted Ti (Ti-poly (VBP)). Table 1 summarizes the atomic composition determined by XPS measurements. A thin oxide layer of TiO_2 naturally occurs on the non-treated Ti surface, as shown in **Figure 4.5** by the presence of oxygen (O1s) at 530 eV; in addition, adventitious carbonaceous contamination is also observed by the presence of C1s signal at 285 eV. As a result, Ti2p (458 eV), O1s (530 eV), C1s (285 eV) are components classically seen on titanium surfaces [20].

After activation, less carbon contamination was observed at 289.3 eV, **Figure 4.6** (a) on the activated titanium surfaces with a more intense contribution at 285.4 eV. In addition, in the oxygen region, **Figure 4.6** (b), a very intense peak observed at 532.3 eV, assigned to hydroxyls and oxygen radicals, confirmed the activation of the titanium surface.

The titanium surface grafted with poly (VBP) causes a rise in carbon (by 2.17) and an oxygen reduction. The polymer has a high carbon and low oxygen content, which accounts for the observed fluctuation. The primary marker of poly (VBP) is the appearance of the P2p peak at 132 eV, clearly confirming the successful grafting of poly (VBP) at the titanium surface. Moreover, after the poly (VBP) grafting, the titanium substrate is hardly distinguishable, suggesting a polymer equivalent thickness around 10 nm. This conclusion was made by observing the results of the XPS measurements in Table 1. The Ti2p peak (458 eV) decreases with grafting of poly (VBP) (18.7 at. % on ungrafted Ti samples and 0.6 at. % on grafted Ti samples), the titanium substrate becomes hardly visible.

Table 4.1 Surface composition (at. %) of the various titanium samples as revealed by XPS analysis.

Element	Position (eV)	Ti-NG (atomic %)	Ti-OH (atomic %)	Ti-poly (VBP) (atomic %)
Ti 2p	458	18.7 ± 0.6	12.7 ± 0.2	0.6 ± 0.4
C 1s	285	33.5 ± 1	42.2 ± 2.6	72.7 ± 2.5
O 1s	530	47.8 ± 0.3	45.1 ± 2.3	20.5 ± 0.6
P 2p	132	/	/	**6.2** ± 0.5

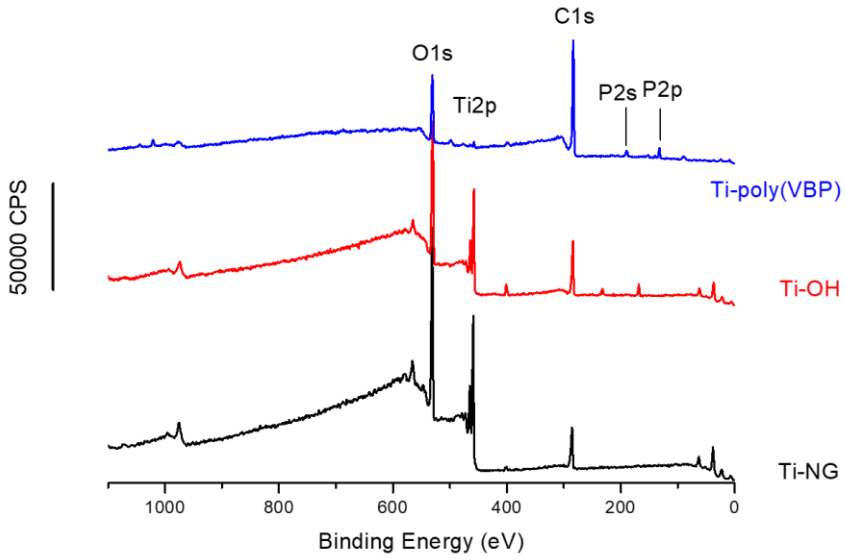

FIGURE 4.5 XPS SURVEY SPECTRA OF TITANIUM SURFACES: NON GRAFTED (TI-NG), OXIDIZED (TI-OH), AND GRAFTED WITH POLY (VBP) (TI-POLY (VBP))

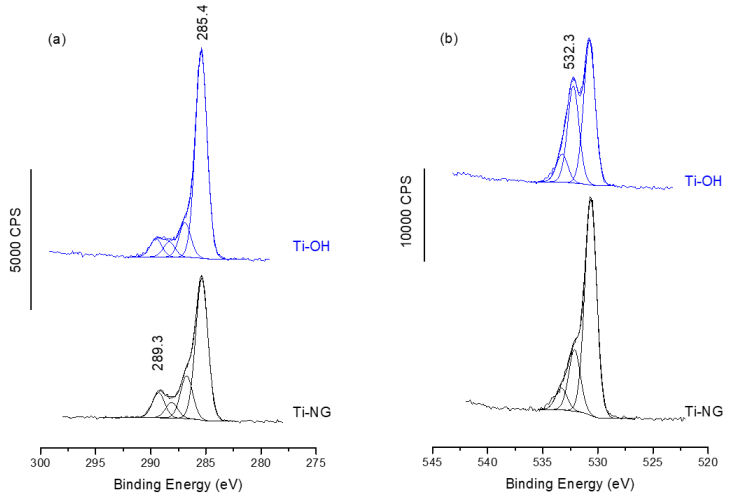

FIGURE 4.6 HIGH-RESOLUTION XPS DATA FOR (A) C1S AND (B) O1S

To investigate the surface's wettability, WCA was measured on polished Ti, stripped Ti, oxidized Ti, and poly (VBP) grafted Ti (**Figure 4.7**). The hydrophilic nature of the surface is enhanced by the production of Ti-OH (contact angle around 25°) in the first step and the presence of poly (VBP) in the second phase (contact angle around 42°). After the grafting procedure, the Ti surface becomes more hydrophilic compared to a stripped Ti surface with a contact angle of around 66°.

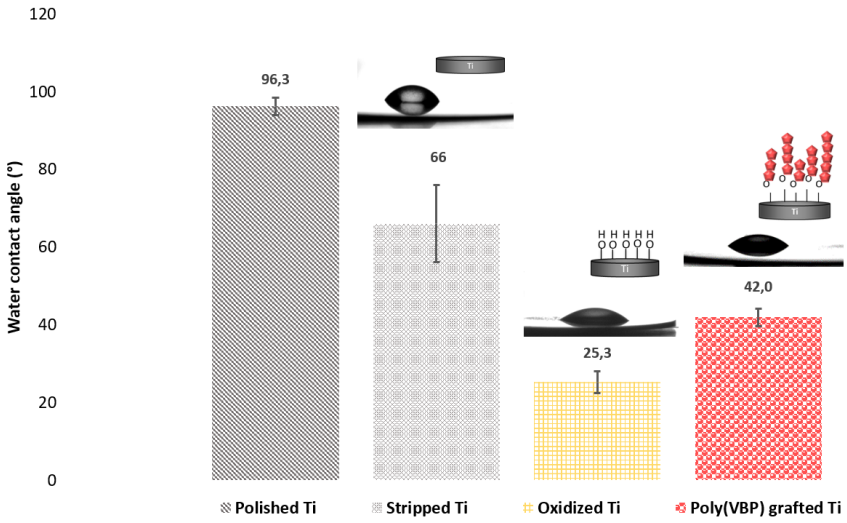

FIGURE 4.7 WATER CONTACT ANGLE MEASUREMENTS ON POLISHED TI, STRIPPED TI, OXIDIZED AND POLY (VBP) GRAFTED TI

After validating the grafting protocol, the effective presence of the polymer was verified by FTIR-ATR, XPS, and WCA analysis. XPS analysis revealed that the poly (VBP) grafted titanium surfaces have a significant atomic percentage of phosphorus (6.2 at. %). Furthermore, compared to the non-functionalized titanium, the grafted surface becomes more hydrophilic (with a contact angle value that decreases by 20°). This value is consistent with the literature's water contact angle measurements results obtained for phosphonic acid [34]. The hydrophilic/hydrophobic balance of a surface influences cellular spreading at the cells/implant contact, with hydrophilic surfaces having a beneficial influence on cell adherence [35,36].

3.3. Cell viability

The percentage of viable cells was determined by MTT assay after 1 day of MC3T3-E1 cells culture (**Figure 4.8**). All Ti surfaces revealed at least 70% of viable cells during the entire assay and were therefore considered non-cytotoxic. These findings demonstrate that functionalized Ti surfaces do not affect the viable cell rate of MC3T3-E1. Moreover, the value found for poly (VBP) grafted Ti surfaces was substantially ($p=0.01$) greater than the non-grafted Ti and the oxidized Ti surfaces, indicating a favourable outcome of poly (VBP) on the osteoblast cell response. Furthermore, when comparing poly (NaSS) grafted surfaces (112±6% viable osteoblast cells) and poly (VBP) grafted surfaces (118±4.2% viable osteoblast cells), it is interesting to note a slightly better cellular response to the surfaces grafted with the phosphonic acid-based polymer.

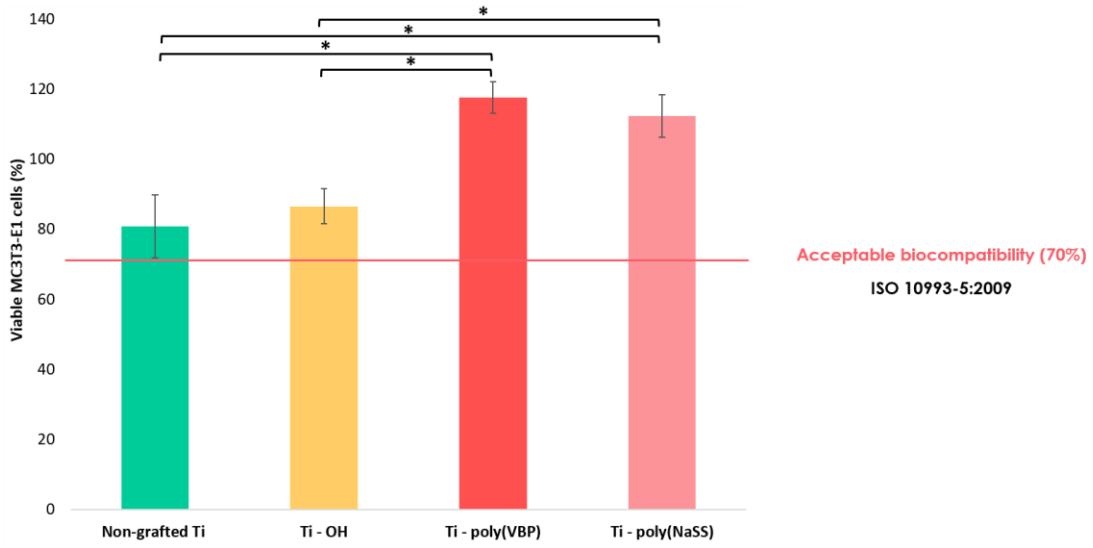

FIGURE 4.8 PERCENTAGE OF VIABLE OSTEOBLAST CELLS OVER NON-GRAFTED TITANIUM, OXIDIZED, POLY (VBP), AND POLY (NASS) GRAFTED TITANIUM AFTER 24H INCUBATION.

3.4. Cellular spreading and morphology

Cell spreading and morphology analyses were performed by environmental scanning electron microscopy (SEM) to take a broad look at the morphology of osteoblast cells. MC 3 T3-E1 osteoblast cells were cultivated on non-grafted Ti, oxidized Ti (Ti-OH), poly (NaSS), and poly (VBP) grafted Ti surfaces at 1 h, 4 h, and 24 h (**Figure 4.9**).

After 1 h of culture, SEM images have shown a considerable variation of the MC3T3-E1 osteoblast cells spreading between Ti surfaces. Osteoblast cells were more confluent on grafted surfaces than on non-grafted surfaces. For the same magnification, the nucleus of the cells was more prominent on the grafted surfaces.

After 4 h of culture, osteoblast cells were connecting with a flattened morphology with lamellipodia extensions on oxidized and grafted surfaces. However, on ungrafted surfaces, the cell expansion was very restrained, with most cells exhibiting a round shape, and no evidence of interconnection between the cells was observed. Osteoblasts cultivated on poly (VBP) grafted surfaces elongate their cytoplasmic across the whole material surface, revealing a solid adhesion capacity of MC3T3-E1 osteoblasts to the presence of poly (VBP) onto the surfaces.

After 1 day of culture, osteoblast cells' morphology onto non-grafted surfaces has a more extended and flattened form than the polygonal shape observed on oxidized and grafted surfaces. In addition, it was immediately apparent that the amount of cells was considerably higher on the poly (VBP) grafted surfaces. This observation is consistent with the cell viability experiment result depicted in **Figure 4.8.**

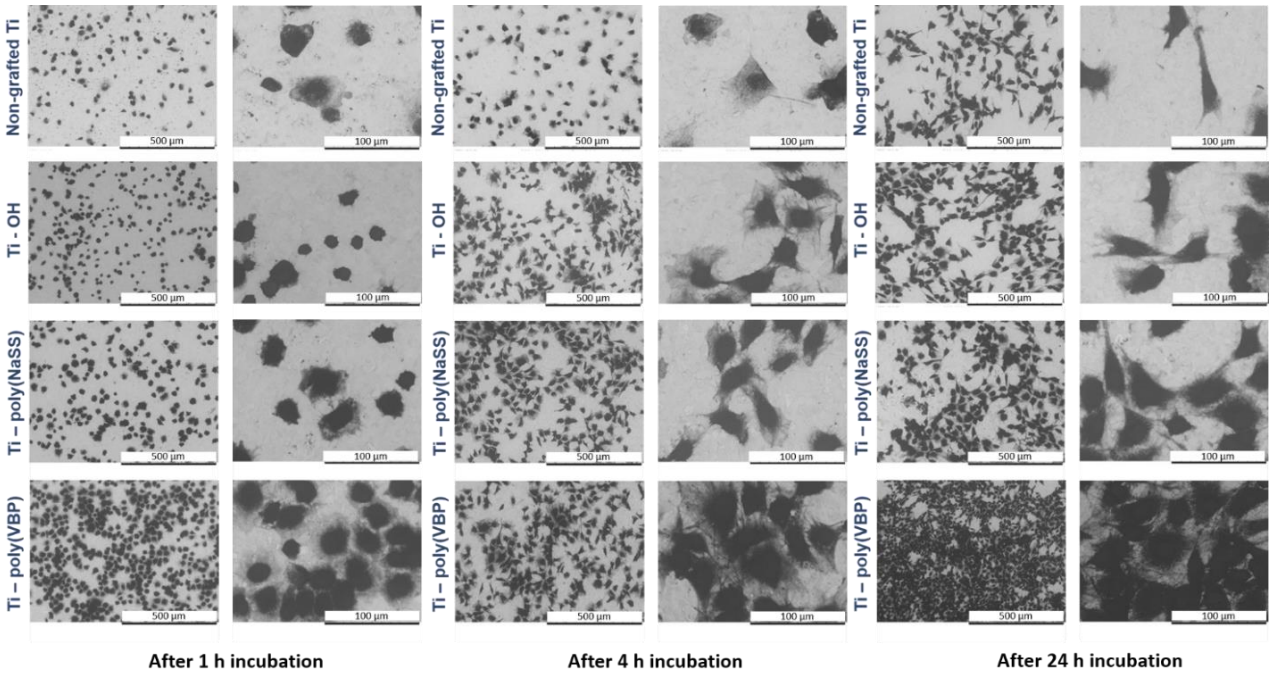

FIGURE 4.9 AFTER 1H, 4H AND 24H INCUBATION, SEM IMAGES OF OSTEOBLAST CELLS ONTO THE NON-GRAFTED, OXIDIZED, POLY (NASS), AND POLY (VBP) GRAFTED TI SURFACES

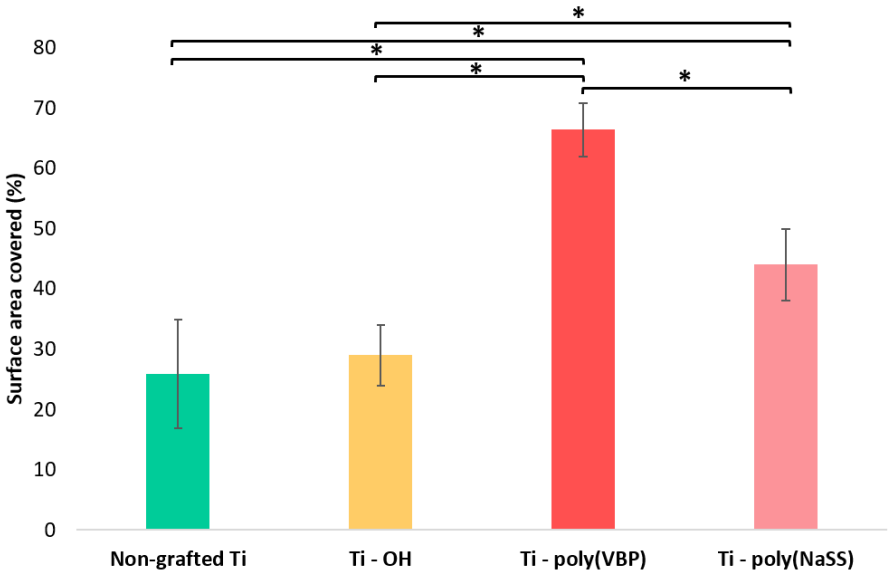

FIGURE 4.10 MEAN PERCENTAGE OF NON-GRAFTED, OXIDIZED (TI-OH), POLY (VBP), AND POLY (NASS) GRAFTED SURFACES COVERED BY OSTEOBLAST CELLS AFTER 2 H INCUBATION.

ImageJ software was used to calculate the surface area covered by the cells after 24 h of culture in each condition. This quantification was done in three separate zones of each sample, and it was discovered that the grafted samples were considerably ($p=0.01$) more covered than the non-grafted (26 ± 9% surface covered) and oxidized surfaces (29 ± 5%). Furthermore, when

compared to surfaces grafted with poly (NaSS) (44 ± 6%), the proportion of osteoblast cells covered on poly (VBP) grafted surfaces (66 ± 4.5%) was more significant (**Figure 4.10**). As a result, adherent cell populations on poly (VBP) grafted surfaces are strikingly improved compared to non-grafted surfaces. The poly (VBP) grafted surfaces promote osteoblast adhesion and spreading, resulting in favourable conditions for future cell growth.

The primary goal of this research was to illustrate the impact of poly (VBP) grafted Ti surfaces on *in vitro* osteogenic properties. In this context, the bioactivity of the chemically modified Ti surfaces grafted with phosphonic acid-based compounds was studied. For this purpose, cell viability, osteoblast cells' morphology, and spreading through SEM and MTT were performed on non-treated titanium and functionalized titanium surfaces. Furthermore, to account for the bioactivity of both bioactive polymers, the grafting of poly (VBP) was compared to the grafting of poly (NaSS). The UV "grafting from" method published by Chouirfa et al [18,26] was used to graft poly (NaSS) onto Ti surfaces. The high values of viable cell density, improvement of cell morphology, and spreading on poly (VBP) grafted surfaces suggested no cellular toxicity and an enhancement in osteoblast cells' growth. Moreover, after 1 h of culture, SEM images revealed the formation of microcellular extensions called filopodia and adherence of the cells to each other in poly (VBP) grafted Ti substrates. The improved cell spreading could be related to the enhanced hydrophilicity of the surface due to the surface-grafting of phosphonate groups.

3.5. Differentiation and mineralization

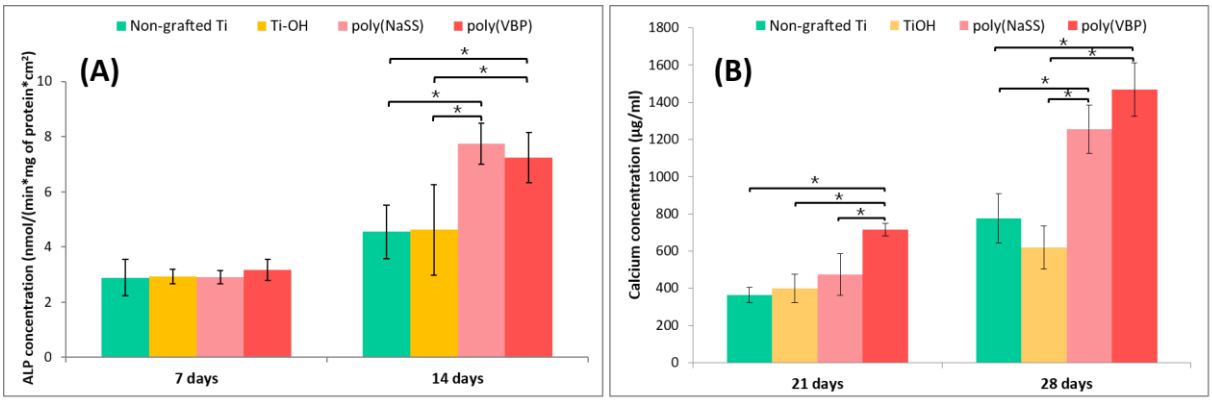

FIGURE 4.11 ALP ACTIVITY (A) AND ECM MINERALIZATION ASSAY (B) OF MC3T3-E1 OSTEOBLAST CELLS ONTO DIFFERENT TITANIUM SURFACES (UNGRAFTED, OXIDIZED, POLY (NASS) AND POLY (VBP) GRAFTED) AFTER RESPECTIVELY 7 AND 14, 21, AND 28 DAYS OF CULTURE

ALP is a primary indicator of osteoblast differentiation [25]. The effect of untreated and functionalized Ti surfaces on osteoblast cell development was initially investigated using ALP activity measurements from 7 to 14 days of culture. Results (**Figure 4.11**) showed that ALP concentration was much improved by the grafting of poly (NaSS) and poly (VBP), with maximum concentration found on day 14, which corresponded to the beginning of the extracellular matrix (ECM) development. Before day 14, ALP production was lower because proliferation was dominant. ALP reduced in result of cell maturation's ECM mineralization phase with the apparition of calcium nodules in the second stage of differentiation [37]. For the poly (VBP) grafted surfaces, the ALP concentration started to decrease from day 14, showing the beginning of the mineralization phase. Ti surfaces were therefore evaluated for calcium content after 21 and 28 days of culture (**Figure 4.11**).

In accord with ALP results, surfaces grafted with poly (NaSS) and poly (VBP) presented statistically superior mineralization than the non-grafted and oxidized surfaces. The difference was even more pronounced after 4 weeks, indicating that the osteoblasts had matured significantly on the poly (VBP) grafted Ti surfaces. These findings revealed that grafting a titanium sample by poly (VBP) promotes osteoblastic differentiation of MC3T3-E1 cells.

Cell differentiation ability in contact with the implant is crucial for bone regeneration. ALP activity and ECM mineralization were assessed quantitatively to examine osteogenic differentiation of MC3T3-E1 *in vitro*. Poly (VBP) grafting has been demonstrated to promote osteoblast differentiation. Together, these outcomes showed that phosphonate groups grafted on Ti surfaces enhanced osteoblasts' early cell adhesion and spreading processes. In previous investigations, phosphate groups have been shown to promote osteoblast adhesion, spreading, proliferation, and osteogenic differentiation [38–40]. One explanation is that phosphate groups are deprotonated under physiological circumstances, which improves calcium ion chelation, a desirable property for transducing osteogenic promptings [41,42]. As a result, phosphonic acid's strong affinity for calcium ions has prompted biological uses [43].

Furthermore, osteoblast attachment and spreading are affected by adsorbed fibronectin (Fn), and vitronectin (Vn) on biomaterial surfaces [17]. Fn and Vn become more stable in the presence of poly (NaSS), facilitating cell adhesion and growth [44,45]. Although the hypothesis mentioned above partially explains why osteoblast responses are improved on phosphonic acid-

based surfaces, follow-up research should be conducted to understand further the protein cells' interaction with poly (VBP).

4. Conclusion

A UV-initiated grafting polymerization technique in a two-step process was successfully developed to graft phosphonate polymers. FTIR-ATR, WCA and XPS data showed that chemically introducing phosphonic acid groups to Ti surfaces was a success. The method developed is easily adaptable to functionalize Ti implants for medical purposes. Moreover, it is possible to extend this process to graft poly (VBP) onto titanium alloys, which are extensively encountered in biomedical equipment. Cell survival, ALP activity, and calcification of MC3T3-E1 osteoblast cells cultured onto the poly (VBP) grafted titanium surfaces revealed increased differentiation of these cells, implying the effect of improved grafted implant osseointegration response. The Ti – metal surface's covalently bonded with phosphonic acid molecules act as a scaffold for new bone growth, allowing the implant to attach to the host tissue. These results indicate that poly (VBP) grafted Ti implants could be used in biological applications.

The next stage of our research will further understand the mechanisms at the atomic and molecular levels involved in cell-protein interaction on grafted titanium and perform in vivo study in a rabbit model.

Acknowledgments

This research was supported by the French Ministry of National Education, Higher Education, and Research. The authors are grateful to University Sorbonne Paris Nord.

IV.4. Conclusion & Perspectives

In this chapter IV, a UV-initiated grafting polymerization technique in a two-step process was successfully developed to graft phosphonate polymers onto titanium surfaces. Now, with Dr Sophie Le Cann (MSME laboratory of University of Créteil), we will be able to study the effect of this new implant surface functionalization (including morphological surface properties due to polymer grafting) to improve osseointegration and to prevent bacterial infection.

Based on different feasibility studies, TiAl6V4 coin-shaped implants will be used because it allows working under standardized and controlled conditions, which is the only solution to obtain a proper and calibrated i) ultrasound response and ii) initiation of crack path selection.

Implants with different surface topography, from electropolished surface to optimal roughness parameters, will be prepared using material additive manufacturing (Electron Beam Melting Additive Manufacturing), which allows a local and accurate control on structural and material parameters. Moreover, samples with “bioactive” surfaces will be prepared, using an efficient chemical way to functionalize TiAl6V4 surfaces with different surface topographies.

Then we will characterize the multiscale mechanical properties of the bone-implant interface (BII) and its dependence on morphological surface properties and functionalization during bone healing by coupling an experimental approach with mechanical modelling (mechanics and acoustics), which will be used in order to analyze the results and to optimize the conception of experiments.

IV.5. References

[1] P.-I. Brånemark, U. Breine, R. Adell, B.O. Hansson, J. Lindström, Å. Ohlsson, Intra-Osseous Anchorage of Dental Prostheses: I. Experimental Studies 3 (1969) 81–100. https://doi.org/10.3109/02844316909036699.

[2] M. Esposito, J.-M. Hirsch, U. Lekholm, P. Thomsen, Biological factors contributing to failures of osseointegrated oral implants, European Journal of Oral Sciences. 106 (1998) 527–551. https://doi.org/10.1046/j.0909-8836..t01-2-.x.

[3] A.M. Roos-Jansaker, S. Renvert, J. Egelberg, Treatment of peri-implant infections: a literature review, J. Clin. Periodontol. 30 (2003) 467–485. https://doi.org/10.1034/j.1600-051X.2003.00296.x.

[4] J.E. Ellingsen, Surface configurations of dental implants, Periodontol 2000. 17 (1998) 36–46. https://doi.org/10.1111/j.1600-0757.1998.tb00121.x.

[5] Y.-J. Park, H.-J. Song, I. Kim, H.-S. Yang, Surface characteristics and bioactivity of oxide film on titanium metal formed by thermal oxidation, J Mater Sci: Mater Med. 18 (2007) 565–575. https://doi.org/10.1007/s10856-007-2303-7.

[6] L. Saldaña, V. Barranco, J.L. González-Carrasco, M. Rodríguez, L. Munuera, N. Vilaboa, Thermal oxidation enhances early interactions between human osteoblasts and alumina blasted Ti6Al4V alloy, J. Biomed. Mater. Res. 81A (2007) 334–346. https://doi.org/10.1002/jbm.a.30994.

[7] A. Carradó, Structural, Microstructural, and Residual Stress Investigations of Plasma-Sprayed Hydroxyapatite on Ti-6Al-4 V, ACS Appl. Mater. Interfaces. 2 (2010) 561–565. https://doi.org/10.1021/am900763j.

[8] Y. Liu, P. Layrolle, J. de Bruijn, C. van Blitterswijk, K. de Groot, Biomimetic coprecipitation of calcium phosphate and bovine serum albumin on titanium alloy, J. Biomed. Mater. Res. 57 (2001) 327–335. https://doi.org/10.1002/1097-4636 (20011205)57:3 <327::AID-JBM1175>3.0.CO;2- J.

[9] Y.-T. Sul, C.B. Johansson, S. Petronis, A. Krozer, A. Wennerberg, T. Albrektsson, Characteristics of the surface oxides on turned and electrochemically oxidized pure titanium implants up to dielectric breakdown: the oxide thickness, micropore configurations, surface roughness, crystal structure and chemical composition, Biomaterials 23 (2002) 491–501. https://doi.org/10.1016/S0142-9612 (01)00131-4.

[10] L. Le Guéhennec, A. Soueidan, P. Layrolle, Y. Amouriq, Surface treatments of titanium dental implants for rapid osseointegration, Dental Materials. 23 (2007) 844–854. https://doi.org/10.1016/j.dental.2006.06.025.

[11] Y.-J. Park, H.-J. Song, I. Kim, H.-S. Yang, Surface characteristics and bioactivity of oxide film on titanium metal formed by thermal oxidation, J Mater Sci: Mater Med. 18 (2007) 565–575. https://doi.org/10.1007/s10856-007-2303-7.

[12] A. Michiardi, G. Hélary, P.-C.T. Nguyen, L.J. Gamble, F. Anagnostou, D.G. Castner, V. Migonney, Bioactive polymer grafting onto titanium alloy surfaces, Acta Biomaterialia. 6 (2010) 667–675. https://doi.org/10.1016/j.actbio.2009.08.043.

[13] H. Chouirfa, M.D.M. Evans, D.G. Castner, Grafting of architecture controlled poly (styrene sodium sulfonate) onto titanium surfaces using bio-adhesive molecules: Surface

characterization and biological properties, Biointerphases 12, 02C418 (2017). http://dx.doi.org/10.1116/1.4985608.
[14] N. Adden, L.J. Gamble, D.G. Castner, A. Hoffmann, G. Gross, H. Menzel, Phosphonic Acid Monolayers for Binding of Bioactive Molecules to Titanium Surfaces, Langmuir. 22 (2006) 8197–8204. https://doi.org/10.1021/la060754c.
[15] F. El Khadali, G. Hélary, G. Pavon-Djavid, V. Migonney, Modulating Fibroblast Cell Proliferation with Functionalized Poly (methyl methacrylate) Based Copolymers: Chemical Composition and Monomer Distribution Effect, Biomacromolecules. 3 (2002) 51–56. https://doi.org/10.1021/bm015563x.
[16] F. Anagnostou, A. Debet, G. Pavon-Djavid, Z. Goudaby, G. Hélary, V. Migonney, Osteoblast functions on functionalized PMMA-based polymers exhibiting Staphylococcus aureus adhesion inhibition, Biomaterials. 27 (2006) 3912–3919. https://doi.org/10.1016/j.biomaterials.2006.03.004.
[17] H.P. Felgueiras, M.D.M. Evans, V. Migonney, Contribution of fibronectin and vitronectin to the adhesion and morphology of MC3T3-E1 osteoblastic cells to poly (NaSS) grafted Ti6Al4V, Acta Biomaterialia. 28 (2015) 225–233. https://doi.org/10.1016/j.actbio.2015.09.030.
[18] H. Chouirfa, V. Migonney, C. Falentin-Daudré, Grafting bioactive polymers onto titanium implants by UV irradiation, RSC Adv. 6 (2016) 13766–13771. https://doi.org/10.1039/C5RA24497H.
[19] P. Datta, J. Chatterjee, S. Dhara, Electrospun nanofibers of a phosphorylated polymer – A bioinspired approach for bone graft applications, Colloids and Surfaces B: Biointerfaces. 94 (2012) 177–183. https://doi.org/10.1016/j.colsurfb.2012.01.033.
[20] C. Viornery, Y. Chevolot, D. Léonard, B.-O. Aronsson, P. Péchy, H.J. Mathieu, P. Descouts, M. Grätzel, Surface Modification of Titanium with Phosphonic Acid To Improve Bone Bonding: Characterization by XPS and ToF-SIMS, Langmuir. 18 (2002) 2582–2589. https://doi.org/10.1021/la010908i.
[21] C. Viornery, H.L. Guenther, B.-O. Aronsson, P. Péchy, P. Descouts, M. Grätzel, Osteoblast culture on polished titanium disks modified with phosphonic acids: Osteoblast Culture on Polished Titanium, J. Biomed. Mater. Res. 62 (2002) 149–155. https://doi.org/10.1002/jbm.10205.

[22] R.E. Dey, I. Wimpenny, J.E. Gough, D.C. Watts, P.M. Budd, Poly (vinylphosphonic acid – *co* – acrylic acid) hydrogels: The effect of copolymer composition on osteoblast adhesion and proliferation: PVPA – *co* – AA HYDROGELS, J. Biomed. Mater. Res. 106 (2018) 255–264. https://doi.org/10.1002/jbm.a.36234.

[23] R.E. Dey, X. Zhong, P.J. Youle, Q.G. Wang, I. Wimpenny, S. Downes, J.A. Hoyland, D.C. Watts, J.E. Gough, P.M. Budd, Synthesis and Characterization of Poly (vinylphosphonic acid – *co* – acrylic acid) Copolymers for Application in Bone Tissue Scaffolds, Macromolecules. 49 (2016) 2656–2662. https://doi.org/10.1021/acs.macromol.5b02594.
[24] P.M. López-Pérez, R.M.P. da Silva, R.A. Sousa, I. Pashkuleva, R.L. Reis, Plasma-induced polymerization as a tool for surface functionalization of polymer scaffolds for bone tissue

engineering: An in vitro study, Acta Biomaterialia. 6 (2010) 3704–3712. https://doi.org/10.1016/j.actbio.2010.03.008.
[25] G. Helary, F. Noirclere, J. Mayingi, V. Migonney, A new approach to graft bioactive polymer on titanium implants: Improvement of MG 63 cell differentiation onto this coating, Acta Biomaterialia. 5 (2009) 124–133. https://doi.org/10.1016/j.actbio.2008.07.037.
[26] C. Falentin-Daudré, V. Migonney, H. Chouirfa, and J. S. Baumann, WO patent PCT/EP2016/068909 (August 7th, 2015).
[27] M.C. Porté-Durrieu, F. Guillemot, S. Pallu, C. Labrugère, B. Brouillaud, R. Bareille, J. Amédée, N. Barthe, M. Dard, C. Baquey, Cyclo-(DfKRG) peptide grafting onto Ti–6Al–4V: physical characterization and interest towards human osteoprogenitor cells adhesion, Biomaterials. 25 (2004) 4837–4846. https://doi.org/10.1016/j.biomaterials.2003.11.037.

[28] R. Müller, J. Abke, E. Schnell, D. Scharnweber, R. Kujat, C. Englert, D. Taheri, M. Nerlich, P. Angele, Influence of surface pretreatment of titanium- and cobalt-based biomaterials on covalent immobilization of fibrillar collagen, Biomaterials. 27 (2006) 4059–4068. https://doi.org/10.1016/j.biomaterials.2006.03.019.
[29] C. Chollet, C. Chanseau, B. Brouillaud, M.C. Durrieu, RGD peptides grafting onto poly (ethylene terephthalate) with well controlled densities, Biomolecular Engineering. 24 (2007) 477–482. https://doi.org/10.1016/j.bioeng.2007.07.012.
[30] Nakanishi, K. Infrared absorption spectroscopy (Holden-Day, San Francisco, 1962).
[31] M.J. Danilich, D.J. Burton, R.E. Marchant, Infrared study of perfluorovinylphosphonic acid, perfluoroallylphosphonic acid, and pentafluoroallyldiethylphosphonate, Vibrational Spectroscopy. 9 (1995) 229–234. https://doi.org/10.1016/0924-2031 (95)00018-P.
[32] A. Popa, C.-M. Davidescu, P. Negrea, G. Ilia, A. Katsaros, K.D. Demadis, Synthesis and Characterization of Phosphonate Ester/Phosphonic Acid Grafted Styrene−Divinylbenzene Copolymer Microbeads and Their Utility in Adsorption of Divalent Metal Ions in Aqueous Solutions, Ind. Eng. Chem. Res. 47 (2008) 2010–2017. https://doi.org/10.1021/ie070886g.
[33] M. Yamabe, K. Akiyama, Y. Akatsuka, M. Kato, Novel phosphonated perfluorocarbon polymers, European Polymer Journal. (2000) 7. https://doi.org/10.1016/S0014-3057 (99)00158-5.
[34] M.P. Danahy, M.J. Avaltroni, K.S. Midwood, J.E. Schwarzbauer, J. Schwartz, Self-assembled Monolayers of α,ω-Diphosphonic Acids on Ti Enable Complete or Spatially Controlled Surface Derivatization, Langmuir. 20 (2004) 5333–5337. https://doi.org/10.1021/la036084h.
[35] B. Feng, J.Y. Chen, S.K. Qi, L. He, J.Z. Zhao, X.D. Zhang, Characterization of surface oxide films on titanium and bioactivity, Journal of Materials Science: Materials in Medicine. 13 (2002) 457–464. https://doi.org/10.1023/A:1014737831371.
[36] G. Zhao, Z. Schwartz, M. Wieland, F. Rupp, J. Geis-Gerstorfer, D.L. Cochran, B.D. Boyan, High surface energy enhances cell response to titanium substrate microstructure, J. Biomed. Mater. Res. 74A (2005) 49–58. https://doi.org/10.1002/jbm.a.30320.
[37] J.Y. Martin, D.D. Dean, D.L. Cochran, J. Simson, B.D. Boyan, Z. Schwartz, Proliferation, differentiation, and protein synthesis of human osteoblast-like cells (MG63) cultured on previously used titanium surfaces, Clin. Oral Implants Res. 7 (1996) 27–37.

[38] D.M. Zheng, K.G. Neoh, E.-T. Kang, Immobilization of alendronate on titanium via its different functional groups and the subsequent effects on cell functions., Journal of Colloid and Interface Science. 487 (2017) 1–11. https://doi.org/10.1016/j.jcis.2016.10.014.
[39] M. Dadsetan, M. Giuliani, F. Wanivenhaus, M.B. Runge, J.E. Charlesworth, M.J. Yaszemski, Incorporation of phosphate group modulates bone cell attachment and differentiation on oligo (polyethylene glycol) fumarate hydrogel, Acta Biomaterialia. 8 (2012) 1430–1439. https://doi.org/10.1016/j.actbio.2011.12.031.
[40] R. Nakaoka, Y. Yamakoshi, K. Isama, T. Tsuchiya, Effects of surface chemistry prepared by self-assembled monolayers on osteoblast behavior., Journal of Biomedical Materials Research. Part A. 94 2 (2010) 524–32.
[41] A.-S. Wagner, K. Glenske, V. Wolf, D. Fietz, S. Mazurek, T. Hanke, A. Moritz, S. Arnhold, S. Wenisch, Osteogenic differentiation capacity of human mesenchymal stromal cells in response to extracellular calcium with special regard to connexin 43, Annals of Anatomy – Anatomischer Anzeiger. 209 (2017) 18–24. https://doi.org/10.1016/j.aanat.2016.09.005.
[42] L.F. Mellor, M. Mohiti-Asli, J. Williams, A. Kannan, M.R. Dent, F. Guilak, E.G. Loboa, Extracellular Calcium Modulates Chondrogenic and Osteogenic Differentiation of Human Adipose-Derived Stem Cells: A Novel Approach for Osteochondral Tissue Engineering Using a Single Stem Cell Source, Tissue Engineering. Part A. 21 (2015) 2323–2333. https://doi.org/10.1089/ten.tea.2014.0572.
[43] C.M. Sevrain, M. Berchel, H. Couthon, P.-A. Jaffrès, Phosphonic acid: preparation and applications, Beilstein J. Org. Chem. 13 (2017) 2186–2213. https://doi.org/10.3762/bjoc.13.219.
[44] D.F. Mosher, L.T. Furcht, Fibronectin: Review of its Structure and Possible Functions, Journal of Investigative Dermatology. 77 (1981) 175–180. https://doi.org/10.1111/1523-1747.ep12479791.[45] J.R. Potts, I.D. Campbell, Structure and function of fibronectin modules, Matrix Biology. 15 (1996) 313–320. https://doi.org/10.1016/S0945-053X (96)90133-X.

Conclusions And Perspectives

CONCLUSION

The objective of this work was to develop of functionalized Ti/PMMA/Ti sandwich structure by grafting different bioactive polymers carrying sulfonate and phosphonate groups in order to improve the biological response of sandwich structures.

This thesis has two main parts:
A "chemistry" part in which the different grafting methods of PMMA, polyNaSS and polyVBP on titanium are described - two grafting methods are used in this thesis:
- a "grafting to" method which uses a functionalized anchor molecule followed by a "click" reaction to bind the PMMA of controlled architecture previously synthesized by RAFT polymerization.
- a "grafting from" method developed at the LBPS in 2016 (patented USPN - CERAVER license) which consists of radical grafting using UV radiation instead of a temperature rise, to initiate the radical polymerization of the PMMA, NaSS and VBP from the surface.
This "chemistry" part gave rise to the writing of 3 articles. An article is devoted to the double functionalization of titanium surfaces (Chapter II), another article reports the surface functionalization of Ti-PMMA with a bioactive polymer, polyNaSS (Chapter III), the last article relates the functionalization of titanium surfaces by the polymer carrying phosphonate groups (Chapter IV).

In parallel, a "biology" part was carried out. The study of the cellular response to different functionalized titanium surfaces was assessed in the LBPS laboratory. Cell survival, ALP activity, and calcification of MC3T3-E1 osteoblast cells cultured onto the different functionalized surfaces were performed.

In the chapter II, both grafting methods, "grafting to" and "grafting from" previously developed for the NaSS monomer, have been successfully transposed to another monomer such as MMA. This polymer is particularly interesting since it aims at improving the mechanical properties of the targeted Ti / PMMA / Ti sandwich structure. The originality of our study is based on the development of a double functionalization of Ti surfaces. It has been shown by different characterizations (TB colorimetric method, WCA, FTIR, EDS) that it is possible to selectively graft a polymer to the surface of Ti using UV irradiation. The protocol developed will allow us to functionalize the external surface of our sandwich structure.

In the chapter III, the work focuses on the surface modification of Ti-PMMA grafted substrates with a simple UV photochemical technique. During the modification of Ti-PMMA surfaces, a monolayer of carboxylic functional group formation occurs. This non-destructive surface process further leads to the grafting of bioactive polymers such as PNaSS. FTIR-ATR, WCA, and TB colorimetric method results proved that PNaSS was successfully grafted onto Ti-PMMA surfaces. Biological studies with osteoblast cells have shown that surface activity is enhanced by PNaSS grafting. The enhancement of cell spreading demonstrated by the morphological study and the improvement of cell differentiation at 28 days of culture indicate the usefulness of this surface functionalization procedure.

In the chapter IV, a UV-initiated grafting polymerization technique in a two-step process was successfully developed to graft phosphonate polymers. FTIR-ATR, WCA and XPS data showed that chemically introducing phosphonic acid groups to Ti surfaces was a success. The method developed is easily adaptable to functionalize Ti implants for medical purposes. Cell survival, ALP activity, and calcification of MC3T3-E1 osteoblast cells cultured onto the poly (VBP) grafted titanium surfaces revealed increased differentiation of these cells, implying the effect of improved grafted implant osseointegration response. The Ti – metal surface's covalently bonded with phosphonic acid molecules act as a scaffold for new bone growth, allowing the implant to attach to the host tissue. These results indicate that poly (VBP) grafted Ti implants could be used in biological applications.

PERSPECTIVES

A thesis work is rarely finished and only represents a building block for a much larger project. Below you will find a description of some perspectives that could be considered in the near future within the LBPS.

One of the first perspectives would be to study the antibacterial effect of the different functionalizations carried out during this thesis, in particular, the effect of polyNaSS grafting on PMMA and the effect of polyVBP on titanium surfaces. In parallel, it would also be interesting to study the behaviour of plasma proteins on these modified titanium surfaces. During implantation, the first reaction that occurs is the adsorption of plasma proteins onto the surface. These proteins have a key role in the adhesion of bacteria and cells to the surfaces, therefore it would be interesting to study their behaviour in relation to the different functionalizations.

A second perspective would be to develop the grafting of polyVBP on Ti-PMMA surfaces in order to increase the osteointegrative response of elaborate sandwich structures.

Another perspective would be to evaluate the cellular response on the sandwich structures in order to evaluate the biological response of the complete structure.

In parallel with this thesis work, an *in vivo* study in rabbits is being conducted with Dr. Sophie Le Cann on titanium surfaces functionalized with polyVBP. These results will complement the *in vitro* part presented in the manuscript.

Annexe

ANNEXE

Liste des Publications :

1. **“Ultraviolet irradiation modification of poly(methylmethacrylate) titanium grafted surface for biological purpose”** Pereira C., Semedo Da Moura C., Carrado A., Falentin-Daudré C.* *Colloids and Surfaces A Physicochemical and Engineering Aspects*, **2022**, 655 (5), 130295.
2. **“Biological properties of direct grafting by ultraviolet irradiation of vinyl benzyl phosphonic acid onto titanium surfaces”** Pereira C., Baumann JS., Humblot V., Falentin-Daudré C.*, *Reactive & Functional Polymers*, **2022,** 173 (17), 105215.
3. **"Trends in Metal-Based Composite Biomaterials for Hard Tissue Applications”** Shankar Nayak G., Carradò A., Masson P., Pourroy G., Mouillard F., Migonney V., Falentin-Daudre C., Pereira C., Palkowski H., *JOM the journal of the Minerals, Metals & Materials Society* , **2022**, 74, 102-125.
4. **“Double Functionalization for the Design of Innovative Craniofacial Prostheses”** Pereira C., Baumann J.S., Masson P., Pourroy G., Carrado A., Migonney V., Falentin-Daudre C.* *JOM the journal of the Minerals, Metals & Materials Society*, **2022**, 74, 87-95.

Communications orales :

1. **"Grafting phosphonic acid polymers onto titanium implant by UV irradiation” C. Pereira**, JS. Baumann, V. Humblot, C. Falentin-Daudré, GDR B2I, Paris, **25 mars 2022.**
2. **"Grafting phosphonic acid polymers onto titanium implant by UV irradiation” C. Pereira**, C. Falentin-Daudré, TMS 2022, (**Advanced Functional and Structural Thin Films and Coatings symposium)**, Anaheim (Etats-Unis), **3 mars 2022.**
3. **"Greffage de polymères à base d'acide phosphonique par irradiation UV sur des implants en titane"**, **Caroline Pereira**, C. Falentin-Daudré GEPO 2021, Porquerolles, 4 octobre 2021.
4. **"Design of Innovative Hybrid Structures Using Grafting of Architecture-controlled Polymers for Biomedical Applications" C. Pereira**, JS. Baumann, P. Masson, G. Pourroy, H. palkowsky, A. Carrado, V. Migonney, C. Falentin-Daudré, TMS 2021 (Advanced Functional and Structural Thin Films and Coatings symposium), Orlando (Etats-Unis), **18 Mars 2021**.

Communications par affiche :

1. **"Greffage de polymères à base d'acide phosphonique par irradiation UV sur des implants en titane"**, **Caroline Pereira**, C. Falentin-Daudré, GFP 2021, Lyon, Novembre 2021.
2. **"Influence de l’architecture de polymères bioactifs greffés sur la réponse biologique sur des implants de titane”** C. Falentin-Daudré, **C. Pereira**, JS. Baumann, H. Chouirfa,

V. Migonney, Tour du CNRS en 80 jours : Matériaux Hybrides, Bobigny, **14 Juin 2019**.

<u>Enseignements</u> :

64h de monitorat par année :

- Travaux pratiques Chimie des solutions
- Travaux dirigés Atomistique, Chimie des solutions et Thermodynamique
- Cours sur les biomatériaux à base de titane

<u>Formation école doctorale</u> :

Modules suivis dans les formations disciplinaires (60h) :

- Participation à la journée thématique "*Procédés Physiques appliqués aux Biointerfaces*
- *Focus sur le Plasma*"
- Congrès international - TMS 2021 virtual meeting (Orlando)
- Journée thématique du GDR B2i
- GDR B2i E-journée d'été

Modules suivis dans les formations transversales (60h) :

- **Participation aux formations proposées par l'Université Paris 13**
  - Formation « Prévention contre les violences sexistes et sexuelles » Woman safe
  - Formation « Premier pas sur HAL »
  - Formation « Intro aux données de la recherche »
  - Formation « Intro à l'identité numérique »
  - « Habilitation aux risques chimiques »
  - « Initiation à Zotero, logiciel de gestions des références »
  - Scientific Writing
  - Journée transversale sciences
  - 48ème Journées d'Etudes des Polymères 2021

- **Formations à la recherche et méthodologie de la recherche**
  - Une heure pour comprendre le dépôt et la diffusion de la thèse

- **Qualité de la recherche**
  - Info Compilatio
  - Protection des données à caractère personnel
  - Intégrité scientifique dans les métiers de la recherche

<u>Autre activité</u> :

Représentante des doctorants du laboratoire CSPBAT lors des conseils de laboratoire

Abstract

Elaboration of Titanium/Polymer hybrid materials to improve the biological response of bone cells

Skull injuries caused by trauma and pathologies, such as tumor or congenital deformities, require the reconstruction of craniofacial prostheses. Titanium (Ti) is one of the most used material for cranioplasty. However, this mono-material alone presents many drawbacks such as inappropriate mechanical properties compared to the bone. To solve this problem, the idea is to combine polymers and metals. Developing layered structures like sandwich materials composed by two metallic skin sheets and a copolymer core can be an interesting alternative to design innovative biomedical prostheses. To avoid Ti/Polymer/Ti structure's delamination, we propose to chemically link polymer chains on metal surfaces by using "grafting to" technique involving an anchorage molecule onto which the polymer synthesized by reversible addition-fragmentation chain transfer (RAFT) polymerization is clicked. Moreover, to confer antibacterial and osseointegration properties, bioactive polymers such as poly(sodium styrene sulfonate) (polyNaSS) and poly (vinyl benzyl phosphonic acid) (polyVBP) will be graft on the exterior surfaces of our sandwich.

Key words : Titanium, grafting, bioactif, polymers

Résumé

Élaboration de matériaux hybrides Titane/Polymère pour améliorer la réponse biologique des cellules osseuses

Les lésions crâniennes causées par des traumatismes et des pathologies, telles que des tumeurs ou des malformations congénitales, nécessitent la reconstruction de prothèses craniofaciales. Le titane (Ti) est l'un des matériaux les plus utilisés pour la cranioplastie. Cependant, ce mono-matériau présente à lui seul de nombreux inconvénients tels que des propriétés mécaniques inappropriées par rapport à l'os. Pour résoudre ce problème, l'idée est d'associer des polymères et des métaux. Développer des structures stratifiées comme des matériaux sandwich composés de deux feuilles de peau métalliques et d'un noyau en copolymère peut être une alternative intéressante pour concevoir des prothèses biomédicales innovantes. Pour éviter le délaminage de la structure Ti/Polymère/Ti, nous proposons de lier chimiquement des chaînes polymères sur des surfaces métalliques en utilisant la technique de « greffage sur » impliquant une molécule d'ancrage sur laquelle le polymère synthétisé par polymérisation réversible par transfert de chaîne par addition-fragmentation (RAFT) est cliqué. De plus, pour conférer des propriétés antibactériennes et d'ostéointégration, des polymères bioactifs tels que le poly(sodium styrène sulfonate) (polyNaSS) et le poly (vinyl benzyl phosphonic acid) (polyVBP) seront greffés sur les surfaces extérieures de notre sandwich.

Mots clés : Titane, greffage, bioactif, polymères